Depositional environment of the Branch Sandstone and correlative sequences:

Late Cretaceous changes in relative sea level in the East Coast Basin of New Zealand

By

Lisa Jan McCarthy

A thesis submitted to Victoria University of Wellington in partial fulfilment of the requirements for the degree of Master of Science in Geology

School of Geography, Environment and Earth Sciences

Victoria University of Wellington

2018

Abstract

The Branch Sandstone is located within an overall transgressive, marine sedimentary succession in Marlborough, on the East Coast of New Zealand's South Island. It has previously been interpreted as an anomalous sedimentary unit that was inferred to indicate abrupt and dramatic shallowing. The development of a presumed short-lived regressive deposit was thought to reflect a change in relative sea level, which had significant implications for the geological history of the Marlborough region, and regionally for the East Coast Basin.

The distribution and lithology of Branch Sandstone is described in detail from outcrop studies at Branch Stream, and through the compilation of existing regional data. Two approximately correlative sections from the East Coast of the North Island (Tangaruhe Stream and Angora Stream) are also examined to provide regional context. Depositional environments were interpreted using sedimentology and palynology, and age control was developed from dinoflagellate biostratigraphy. Data derived from these methods were combined with the work of previous authors to establish depositional models for each section which were then interpreted in the context of relative sea level fluctuations.

At Branch Stream, Branch Sandstone is interpreted as a shelfal marine sandstone, that disconformably overlies Herring Formation. The Branch Sandstone is interpreted as a more distal deposit than uppermost Herring Formation, whilst the disconformity is suggested to have developed during a fall in relative sea level. At Branch Stream, higher frequency tectonic or eustatic sea-level changes can therefore be distinguished within a passive margin sedimentary sequence, where sedimentation broadly reflects subsidence following rifting of the Tasman Sea. Development of a long-lived disconformity at Tangaruhe Stream and deposition of sediment gravity flow deposits at Angora Stream occurred at similar times to the fall in relative sea level documented at the top of the Herring Formation at Branch Stream. These features may reflect a basin-wide relative sea-level event, that coincides with global records of eustatic sea level fall.

Acknowledgements

First and foremost I'd like to thank my long-suffering supervisors, James Crampton and Mike Hannah, who have helped me through this process every step of the way, from formulating this topic, right through to the last push at the end. You have both been endlessly knowledgeable and encouraging, not to mention enthusiastic, despite my best efforts to be negative.

Mike, thanks especially for your help with the HF work, it's never fun dressing up in a bright orange suit twice a day, and you have been exceedingly patient. Thanks also must go to my lab buddy, Matt – for all the chat, knowledge and assistance – I wouldn't have had any slides to analyse if it weren't for you. I'd also like to acknowledge all the Victoria and GNS staff who have kindly given their time, knowledge and assistance, whether it be helping me prepare for field work, getting me up to speed in the lab or enlightening me regarding palynofacies – there is no way I could have done any of this without your help.

Particular thanks must go to Poul Schiøler, I am indebted to you for all the time you sat with me and helped me through all things palynology, it was a steep learning curve and your extensive knowledge was invaluable.

Thanks to the Murrays of Bluff Station, Brian in Wimbledon and Craig and Tom at Longview for kindly granting me access to the field sites. This research would not have been possible without you, nor would I have got to visit such stunning locations.

I am hugely grateful to everyone at NZOG, firstly for inspiring and encouraging me to undertake a geology degree in the first place, and also for the financial assistance. Chris, AJ, and Dan, thank you a thousand times over for your patience with me and your ability to provide humour when I was at my grumpiest. Bernice, you have been a constant source of wisdom, belief, humour and support over the years, I can only hope you don't cut me off now. Old Mate, I can't begin to thank you for your friendship, help and encouragement, thanks for putting up with me over the years.

Cheers to all the university people who have made this such an enjoyable experience. Tom, Jack, Adam, Brad, Melanie, Lucas and Georgia thanks for all the help, encouragement, beers and entertainment. Special thanks for your help with the fieldwork Tom and Adam, it was a great time and I couldn't have asked for better, more photogenic field assistants.

Thanks to my friends and family for always being there. Tim, it kills me to admit it, but all that constant grammar-related pestering in my youth probably came in useful. Andrew, you are a bit of an inspiration to me (it would have been helpful if I'd worked that out a bit earlier in life). Jan, thanks for all the cheery phone calls and support, you are the best.

Finally, and not least, thanks Nick. For everything. You have been endlessly patient, helpful and supportive. I couldn't have done it without you.

Contents

List of Figures

List of Tables

1 Introduction

The introductory chapter gives an overview of this thesis. This introduction explains the rationale and aims of the research. Section 1.3 discusses the regional setting and modern-day locations of field areas and Section 1.4 outlines the geological history of the East Coast Basin.

1.1 General Introduction

This thesis describes and interprets a Late Cretaceous rock formation, the Branch Sandstone, and its correlatives in eastern New Zealand. The Branch Sandstone is an apparently anomalous unit, which seems to indicate abrupt and dramatic shallowing, within an overall transgressive, marine sedimentary succession in southern Marlborough, on the East Coast of New Zealand's South Island. This succession formed following New Zealand's separation from Gondwana and the opening of the Tasman Sea, and records a prolonged period of thermal subsidence in New Zealand's geologic history (King et al., 1999). Reconnaissance level analysis of Branch Sandstone indicates the formation is a shallow marine deposit of Late Cretaceous age, which was deposited along the paleo-north facing margin of proto-New Zealand (Crampton et al., 2003; Reay, 1993; Reay & Strong, 1992).

In Marlborough, the Branch Sandstone overlies the Herring Formation, a sequence of mudstone, siltstone and very fine sandstone that has been interpreted as being deposited at shelfal or greater depths (Field et al., 1997; Laird et al., 1994). The Branch Sandstone is sharply overlain by Mead Hill Formation, a chert rich, micritic limestone with facies indicative of a progressively deepening inner to outer shelfal marine environment (Reay, 1993; Strong et al., 1995; Crampton et al., 2003). The Mead Hill Formation is thought to reflect ongoing relative sea level rise and/or subsidence until at least the end of the Cretaceous (Crampton et al., 2003).

This project examines the Branch Sandstone at Branch Stream in Marlborough, as well as two other comparable field sites in the North Island, with the aim of evaluating a broader, regional trend in paleoenvironmental changes around the time of Branch Sandstone deposition.

Originally, this research planned to exclusively evaluate Branch Sandstone and incorporated a significant field mapping component, to be undertaken in the Clarence valley. In November 2016, the Mw7.8m Kaikoura earthquake caused extensive damage in the upper South Island and rendered much of the proposed field area inaccessible and the scope of the project was subsequently revised.

Potentially analogous sedimentary sequences of a similar age in the East Coast Basin of the North Island have previously been described by Crampton (1997) and Crampton et al. (2006). At Angora Stream (Figure 1), a ca. 4m thick, unnamed sandstone deposit (sandstone A) overlies the Glenburn Formation, which is considered to be a series of bathyal fan deposits (Crampton, 1997; Moore, 1988a). Sandstone A is in turn overlain by Whangai Formation, a progressively deepening shelfal-bathyal deposit. The depositional setting at Tangaruhe Stream, in southern Hawke's Bay, through the same period is thought to have been more proximal to the paleo-shoreline (Crampton et al., 2006). Existing data suggest that an unconformity at the top of Tangaruhe Formation, which is overlain by Whangai sediments, correlates with the timing of deposition of Branch Sandstone and sandstone in Angora Stream.

The suggestion that short-lived, apparently regressive deposits lie between progressively deepening facies has implications for the geological history of southeastern Marlborough, and more regionally, for the East Coast Basin. This sedimentary event would reflect either a substantial change in eustatic sea level, a significant tectonic event, or both. The present MSc research project is the first study to target this putative event at a basin wide scale and derive a depositional model for the Branch Sandstone and correlatives during the Late Cretaceous.

1.2 Aims

This research aims to understand the depositional environment of the Branch Sandstone and proposed correlative sequences, and the paleoenvironmental circumstances that lead to their deposition. To accomplish these aims, the following steps will be undertaken:

- Compile existing field data to establish the modern day geographic distribution of Branch Sandstone
- Measure sections and collect samples at key localities, including Branch Stream, Angora Stream and Tangaruhe Stream
- Interpret depositional environment based on lithology, grain-size analyses, and stratigraphic relationships
- Use dinoflagellate biostratigraphy to constrain the age and depositional setting of Branch Sandstone and correlatives, and identify any depositional hiatuses associated with these units
- Use palynofacies analysis to constrain the depositional setting of Branch Sandstone and correlatives, and any fluctuations in relative sea level associated with their deposition
- Interpret findings from these analyses in the context of stratigraphic relationships, regional tectonic and depositional models, and available Late Cretaceous eustatic sea-level curves

1.3 Study Area

This research was carried out at various localities within the East Coast Basin of New Zealand. The East Coast Basin stretches from the East Cape of the North Island (~36°S) to the northern edge of the Chatham Rise (42°S), which extends from the central South Island in an eastward direction. The Basin is delineated to the west by the axial ranges of the North Island and the Wairau Fault in the South Island and extends offshore, where it is laterally constrained by the modern day Hikurangi trough (Field et al., 1997). Data were collected from three field sites including Branch Stream (southeast Marlborough), Angora Stream (northern Wairarapa) and Tangaruhe Stream (southern Hawkes Bay) (Figure 1).

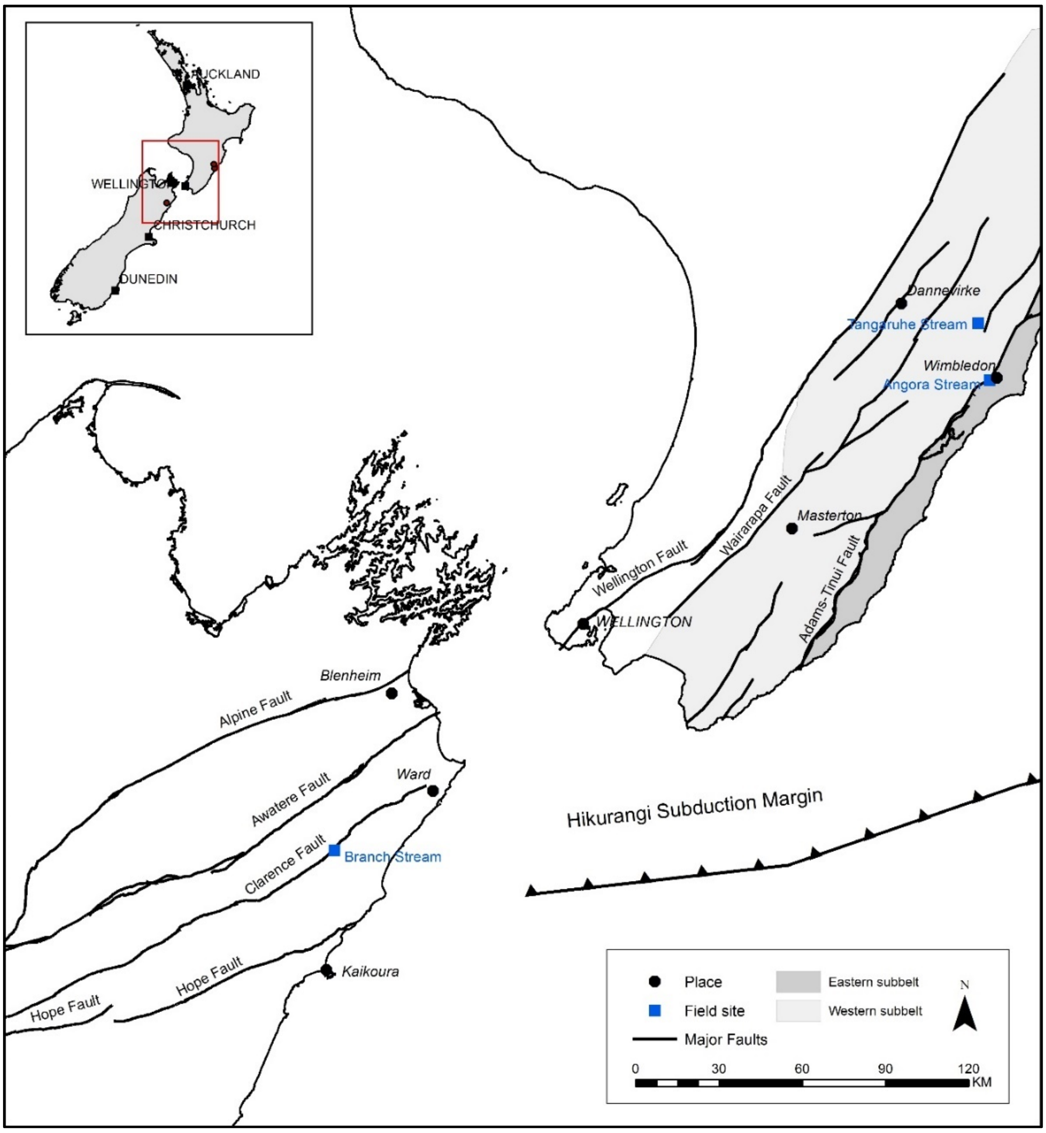

Figure 1. Simplified structural map, showing locations of field sites. Fault data from QMAP (GNS, 2014), subbelt configuration from Field et al. (1997).

Table 1. Coordinates of field sites

Site	Latitude (NZGD 2000)	Longitude (NZGD 2000)	X (NZTM)	Y (NZTM)
Branch Stream	-42.02214	173.71610	1659285	5347518
Angora Stream	-40.44791	176.47974	1895109	5516710
Tangaruhe Stream	-40.2661	176.42263	1891046	5537085

For simplicity and due to differences in lithostratigraphic nomenclature, discussion in the following sections will be separated by region: a) Marlborough and b) northern Wairarapa/southern Hawkes Bay. Localities of field sites are given a NZMS 260 map reference within the text below, whilst Table 1 gives approximate geographic coordinates in NZGD2000 and projected coordinates in the New Zealand Tranverse Mercator (2000) reference system.

1.3.1 Marlborough

The present day landscape of southeastern Marlborough is dominated by two northeast-trending mountain belts, the Inland and Seaward Kaikoura Ranges (Figure 2 inset). These ranges are separated by the Clarence River valley, which contains a well preserved Late Cretaceous sedimentary succession. A number of streams drain into the Clarence River and flow perpendicular to strike of the strata, and thereby expose a number of sedimentary sections for analysis (Strong & Beggs, 1990). One of these rivers, Branch Stream, is the type locality for Branch Sandstone. Branch Stream is located in the middle Clarence Valley (O30/693092) and is only accessible with a 4WD vehicle, on private farm tracks.

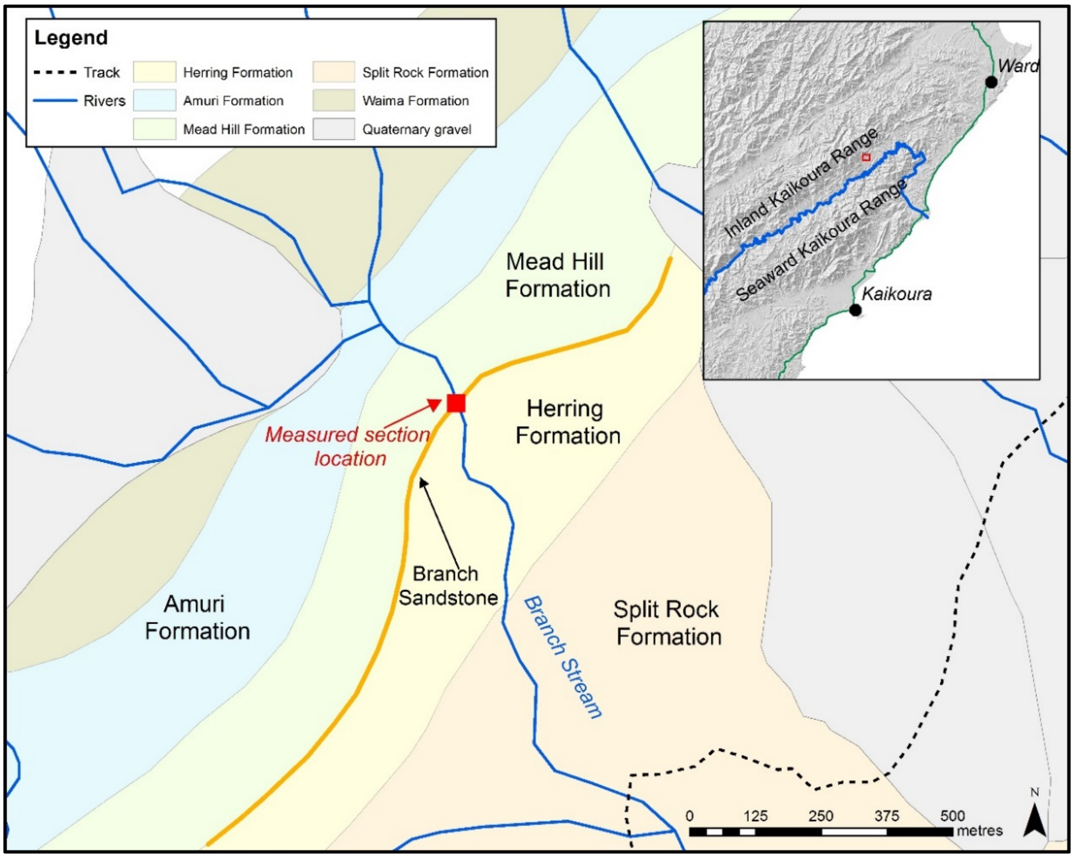

Figure 2. Branch Stream field site showing measured section locality, as well as regional geology, modified from 250:000K QMAP series (GNS, 2014).

1.3.2 Northern Wairarapa/Southern Hawkes Bay

The Cretaceous sedimentary succession in the Wairarapa and southern Hawkes Bay is divided into two distinct NE-SW oriented structural blocks due to variations in lithology, deformation and igneous content: the Eastern and Western subbelts (Figure 1) (Moore, 1988b). In general, the Eastern Sub-belt is structurally complex and contains a sequence of Cretaceous flysch facies (Moore, 1988b). Conversely, the western sub-belt exhibits less deformation and the Cretaceous sedimentary sequence is mudstone dominated (Moore, 1988b).

Angora Stream is located within the Eastern Sub-belt, within rolling hill country in northern Wairarapa, around 50 minutes drive southeast of Dannevirke (U24/051784). The section logged for this research is situated on private farmland, just off Angora Road. The sediments described herein crop out along the river banks, around 250m from the intersection of Angora Road and Route 52 (Figure 3).

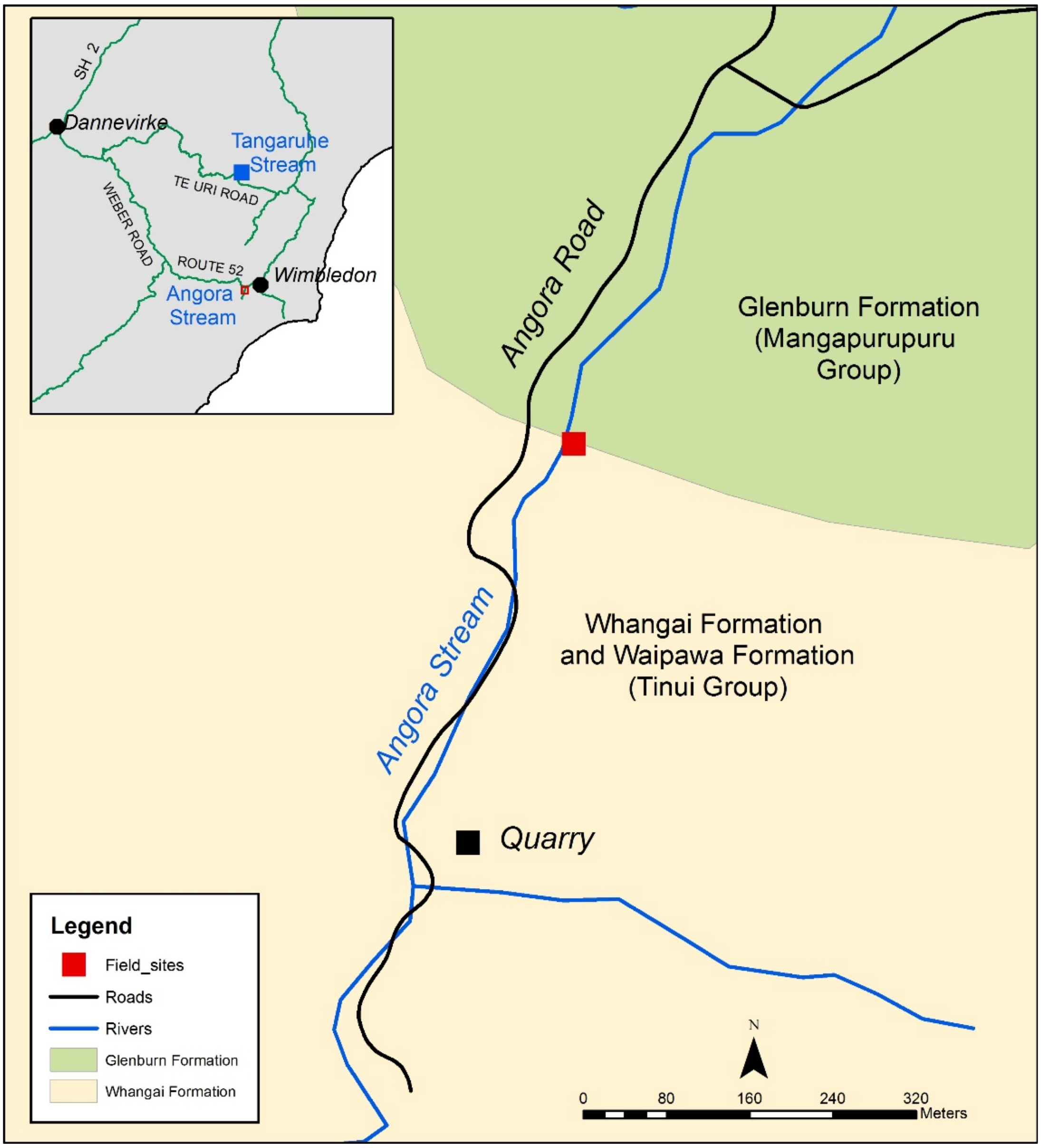

Figure 3. Angora Stream field site showing measured section locality, as well as regional geology, modified from 250K QMAP series (GNS, 2014).

Tangaruhe Stream (Figure 4) sits within the western subbelt, and is located in the eastern Whangai Range area, approximately due east of Dannevirke (U24/010988). The section is located on private farmland, off Te Uri Road.

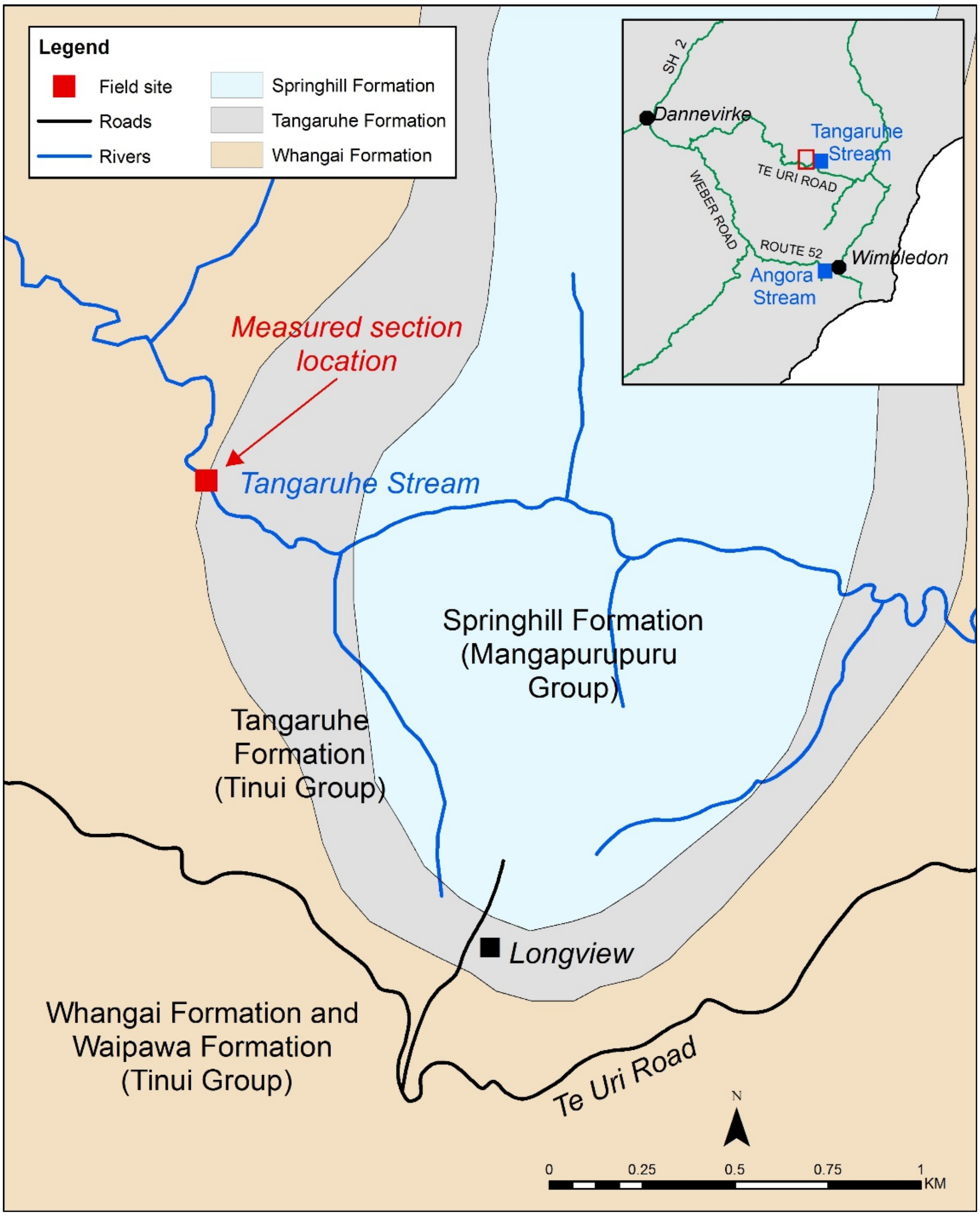

Figure 4. Tangaruhe Stream field site showing measured section locality, as well as regional geology from 250K QMAP series (GNS, 2014).

1.4 Geological setting and tectonic history

The Branch Sandstone forms part of the Late Cretaceous sedimentary succession in Marlborough, where it is thought to indicate shallowing within an overall transgressive sedimentary package (Reay, 1993; Reay & Strong, 1992). At a regional scale, the evolution of the East Coast Basin's Late Cretaceous and Paleogene sedimentary record can be attributed to post rift subsidence following the separation of Zealandia from Gondwana. The separation of proto-Zealandia (Mortimer et al., 2017) from Gondwana commenced around 100 Ma, at which time, the East Coast Basin was situated on the northwest-facing, paleo-Pacific passive margin of the continent (King et al., 1999).

Late Cretaceous – Paleocene sediments of the East Coast Basin comprise a broadly upward fining assemblage of shelfal marine sands, flysch and siliceous shales, that belong to the Tinui (Wairarapa), Seymour and Muzzle Groups (Marlborough) (Field et al., 1997; King, 2000). These sediments were deposited during a widespread marine transgression that initiated around 85 Ma in association with Tasman Sea spreading (Bradshaw, 1989; Laird & Bradshaw, 2004). During this period, the Zealandia continent slowly subsided as it drifted away from the remaining Gondwanan landmass (Ballance, 1993; King, 2000; Laird, 1992). By Eocene times, the marine transgression culminated in deposition of micritic limestone in Marlborough and calcareous muds further north (King et al., 1999).

The modern East Coast Basin sits atop the Hikurangi margin, where the Australian Plate overrides the Pacific Plate. Westward directed, oblique subduction of the Pacific Plate commenced during the early Miocene, transforming the area from a passive margin to a convergent forearc setting (Beanland et al., 1998; Rait et al., 1991). The Hikurangi trench runs roughly parallel to the coastline of northern Wairarapa, with associated deformation distributed over a distance of around 200km (Lewis & Pettinga, 1993). East-west oriented compression is manifest as numerous active folds, extensive right lateral strike slip faults and westward directed thrust faults (Barnes et al., 1998; Beanland et al., 1998; Lee & Begg, 2002).

In the Marlborough region, the subduction zone passes into a transcurrent fault system, and motion is distributed across a network of major dextral strike slip faults collectively termed the Marlborough Fault System (Figure 1) (Roberts, 1995).

Extensive Neogene deformation associated with the active plate boundary has therefore complicated stratigraphic relationships among Late Cretaceous sediments in the wider East Coast region (Crampton et al., 2003). Presently, and largely because of the deformation discussed above, the Late Cretaceous paleogeography of the East Coast Basin is not well constrained. Basic paleogeographic maps are presented by Field et al. (1997), whilst King (2000) depicts the broad position of the basin through the past 100 Ma. Crampton et al. (2003) provided detailed palinspastic reconstructions for the southeastern Marlborough region for the Late Cretaceous – Paleogene period. These maps indicate progressive drowning of a paleo west-northwest facing portion of continental shelf, associated with thermal subsidence.

2 Previous research

Chapter 2 describes work undertaken by previous authors, who have subdivided the Late Cretaceous successions in Marlborough and the lower eastern North Island into various lithostratigraphic units. The regional geology of the East Coast Basin has been synthesised by Field et al. (1997), who split the basin into four distinct areas: Marlborough, Wairarapa, Hawkes Bay and Raukumara. Here, only the lithostratigraphy pertinent to this study's field localities of Marlborough and Wairarapa/Hawkes Bay is discussed (Figure 5).

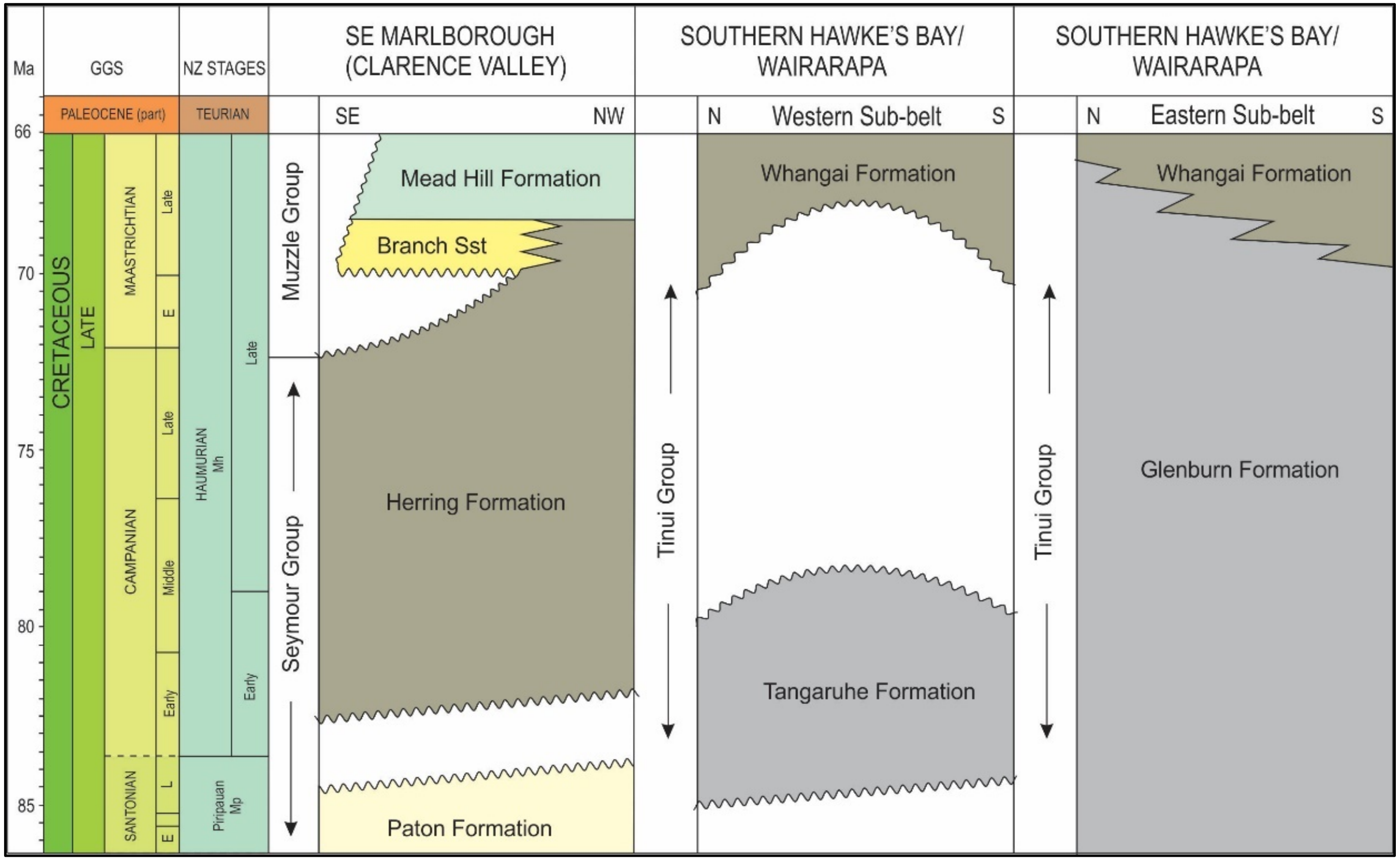

Figure 5. Simplified stratigraphy of the SE Marlborough and southern Hawkes Bay/Wairarapa regions. Modified from Crampton et al. (2006) and Crampton et al. (2003).

2.1 Previous work

2.1.1 Marlborough

The Marlborough region has a long history of geological study, beginning in the 1800's when Hutton (1877) and McKay (1886) conducted reconnaissance mapping in the area. Thomson (1919) published a detailed synthesis of the stratigraphy of the middle Clarence and Ure valleys, based on his own and McKay's mapping. Suggate (1958) discussed Cretaceous sections of the middle Clarence Valley, describing the Cretaceous type section for Seymour Formation at Seymour Stream. A generalised section of Middle Clarence valley sedimentary rocks was provided by Wellman (1959), which made mention of Mata series glauconitic sandstones and greensands. Webb (1971) compiled faunal lists of Late Cretaceous foraminifera from localities within the present study area, including Branch Stream. This work placed the upper Herring Formation and lower Amuri Formation in Marlborough within the Haumurian stage.

The Branch Sandstone was first described (informally) as a distinct unit by Reay and Strong (1992), who proposed that the formation was lithologically unique in central Marlborough. Prior to this Morris (1987) assigned Branch Sandstone from the type locality to the Claverley Sandstone formation. Laird (1992) briefly described Branch Sandstone as part of efforts to compile a regional synthesis of the Cretaceous geology of the Marlborough region, but did not go into detail due to the localised nature of the unit.

Reay (1993) produced a monograph on the Geology of the Middle Clarence Valley, in which the most comprehensive descriptions of Branch Sandstone appear. This publication documented the lithostratigraphy of the study region, and Reay's nomenclature is used, where possible, here. A more regional synthesis of the stratigraphy of the East Coast is given in Field et al. (1997), which suggests that the Branch Sandstone could be a lateral equivalent of the Claverley Sandstone of North Canterbury.

Prior to the present study, detailed biostratigraphic analysis has not been undertaken on the Branch Sandstone, although the presence of dinoflagellate cyst remains has been noted within the formation (Reay & Strong, 1992). Biostratigraphic studies are relatively common in Marlborough, but have focussed on units above and below the Branch Sandstone. The K-Pg boundary is well exposed in the region and has been researched extensively (e.g. Hollis, 2003; Hollis et al., 2003; Strong et al., 1995). Likewise, the underlying Paton and Herring formations have been examined in some detail (Crampton et al., 2006; Schiøler et al., 2002; Schiøler & Wilson, 1998).

2.1.2 Hawkes Bay/Wairarapa

Early geological mapping in the Southern Hawkes Bay-Northern Wairarapa region was undertaken by Hector (1871) and McKay (1877, 1879). Oil and gas exploration companies later conducted field studies in the Dannevirke and Whangai Range regions. An initial wave of reconnaissance mapping and sampling in the 1930's was undertaken on behalf of NZ Exploration Limited (Walpole & Burr, 1939; Walpole, Quennell, & Burr, 1938). In the 1960's, renewed interest in the area saw extensive field mapping and biostratigraphic studies carried out by BP Shell Todd Exploration Limited (Laing, 1961; Ridd, 1964).

Academic studies initially targeted localised parcels of land for geological mapping projects. Projects that examined the late Cretaceous sedimentary sequence in the Lower North Island were undertaken by Lillie (1953); Eade (1963); Johnston (1971); Moore (1980) and Johnston (1980) and Neef (1995). Kingma (1960) discussed the regional distribution of Cretaceous and Tertiary facies in the East Coast whilst Moore (1986) presented a regional synthesis of Cretaceous and Tertiary stratigraphy for the eastern North Island.

Moore (1986, 1988b) subdivided the East Coast Basin of the lower North Island into five structural blocks, and two separate subbelts, due to significant variations in geological history. This work was noteworthy as it provided an improved tectonostratigraphic foundation with which to examine the stratigraphy of the area. Additionally, Moore (1988a) undertook comprehensive studies of the distribution, sedimentology and stratigraphy of the late Cretaceous Whangai Formation and associated rocks in the Eastern North Island. Notably, this work makes mention of a 'four metre thick, glauconitic sandstone bed' immediately beneath Whangai facies at Angora Stream. This same deposit has been logged and described elsewhere, where it is similarly attributed to the Glenburn Formation (Crampton, 1997; Crampton et al., 2006).

Crampton (1997) outlined and interpreted the stratigraphy of the southern Hawkes Bay and Wairarapa area. This synthesis documents the lithostratigraphy of the sites examined in this project, and the terminology suggested by Crampton (1997) is used here. Field et al. (1997) also contains a regional guide to the stratigraphy of the East Coast Basin, whilst a 250,000 geological map of the Wairarapa region is provided by Lee and Begg (2002).

2.2 Stratigraphic framework

2.2.1 Marlborough

The geology of the middle Clarence valley is described in detail by Reay (1993), whilst the Late Cretaceous-Paleogene stratigraphy of the wider southeastern Marlborough region is documented by Rattenbury et al. (2006) and references therein; Lensen (1978) Morris (1987) Hollis et al. (2003); and Field et al. (1997).

In Marlborough, the Late Cretaceous and Paleocene sedimentary succession encompasses the upper Seymour Group and the lower Muzzle Group. With the exception of Branch Sandstone, the sequence broadly corresponds to an upward fining assemblage, indicative of progressively deepening marine environments (Crampton et al., 2003; Hollis et al., 2013; Reay, 1993).

The lithostratigraphic units described herein include (from base) Herring Formation (Seymour Group); Branch Sandstone and the Mead Hill Formation (Muzzle Group) (Figure 5). These units and their correlatives are the principal constituents of the Haumurian sedimentary record in Marlborough. Whilst this project is primarily concerned with the Branch Sandstone, the enclosing formations are described to place the unit in context.

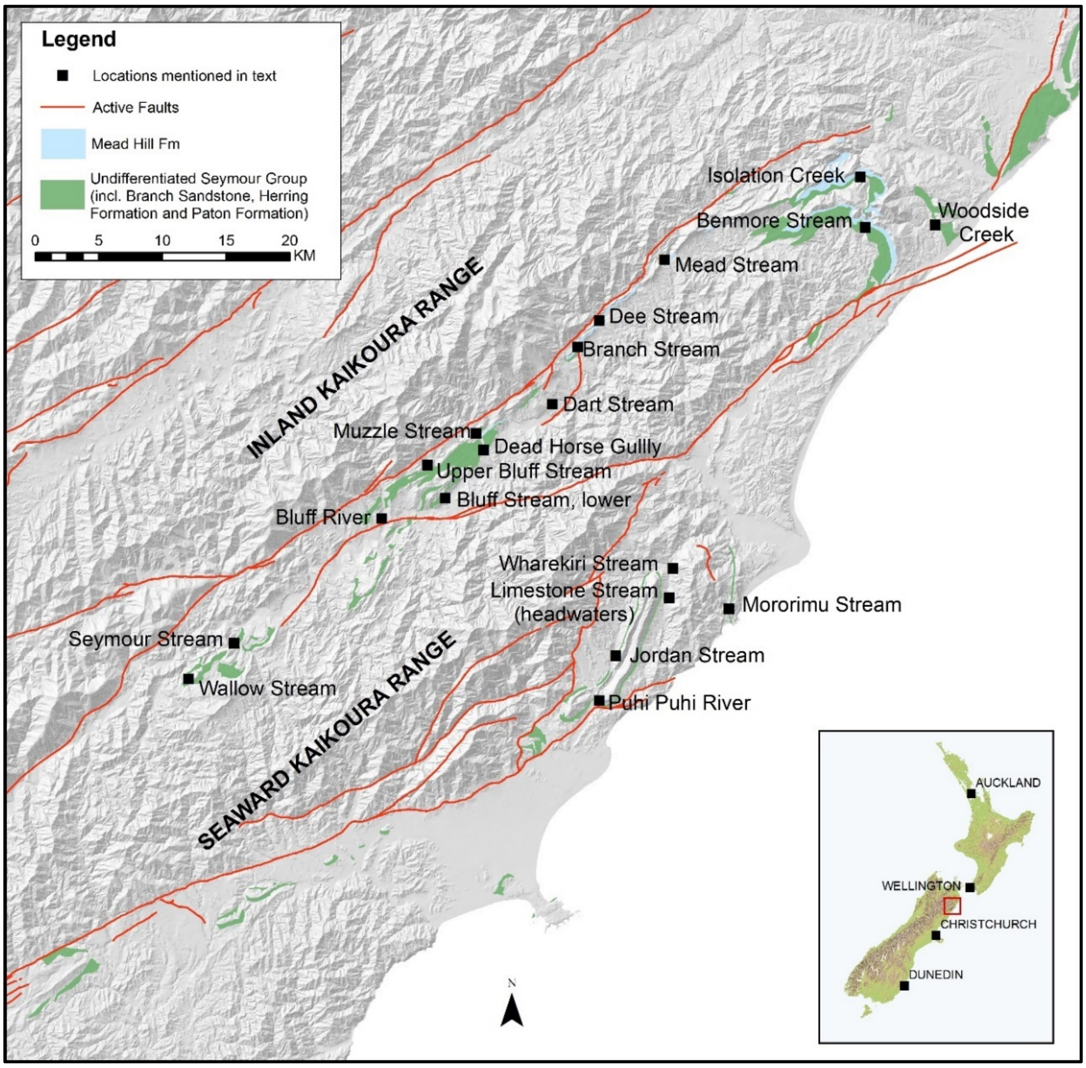

Figure 6. Distribution of Late Cretaceous sediments and known Branch Sandstone occurrences, southern Marlborough. Geological data from QMAP (GNS, 2014).

2.2.1.1 Herring Formation

Widespread marine transgression in the Marlborough region initiated at the base of the Piripauan Stage (ca. 86Ma), with deposition of the Seymour Group (Laird, 1992). The upper Seymour Group includes the Herring Formation, an upward fining assemblage of mudstone, siltstone and very fine sandstone (Field et al., 1997; Laird et al., 1994).

The Herring Formation is ubiquitous in the Middle Clarence Valley, where it ranges in thickness from 45m to >300m, and thickens to the northeast (Crampton et al., 2003; Reay, 1993). The unit consists of jarositic muddy siltstone interbedded with very fine sandstone (Reay, 1993). Dolomitic concretions are common, whilst sandstone dikes are widespread throughout the formation (Reay, 1993).

The depositional environment of Herring Formation is thought to vary laterally in southeastern Marlborough, from inner shelf conditions to mid-outer shelf (Crampton et al., 2003; Laird, 1992). The formation is interpreted to have been primarily deposited in poorly oxygenated, reducing conditions (Laird, 1992). In Marlborough, Herring Formation is thought to represent ongoing marine transgression associated with passive margin subsidence (Crampton et al., 2003).

2.2.1.2 Branch Sandstone

Branch Sandstone outcrops south of the Hope Fault, in Mororimu Stream, Wharekiri Stream and Puhi Puhi River, as well as in the middle Clarence Valley between Seymour and Dee Streams (Figure 6). Branch Sandstone is not present in the northern Clarence Valley, where most sections (e.g. Isolation Creek, Woodside Creek) display a prominent unconformity, and Herring Formation is in sharp contact with Mead Hill Formation (Hollis et al., 2013).

The Branch Sandstone comprises a massive, well sorted, intensely burrowed, fine grained sandstone (Reay & Strong, 1992). Laird (1992) noted the intensely bioturbated, well sorted nature of Branch Sandstone, as well as the presence of a 'thin matrix-supported pebble conglomerate at the base of the sand in some localities'. Further, in keeping with Reay and Strong (1992), Laird (1992) described a carbonaceous rich layer at the top of Branch Sandstone at the unit's type locality.

Morris (1987) inferred that deposition of Branch Sandstone (referred to as the Claverley Sandstone) occurred in high energy conditions in shallow water. The author ascribed lateral variations in thickness of the Claverley Sandstone to prior topography, erosion, remobilisation and expulsion (Morris, 1987).

Despite a lack of macrofossils and very few sedimentary structures, Branch Sandstone has been interpreted as a shallow marine deposit (Laird, et al. 1994). Reay and Strong (1992) inferred the unit was part of a barrier island system, which was deposited in association with marine transgression taking place during the mid-late Haumurian stage. Their work tentatively suggested that the transgression may correlate with a period of eustatic sea level change. Conversely, Hollis et al. (2013) suggested that the relative fall in sea level leading to deposition of Branch Sandstone is related to localised tectonic activity affecting part of the northern South Island.

2.2.1.3 Mead Hill Formation

The Mead Hill Formation crops out along a northeast trending strip, adjacent to the Clarence Fault, west of the Clarence River (Figure 6). The unit displays substantial variation in thickness, attaining a maximum thickness of around 250m in Mead Stream (Reay, 1993). The Formation is absent in the lower Clarence Valley, pinching out south of Bluff River (Rattenbury et al., 2006; Reay, 1993).

Mead Hill Formation overlies Branch Sandstone with sharp contact. The unit comprises a chert-rich, micritic limestone with facies indicative of a progressively deepening inner to outer shelfal marine environment (Reay, 1993; Strong et al., 1995; Crampton et al., 2003).

The Mead Hill Formation is thought to reflect ongoing relative sea level rise and/or subsidence until at least the end of the Cretaceous (Crampton et al., 2003). Assemblages of foraminifera indicate that, at Branch Stream, this unit was deposited in outer shelf-bathyal water depths, in an upwelling zone, or similar nutrient rich locality (Hollis et al., 2003). Mead Hill Formation, where present, often encompasses the Cretaceous-Paleogene boundary in Marlborough, and as such is latest Cretaceous towards its base (Hollis et al., 2003; Hollis & Strong, 2003; Willumsen, 2011).

2.2.2 Wairarapa – Southern Hawkes Bay

Moore (1988a) subdivides the Cretaceous to Paleogene sedimentary sequence of the eastern North Island into three major groups, which together form a first order transgressive cycle:

1. Early-Late Cretaceous clastic sediments including conglomerate, sandstone and mudstone;
2. A Latest Cretaceous-Paleocene succession of predominantly fine grained sediments that become increasingly calcareous upsection; and
3. Fine grained Eocene to Oligocene calcareous sediments, predominantly clay-rich mudstone and limestone.

The units of principal interest to this study form part of the Late Cretaceous-Paleocene succession in the East Coast Basin. These include the Glenburn Formation in the eastern sub-belt, Tangaruhe Formation in the western sub-belt, as well as the overlying Whangai Formation in both regions (Figure 5).

2.2.2.1 Glenburn Formation (Mangapurupuru Group)

Glenburn Formation crops out along the eastern side of the Adams-Tinui Fault, in a northeast-southwest trending belt (Lee & Begg, 2002) (Figure 7). Crampton (1997) described Glenburn Formation as comprising all Ngaterian-Haumurian conglomerate, sandstone and siltstone, or flysch facies of the Eastern sub-belt in the Wairarapa and southern Hawkes Bay region. Sandstone beds commonly exhibit grading, parallel and convolute lamination, whilst mudstone beds are fossiliferous, both may be concretionary (Crampton, 1997; Lee & Begg, 2002).

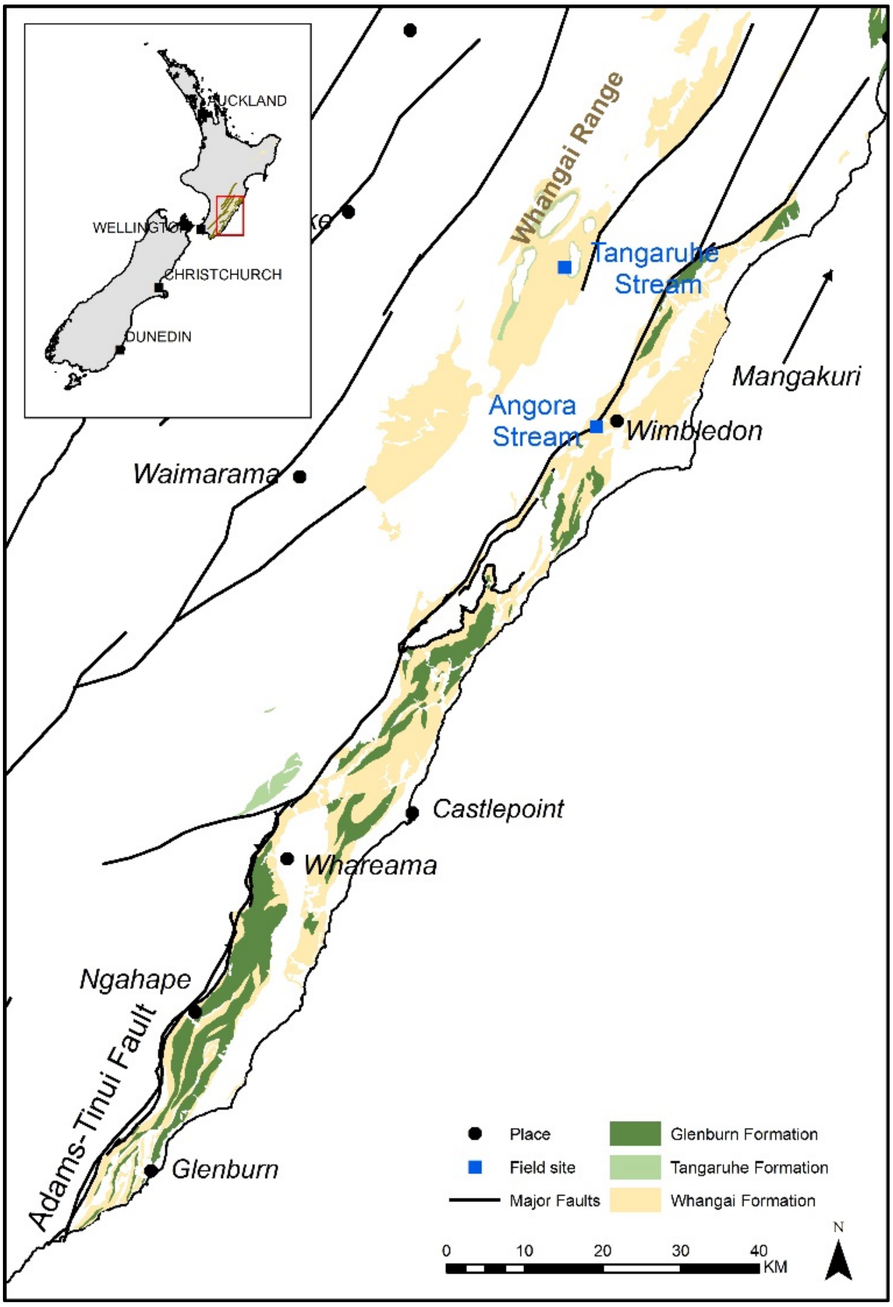

Figure 7. Distribution of the Glenburn, Tangaruhe and Whangai Formations in the lower North Island. Geological data from QMAP (GNS, 2014).

The Glenburn Formation was originally interpreted as shallow marine sediments or tidal strait deposits (Boyes et al., 2011; Eade, 1966; Johnston, 1980; Moore, 1980). This was revised by Crampton (1997) who postulated a deep water origin, suggesting the formation comprises mass flow and turbidity deposits. First pass analysis of palynofacies data mostly gives an outer shelf depth of deposition for Glenburn Formation in samples from Waimarama, Mangakuri and Glenburn (Wilson, 1991, in Crampton, 1997). Interestingly, however, samples from the uppermost Glenburn at Kaiwhata Stream, near Ngahape, may indicate deposition at inner shelf depths (Wilson, 1991, in Crampton, 1997).

2.2.2.2 Tangaruhe Formation (Tinui Group)

Tangaruhe Formation crops out in the Whangai Range area, extending as far north as Otane, and south to the Tinui Region (Crampton, 1997). Tangaruhe Formation generally comprises alternating glauconitic siltstone and sandstone, apart from the basal Mangawarawara Member, which is a poorly sorted pebbly sandy mudstone (Crampton, 1997; Moore, 1986). The unit is quite variable, with sandstone displaying partial bouma sequences in places, but having a massive character in others (Field et al., 1997; Moore, 1986). At the type locality, in Tangaruhe Stream, the formation is disconformably overlain by Whangai Formation (Crampton et al., 2006).

Tangaruhe Formation contains a prominent ichnofauna, and a sparse assemblage of predominantly autochthonous, agglutinated foraminifera (Adams, 1985). Based on these characteristics, and the presence of the presence of highly fragmented macrofossil material, Adams (1985) inferred Tangaruhe Formation was deposited in an anoxic slope basin.

Dinoflagellate and pollen flora, along with foraminifera and macrofossils indicate a lower Piripauan to lower Haumurian age (Adams, 1985; Moore, 1986). Quantitative biostratigraphic analysis suggests that the disconformity separating Whangai and Tangaruhe Formation at this locality may correlate with the timing of deposition of both Branch Sandstone in Marlborough and the top Glenburn Formation at Angora Stream (Crampton et al., 2006).

2.2.2.3 Whangai Formation (Tinui Group)

Whangai Formation occurs throughout the East Coast region, cropping out on the eastern side of the Adams-Tinui Fault in the southern Wairarapa, but extending westward of the fault north of Mataikona (Lee & Begg, 2002). Whangai Formation overlies Tangaruhe Formation in the west and Glenburn Formation in the east (Lee & Begg, 2002; Moore, 1986).

Whangai Formation is subdivided into three major members (Rakauroa Member, Upper Calcareous Member and Porongahau Member) and two local members (Te Uri and Kirks Breccia members) (Moore, 1988a). According to Moore (1988a), Whangai formation is at least 300m thick at Angora Stream, where the lower part of the succession comprises Rakauroa-like facies. Rakauroa Member typically forms the lowest most portion of the Whangai Formation regionally, with foraminifera and dinoflagellate assemblages mostly yielding a Haumurian age (Field et al., 1997; Moore, 1988a). The base of the unit is thought to be diachronous, however, and in some areas may be Piripauan in age (Field et al., 1997), although Crampton et al. (2006) found no evidence of this.

Moore (1980) tentatively suggested that Whangai Formation, in the Whareama-Ngahape region, was deposited in shelfal conditions with restricted sediment supply, but noted a lack of clear evidence for this. Macro- and microfaunas found in other localities similarly were considered to suggest deposition in a shelfal environment under reducing conditions, indicative of restricted oceanic circulation (Moore, 1988a). This interpretation has since been revised, with studies of foraminifera more commonly indicating deposition at bathyal depths (Leckie et al., 1995; Wilson et al., 1989).

Leckie et al. (1995) suggested that the Rakauroa Member lies unconformably on Glenburn Formation at Angora Stream and is therefore representative of the basal portion of a marine transgression over the Glenburn Formation. Moore's (1988) study of Angora Stream places the lower contact of the Whangai Formation above a ca. four-meter-thick glauconitic sandstone bed, sampling of the base Whangai at this locality indicated a Haumurian-Teurian age. Crampton et al. (2006), followed Moore's (1988) definition and determined a Late Haumurian age for the basal Whangai Formation at Angora Stream.

3 Lithostratigraphy of Branch Sandstone and correlatives

3.1 Introduction

This section describes the results of outcrop studies and grain-size analyses undertaken on rock formations from Branch and Angora streams. A measured section from the Tangaruhe Stream field site is presented. Finally, existing measured section data from Marlborough are collated, showing the known outcrop distribution of Branch Sandstone.

3.2 Methods

3.2.1 Measured sections and sample collection

Stratigraphic sections for the interval of interest were logged at three key localities: Branch Stream, Angora Stream and Tangaruhe Stream. At each site, sections were measured to centimetre resolution using a 30m tape and compass. True stratigraphic thickness was calculated from tape and compass data using a Microsoft Excel macro written by James Crampton. Samples were collected at 0.5m – 0.8m intervals, and adjacent to formation contacts this spacing was reduced to ~0.1m.

3.2.2 Data compilation

There are many existing measured sections of the Late Cretaceous succession in Marlborough. GNS houses a number of these, which were compiled for the Cretaceous-Cenozoic basin analysis project (Field et al., 1997). Data were extracted from these measured sections, including:

- Localities where Branch Sandstone is present;

- Thickness of Branch Sandstone;
- Nature of upper and lower contacts;
- Locations where Branch Sandstone is absent; and
- The juxtaposition of under and overlying formations where Branch Sandstone is absent

These data were compiled in Excel, ArcMap and CorelDraw, and maps and panels of the present day Branch Sandstone distribution were produced.

3.2.3 Grain-size studies

Sandstone samples from both Branch and Angora Streams were analysed for grain-size distribution. These samples were prepared at Victoria University of Wellington, where they were first dried in a 40° oven, and then disaggregated manually using wooden blocks. Next, samples were placed in 50ml tubes and placed in a water bath, where they were treated with 27% hydrogen peroxide to remove organic material. After a period of >24 hours, and once the hydrogen peroxide had stopped reacting with organic compounds, the samples were rinsed and centrifuged in distilled water three times. To remove any carbonate, each sample was next treated with 10% hydrochloric acid for a period of around one hour. Samples were again rinsed and centrifuged in distilled water three times.

Samples were then freeze dried and split using the cone and quartering method, in order to obtain the correct sample volume for analysis (0.1-2 grams). The sediments were then placed in a beaker with 0.5 g/L sodium hexametaphosphate solution, and placed in an ultrasonic bath, where each sample was mechanically stirred and sonicated for 10 minutes. Following this, samples were immediately introduced to the Beckman-Coulter LS 13320 Laser Diffraction Particle Size Analyser for grain-size analysis.

Data outputs from the grain-size analysis are provided in Appendix 1.

3.3 Measured section results

3.3.1 Branch Stream

Branch Sandstone is exposed in the middle limb of Branch Steam (O30/693092). Previous mapping of the Branch Sandstone at this locality (Reay & Strong, 1992) produced a continuous section that indicated the formation is approximately 5m thick. Field work for the present study was undertaken shortly after the 2016 Kaikoura earthquake, and on the true right bank of the river, the base of the formation was obscured by rockfall. The upper 3.5m of the section was recorded and sampled here. The base of the formation was measured and sampled on the true left bank of the river, where a clear section was exposed. Poor accessibility and concerns regarding the stability of the slope on the true left of the river meant it was preferable to measure the majority of the section elsewhere. The measured section presented herein, is therefore a composite section, taken from both sides of the river (Figure 8). Figure 9 and Figure 10 show field photographs from the Branch Stream area.

At Branch Stream, beds strike ~040°, dip 69° to the northwest, and young northwest. Here, Branch Sandstone overlies Herring Formation with sharp contact (Figure 9b). Immediately below the contact, Herring Formation comprises a dark brown – blue grey, finely laminated, mudstone. Further down-section, Herring Formation becomes a dominantly dark to light grey jarositic siltstone and fine sandstone that displays both planar lamination and flaser bedding at a centimetre scale (Figure 10b). Additionally, numerous metre to decimetre long sandstone dykes are observed within the Herring Formation (Figure 10c).

Branch Sandstone is a predominantly massive, cream coloured, moderately indurated, quartzo-feldspathic, fine grained sandstone with common glauconite. The upper ~70cm of Branch Sandstone is increasingly carbonaceous, silt rich and finely laminated (Figure 9b). A ~10cm clay-rich horizon is present at the top of Branch Sandstone, which is overlain with sharp contact by Mead Hill Formation.

Mead Hill Formation comprises dark to very light grey, well bedded, chert-rich limestone. On the true left bank of the river, the silt and clay rich layer at the top of Branch Sandstone forms a wedge shaped horizon (Figure 9d). The character of this outcrop appears to differ from that of the corresponding section on the true right bank of the river, and it is possible that the upper contact is faulted.

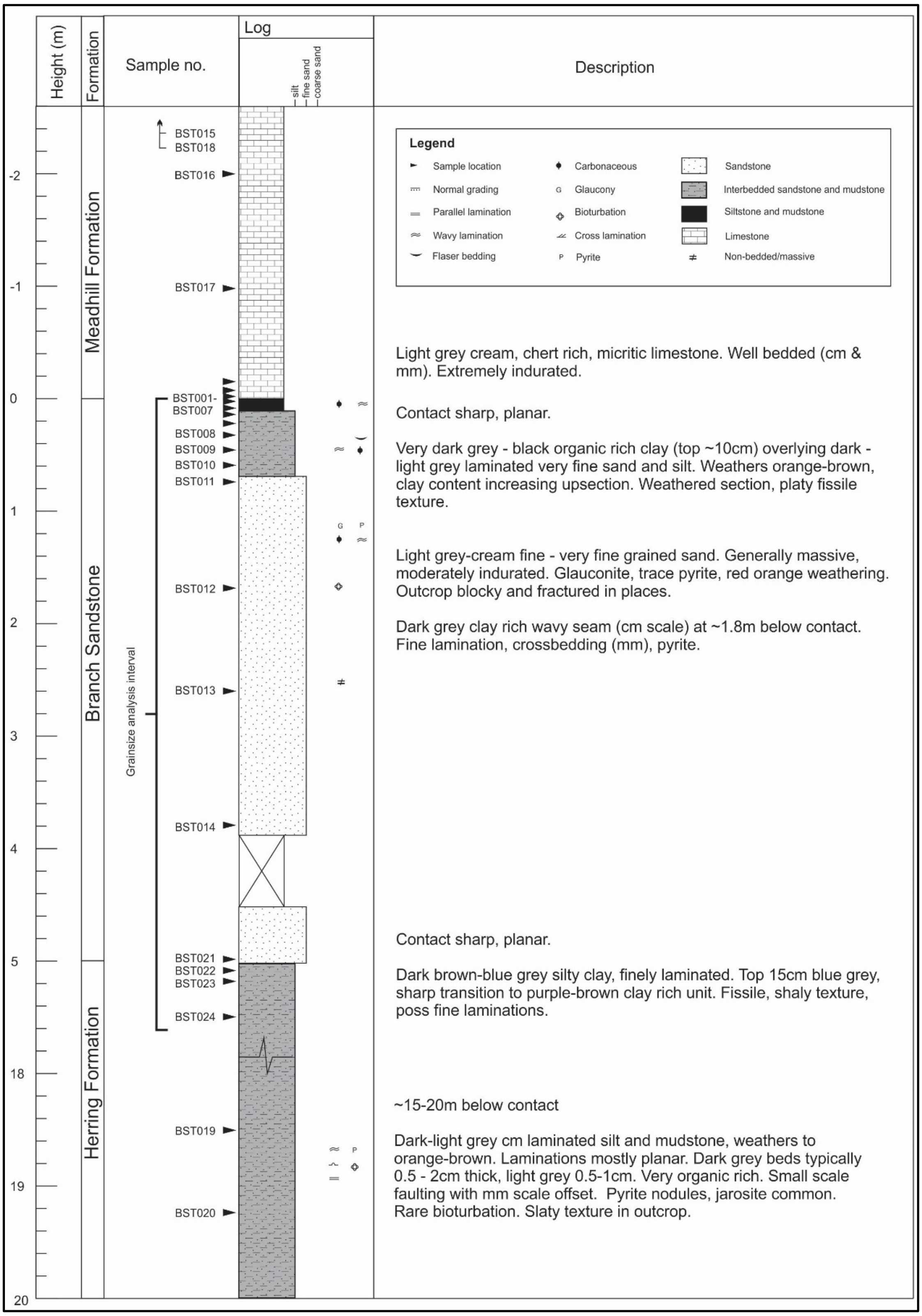

Figure 8. Composite measured section from Branch Stream (O30/693092)

a) Upper contact of Branch Sandstone, showing carbonaceous and silt rich upper section. Light coloured sediments (right) are base Mead Hill Formation. Exposure on true right bank of Branch Stream

b) Lower contact of Branch Sandstone, exposed on true left bank of Branch Stream. Light (cream) coloured rock (left) is base Branch Sandstone. Dark grey to purple mud-rich facies (right) are taken to mark the upper Herring Formation.

c) Very fine scale lamination near top Branch Sandstone, true right bank Branch Stream

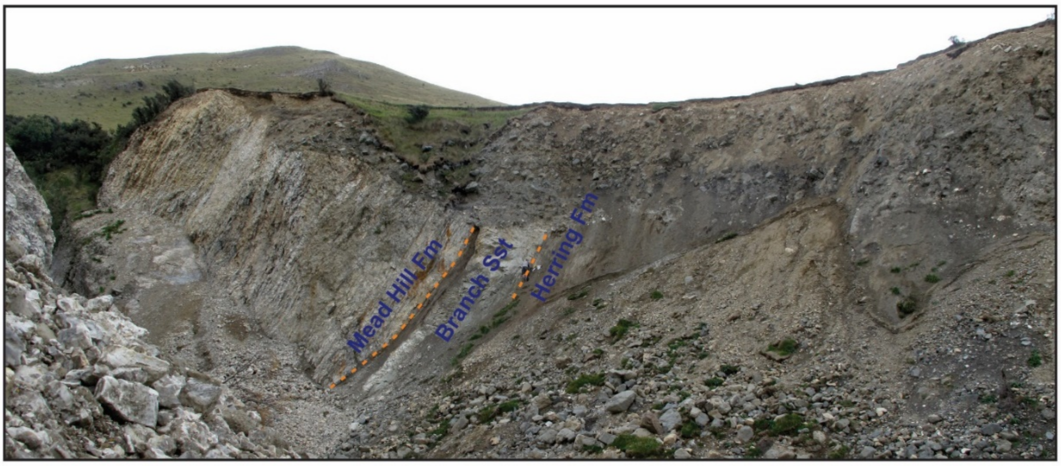

d) Looking upstream, showing Branch Sandstone exposure on true left bank of the river.
Note the dark horizon immediately above unit, which is wedge shaped in outcrop. Additionally, this image demonstrates the volume of loose debris in the valley, which obscured the lower contact of Branch Sandstone on the true right bank.

Figure 9. Images from Branch Stream. See figure text for related captions.

a) Massive character of Branch Sandstone, true left bank of the river. Rock formations young toward the left. Person is 1.6m tall. Photo from J. Crampton.

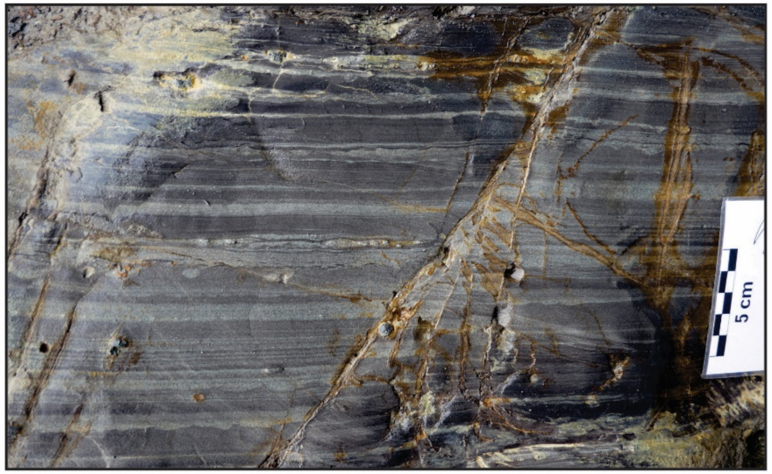

b) Example of planar lamination and wavy/flaser bedding in the Herring Formation, true right bank of Branch Stream, ~20m below the lower contact of Branch Sandstone. Photo from J. Crampton.

c) Metre scale sandstone dyke, intruded in Herring Formation, on true left bank of Branch Stream. Dyke width is approximately 30-50cm. Image courtesy of James Crampton, taken from true right bank, looking across the river valley.

Figure 10. Images from Branch Stream. See figure text for related captions.

3.3.1.1 Grain-size analysis

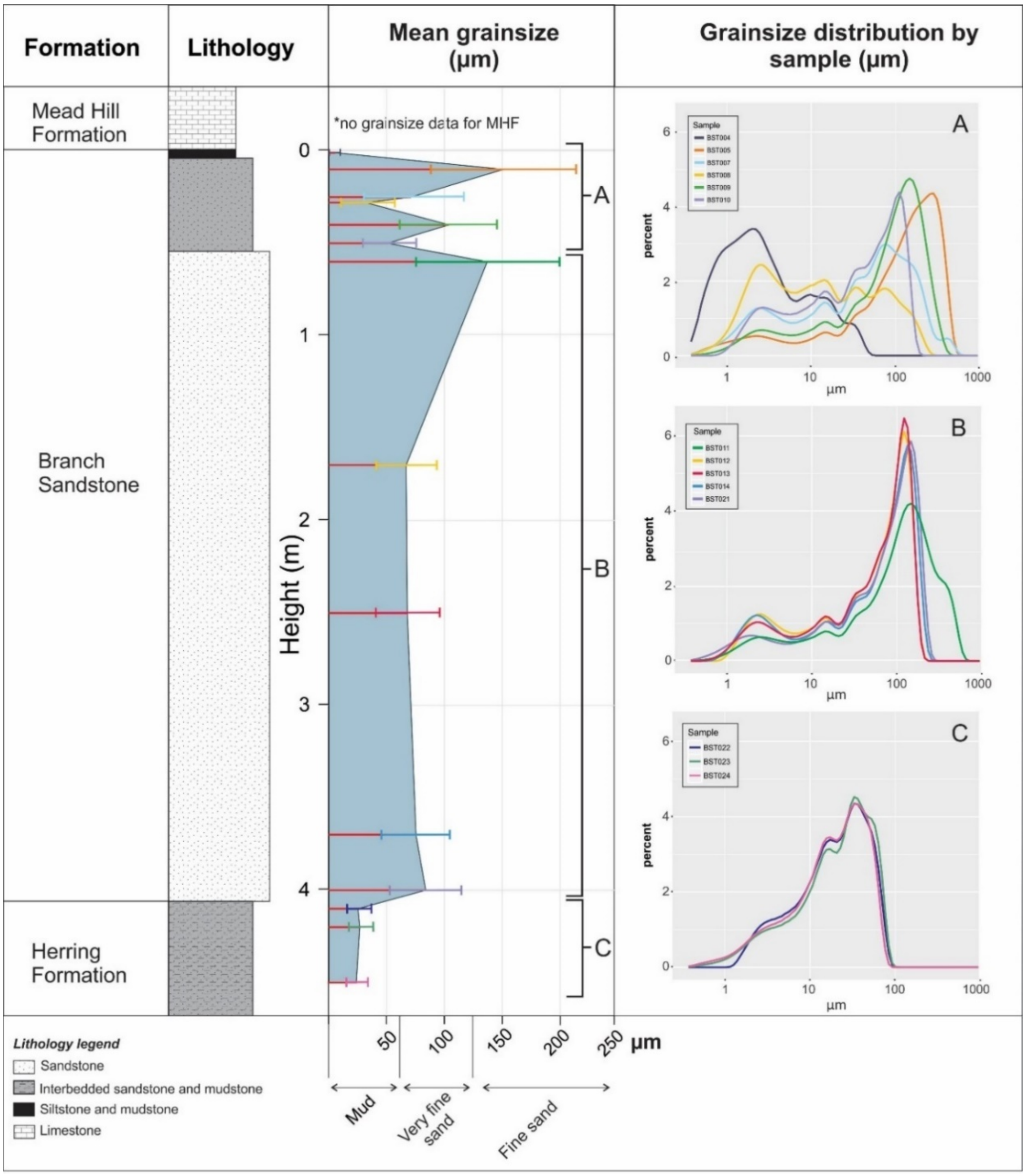

Figure 11. Results of laser particle size analysis of Branch Sandstone. Error bars indicated on mean grain-size column represent standard deviation of each sample. Graphs on right-hand side of figure indicate grain-size distribution from each sample.

At the Branch Stream locality, laser particle grain-size analysis shows that Branch Sandstone dominantly comprises a mud-rich, very fine, moderately sorted sandstone (Figure 11). The uppermost Herring Formation is relatively fine grained in comparison, dominantly comprising silt-sized particles.

Broadly, the massive portion of Branch Sandstone exhibits a skewed profile (Figure 11B), with a pronounced peak of fine grained sand sized particles at around 100µm and long tail of silt sized material. The upper ~70cm of Branch Sandstone comprises a interbedded mudstone and very fine to fine sandstone. Fluctuating grain-size and mudstone content is quantified by the laser particle grain-size analysis, which shows variance in sand content between 25% and 75% (Figure 11A). The uppermost sample, which is extracted from the horizon immediately below the Mead Hill Formation, is a very fine silt to clay-rich lithology.

3.3.2 Angora Stream

A thick sandstone bed (sandstone A) is exposed in Angora Stream at the top of the Glenburn Formation. A measured section encompassing this bed and parts of the under and overlying units is presented in Figure 12. Figure 13 includes field photographs of important features.

Within the Angora Stream section, beds strike 155°, dip 86° to the southwest, and young to the southwest. Glenburn Formation is composed of centimetre to decimetre interbedded sandstone and laminated mudstone containing approximately 30% sandstone. A thin (~15cm) layer of organic rich mudstone is present immediately below sandstone A.

Sandstone A comprises light grey, mostly massive, medium-fine grained, glauconitic, moderately well sorted sandstone. Within ca. 1 metre of the base, the unit is moderately indurated and finely laminated. The top ~50cm of sandstone A is faintly laminated, and becomes increasingly silt rich before grading into a ~30cm horizon of blue grey mudstone.

Whangai Formation overlies sandstone A with gradational contact. At this locality Whangai Formation comprises a micaceous dark-light grey interbedded silt and fine sandstone. It is slightly calcareous, bioturbated and displays localised centimetre scale cross bedding toward the base.

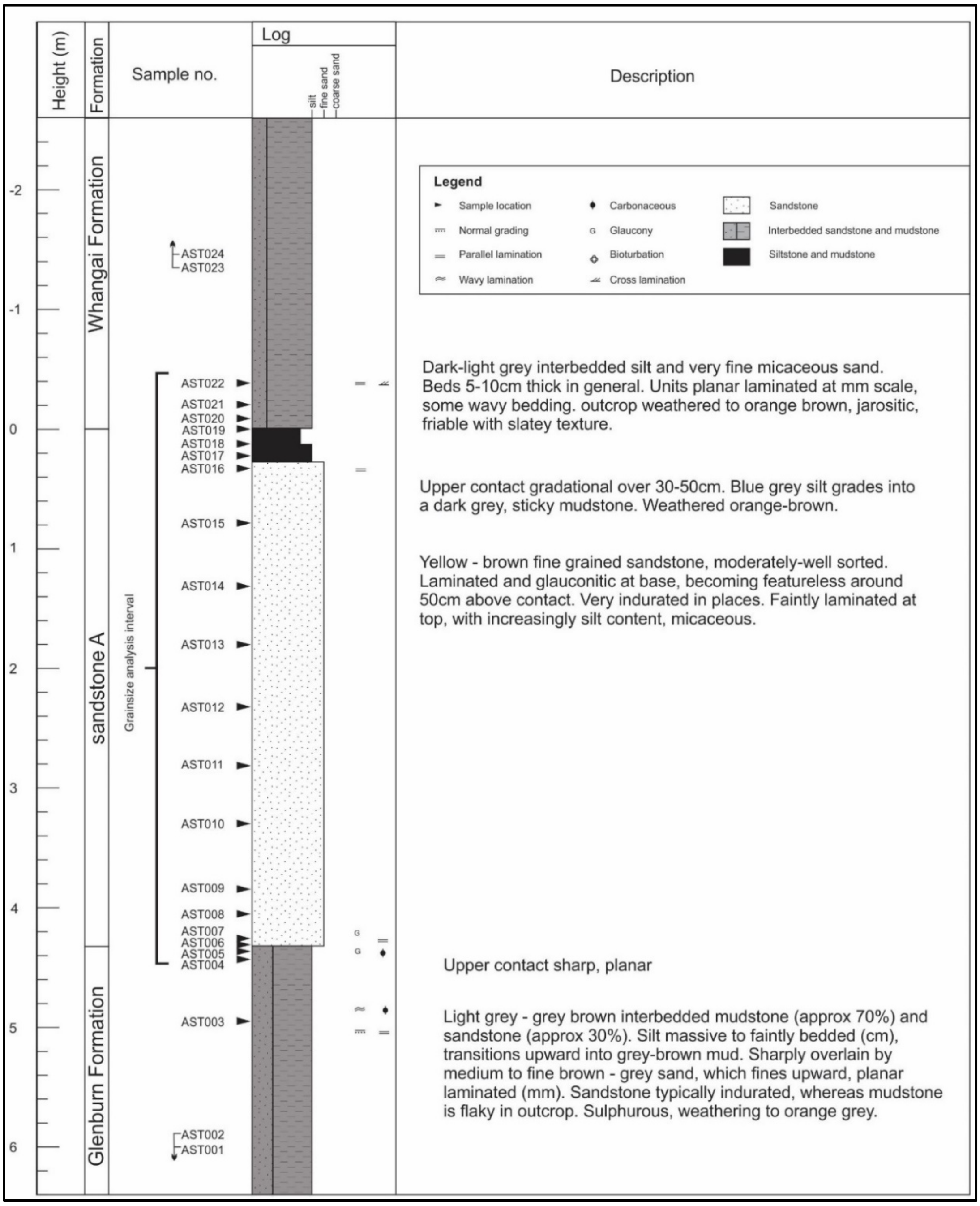

Figure 12. Measured section, Angora Stream (U24/051784).

a) Image taken looking upstream at Angora Stream. The base of sandstone A is indicated by the pale blue dashed polygon on the right hand side of the image.

b) Upper contact of sandstone A on the true left bank of Angora Stream.

The sandstone A-Whangai contact is delineated by the dashed blue line. Note blue-grey mudstone facies immediately below the contact. Beds dip to the southwest and young to the left (upstream in (a)).

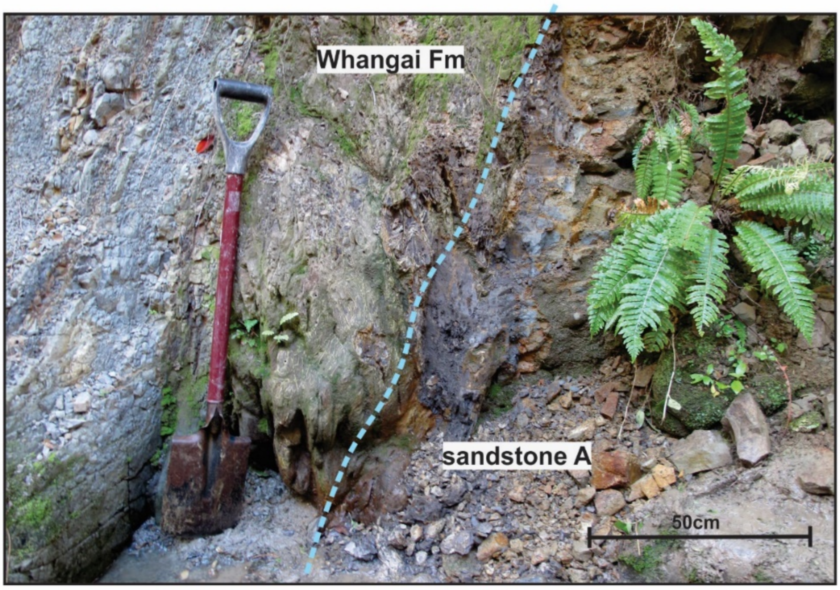

Figure 13. Images from Angora Stream. See figure text for related captions.

3.3.2.1 Grain-size analysis

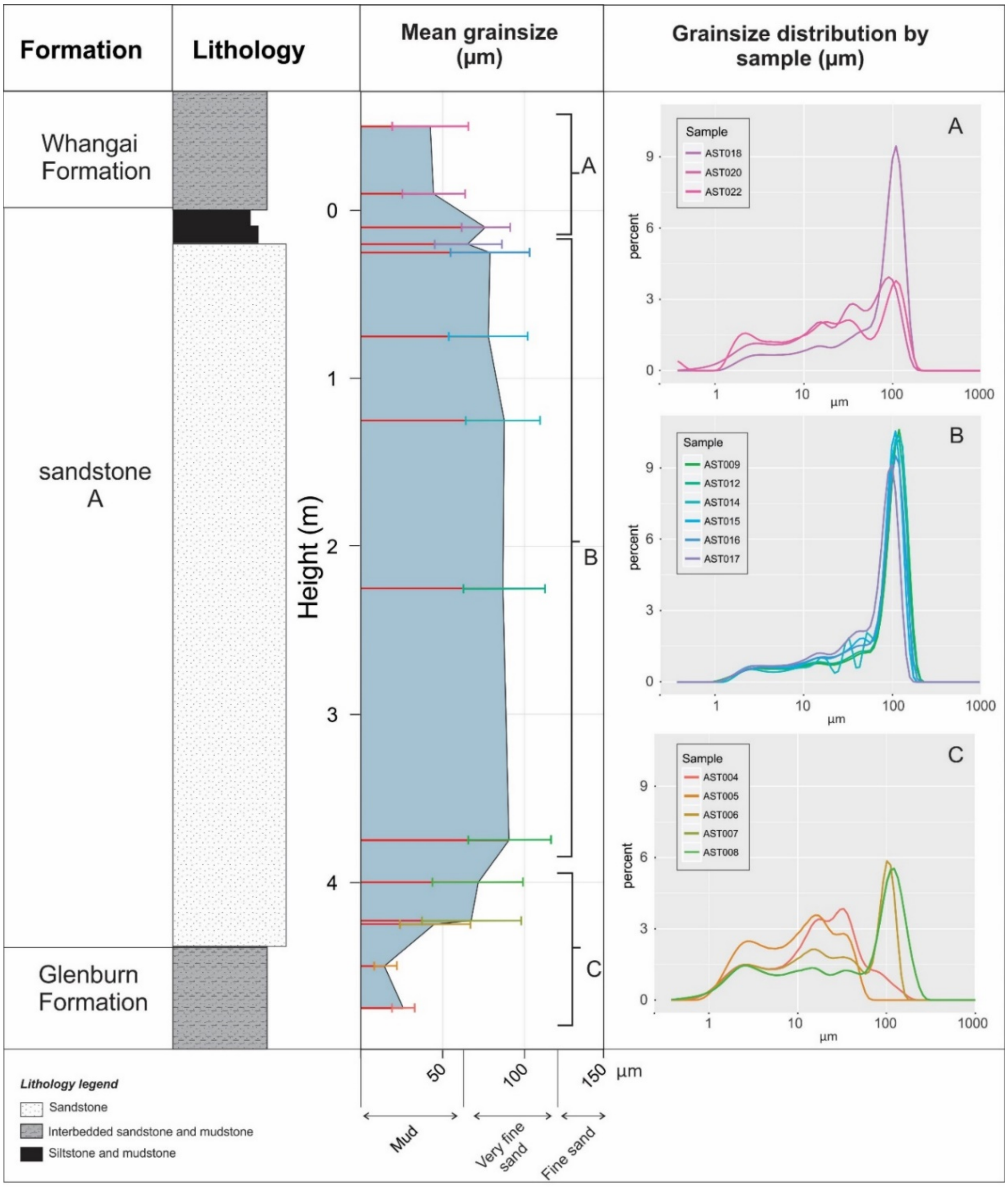

Figure 14. Results of laser particle size analysis of sandstone A from Angora Stream. Error bars indicated on mean grain-size column represent standard deviation of each sample. Graphs on right-hand side of figure indicate grain-size distribution from each sample.

Results from laser particle grain-size analysis of sandstone A at Angora Stream are shown in Figure 14. This analysis shows that sanstone A is a moderately well sorted very fine sandstone, that fines upward. Glenburn Formation immediately underlying the sandstone is fine grained in comparison, dominantly comprising silt with a significant clay fraction. Overlying Whangai Formation is dominantly a mudstone facies, comprising approximately 30% sand overall.

The grain-size distribution plot for Glenburn Formation sandstone displayed in Figure 14B shows that samples exhibit a broadly unimodal distribution, with a distinct peak at around 100µm, comprising around 9% of the volume for each sample. Two samples from the very base of Glenburn Formation sandstone facies (AST007, AST008) exhibit a less pronounced peak, and contain a greater fraction of mud-sized grains (Figure 14C).

3.3.3 Tangaruhe Stream

At Tangaruhe Stream, Whangai Formation unconformably overlies Tangaruhe Formation. A measured section through this unconformity is presented in Figure 15 and field photographs are shown in Figure 16. Tangaruhe Stream flows approximately perpendicular to a north-south trending anticline, where, in the past the Tangaruhe-Whangai contact has repeated in the stream, although the eastern occurrence is not exposed at the present time (c.f. Adams, 1985; Crampton, 1997; Moore, 1988a). The section presented here was therefore measured on the western limb of the anticline but due to poor exposure, comprises a composite section from both the true left and right river banks. Supplementary information from Crampton (1997) is incorporated into the description set out below.

Uppermost Tangaruhe Formation at Tangaruhe Stream comprises a hard, featureless, dark grey, micaceous mudstone, containing sparse concretions. The upper contact is poorly exposed, but is sharp and likely exhibits minor undulation. Overlying Whangai Formation is a well indurated, highly weathered siltstone with minor sand content. The primary aim at this section is to constrain the timing of the unconformity between the Tangaruhe and Whangai Formation. Because of this, the fact there is no sand to evaluate, and the well indurated nature of Whangai Formation, grain-size analyses were not undertaken for this section.

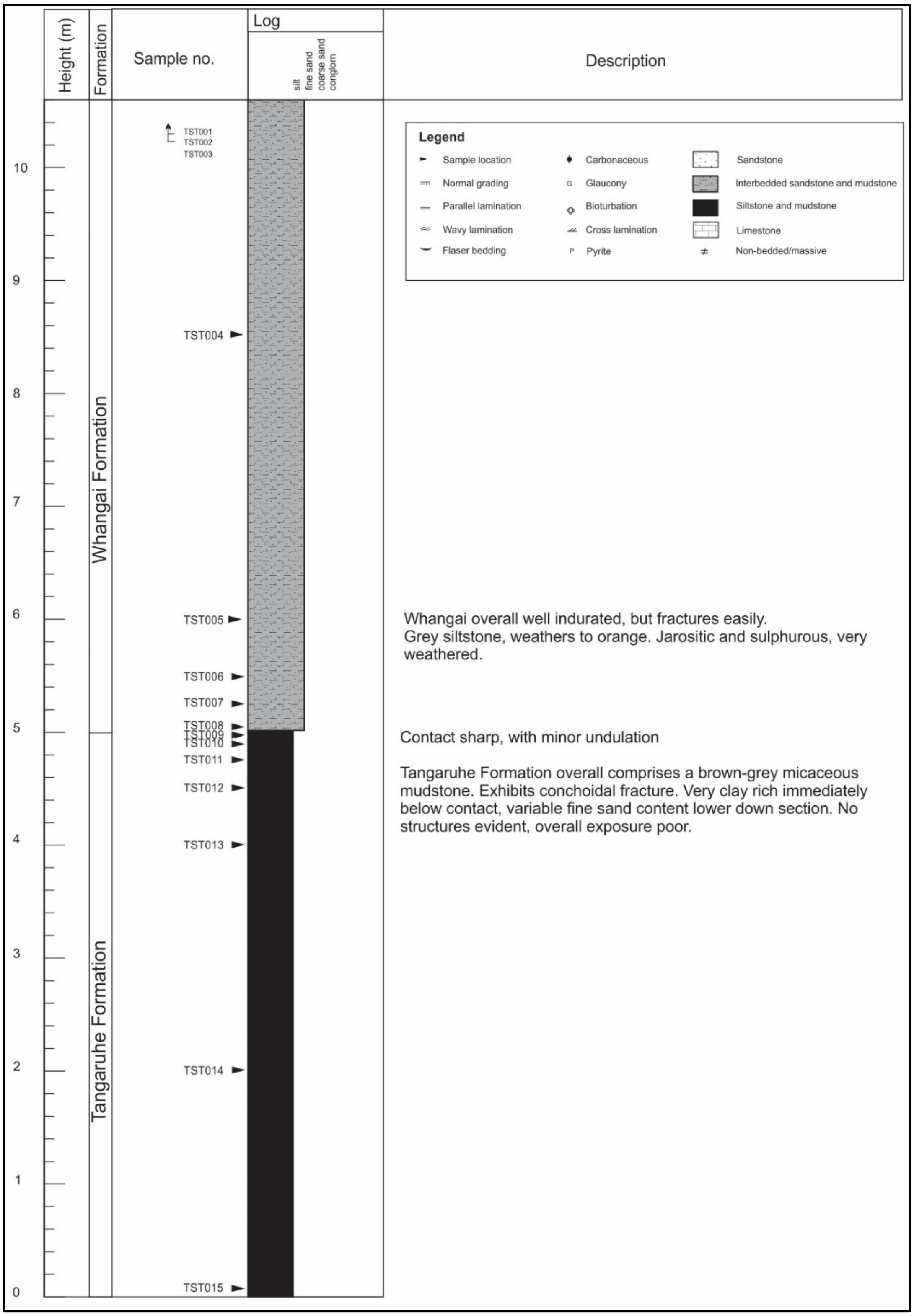

Figure 15. Measured section, Tangaruhe Stream (U24/010988).

a) True left bank of Tangaruhe Stream, on the western limb of the anticline. The section was overall very poorly exposed, due to the proliferation of vegetation on the river banks. The Tangaruhe-Whangai contact is delineated by the dashed blue line, whilst the red box indicates the extent of the image below (b).

b) Close up view of contact (pale blue dashed line) between Tangaruhe and Whangai Formations at Tangaruhe Stream, on western limb of anticline.

c) Whangai Formation outcrop ca~ 2m upstream from Tangaruhe-Whangai contact on true left bank of river.

d) Tangaruhe Formation around 50cm downstream of the Tangaruhe-Whangai contact on true left bank of river.

Figure 16. Images from Tangaruhe Stream. See figure text for related captions.

3.4 Regional distribution and paleogeography – Branch Sandstone

Section 3.4 describes the results from compilation of regional stratigraphic sections in the wider Marlborough region. This compilation aims to develop an understanding of the regional distribution of Branch Sandstone, as well as the paleogeography of southeastern Marlborough in the Late Cretaceous.

According to palinspastic reconstructions, and paleogeographic mapping, by the end Cretaceous southeast Marlborough formed a paleo-embayment on the north facing coast of proto-Zealandia (Crampton et al., 2003; King et al., 1999). At this time, the area that comprises the modern-day lower East Coast of the North Island is believed to have been immediately adjacent to Marlborough in the paleowest, with the Chatham Rise extending to the east (Figure 17).

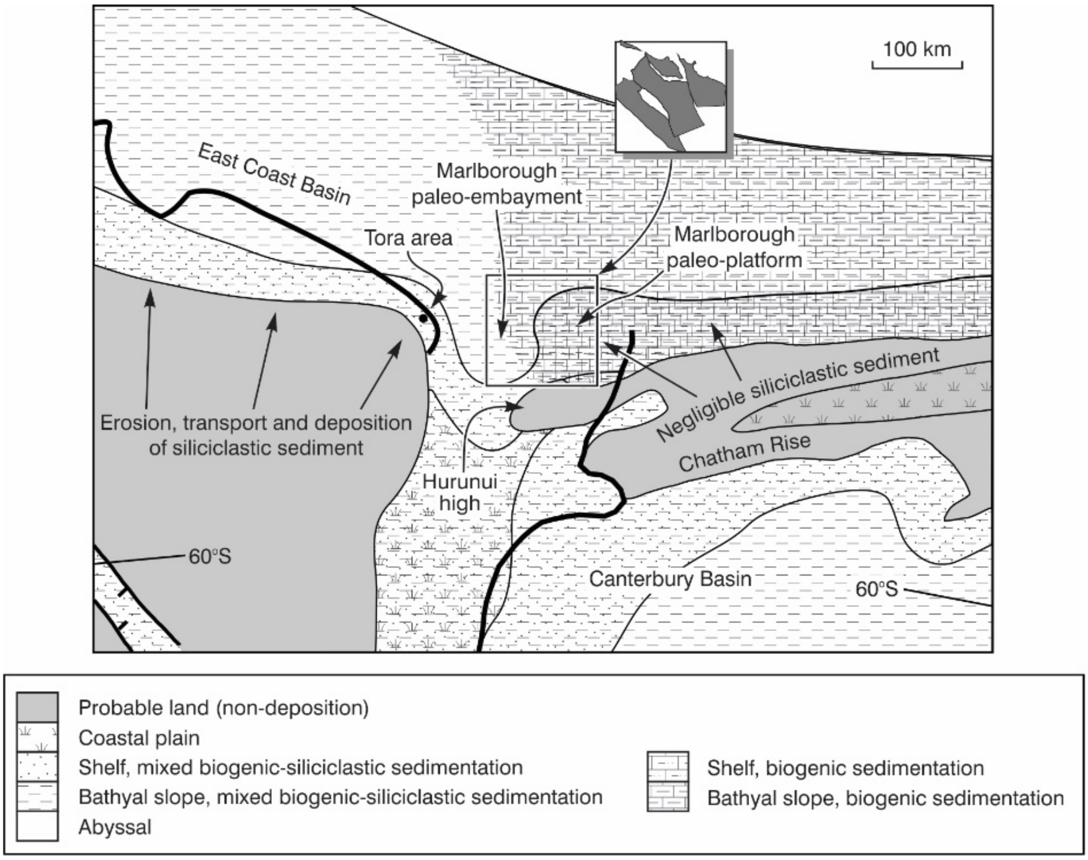

Figure 17. Paleogeography of the East Coast region, ca 65Ma. From Crampton (2003), which incorporates data from Sutherland et al. (2001) and King et al. (1999).

Isopachs show a marked thickening of both Herring Formation and Mead Hill Formation in the northeast Clarence Valley (Laird, 1992; Morris, 1987; Reay, 1993). Paleomagnetic data indicates that Cretaceous and Paleocene sediments in Marlborough have undergone clockwise rotation up to, and in excess of 100°, to attain their present day position (Townsend, 2001). Palinspastic reconstructions for the same time period therefore display thickening to the paleo north-west (Crampton et al., 2003). Additionally, paleobathymetric data incorporated into the reconstruction of Crampton et al. (2003) is indicative of southward-progressing marine transgression.

The palinspastic reconstructions of Crampton et al. (2003) are shown in Figure 16 (Herring Formation) and Figure 17 (Mead Hill Formation). In these diagrams, the grey blocks are major fault-bounded structural blocks from the southeast Marlborough region. White space indicates the area/volume that has been consumed during localized compression, uplift and erosion along the major faults during Neogene evolution of the modern plate boundary. Additionally, blocks have been moved horizontally with respect to each other to account for Neogene strike-slip motion on faults, rotated to account for vertical-axis rotations, and stretched internally to account for plastic, within-block deformation. Further details are available from Crampton et al. (2003).

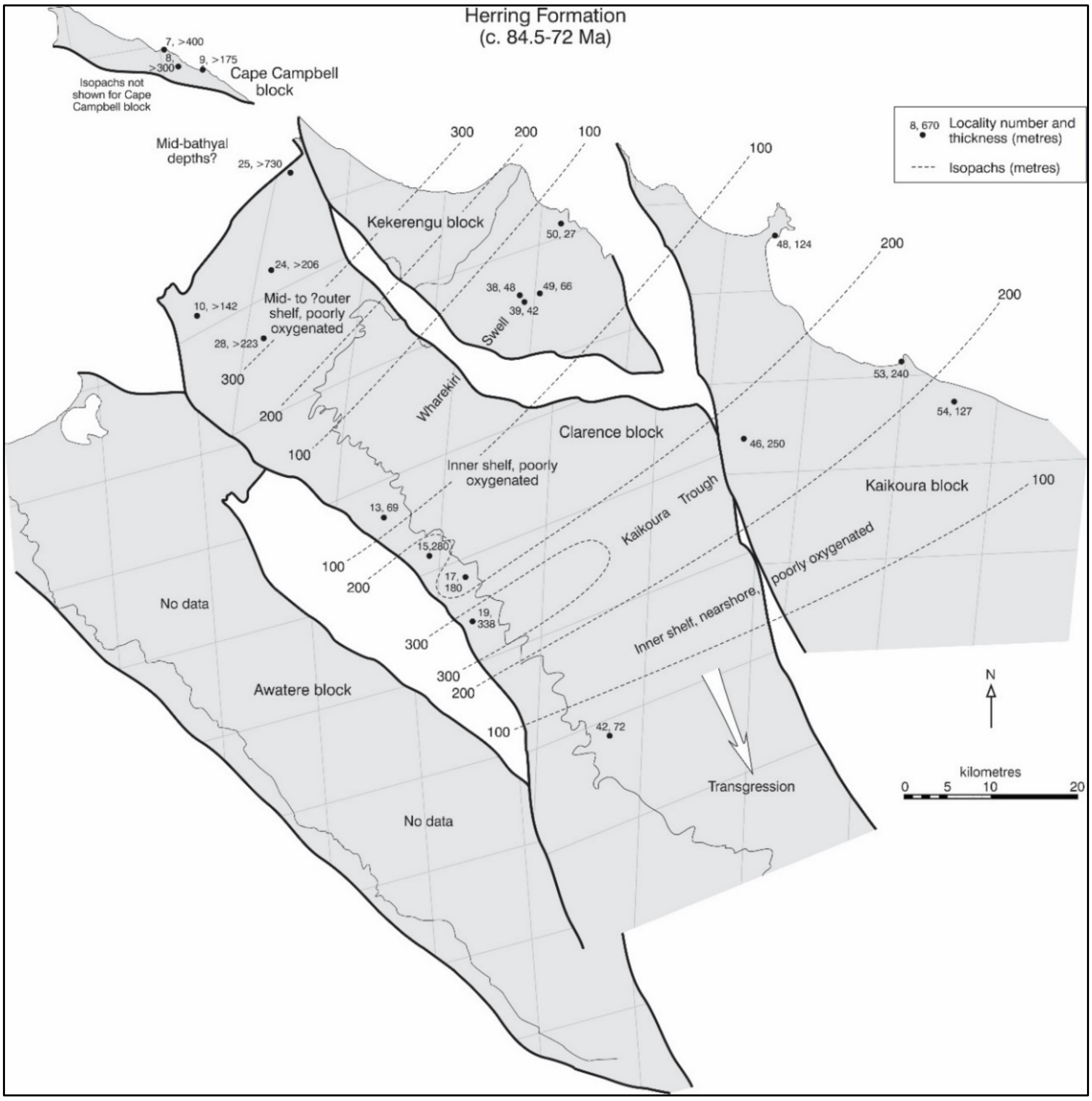

Figure 18. Palinspastic reconstruction of SE Marlborough, showing distribution and thickness of Herring Formation, along with interpretation of depositional environment (Crampton et al., 2003)

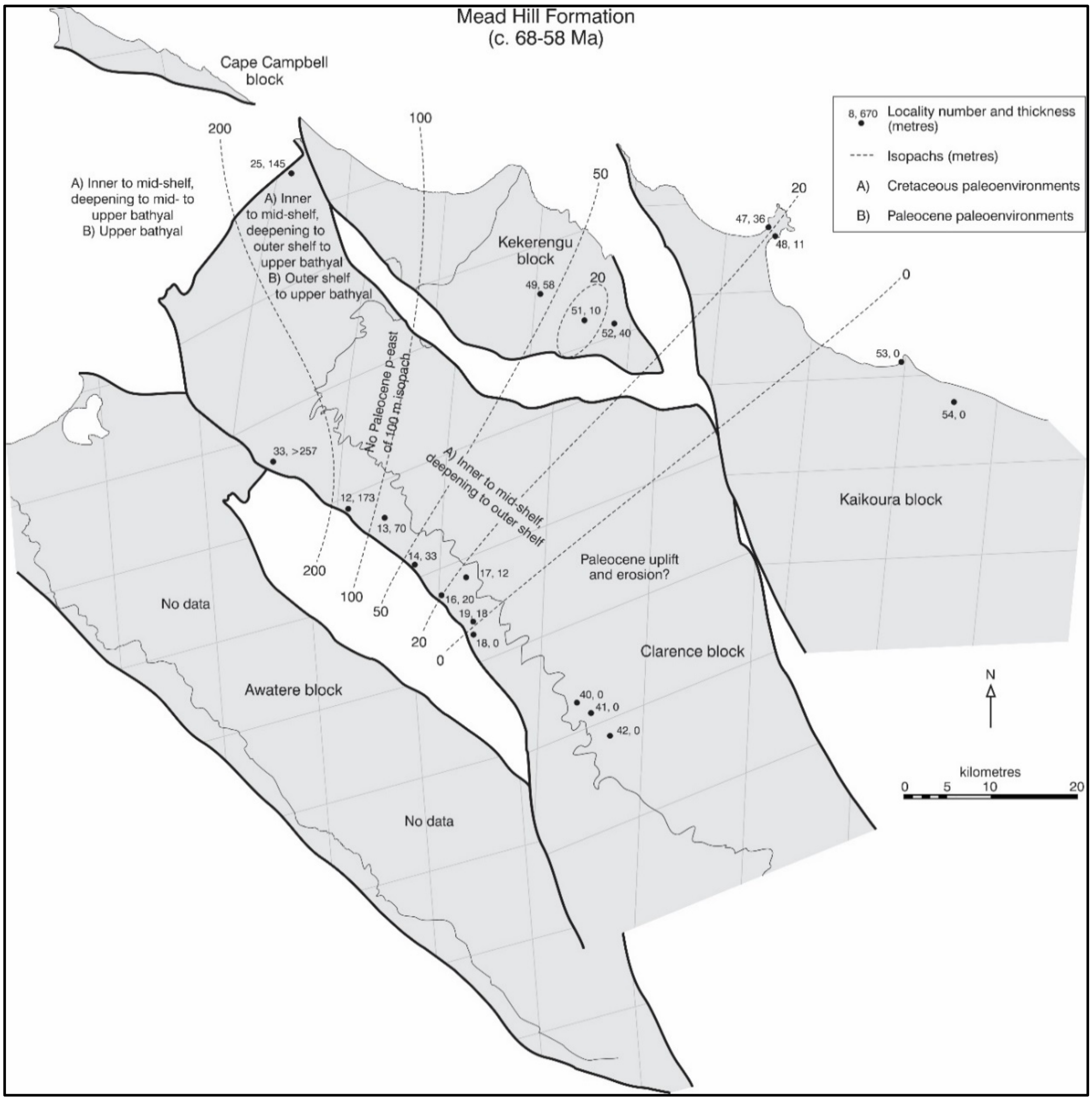

Figure 19. Palinspastic reconstruction of SE Marlborough, showing distribution and thickness of Mead Hill Formation, along with interpretation of depositional environment (Crampton et al., 2003)

Thickness data for Branch Sandstone, compiled from legacy stratigraphic columns (Table 2), is overlaid on the palinspastic reconstruction of Crampton et al. (2003) in Figure 20. The data show that Branch Sandstone is not present paleo-northwest of Dee Stream. Branch Sandstone thickness is variable within the Clarence block, but nowhere exceeds 12m. In the Kekerengu block, Branch Sandstone thickness ranges from a minimum of 3m in the headwaters of Limestone Stream, to a maximum of 42m at Puhi Puhi River, over a distance of ~5km.

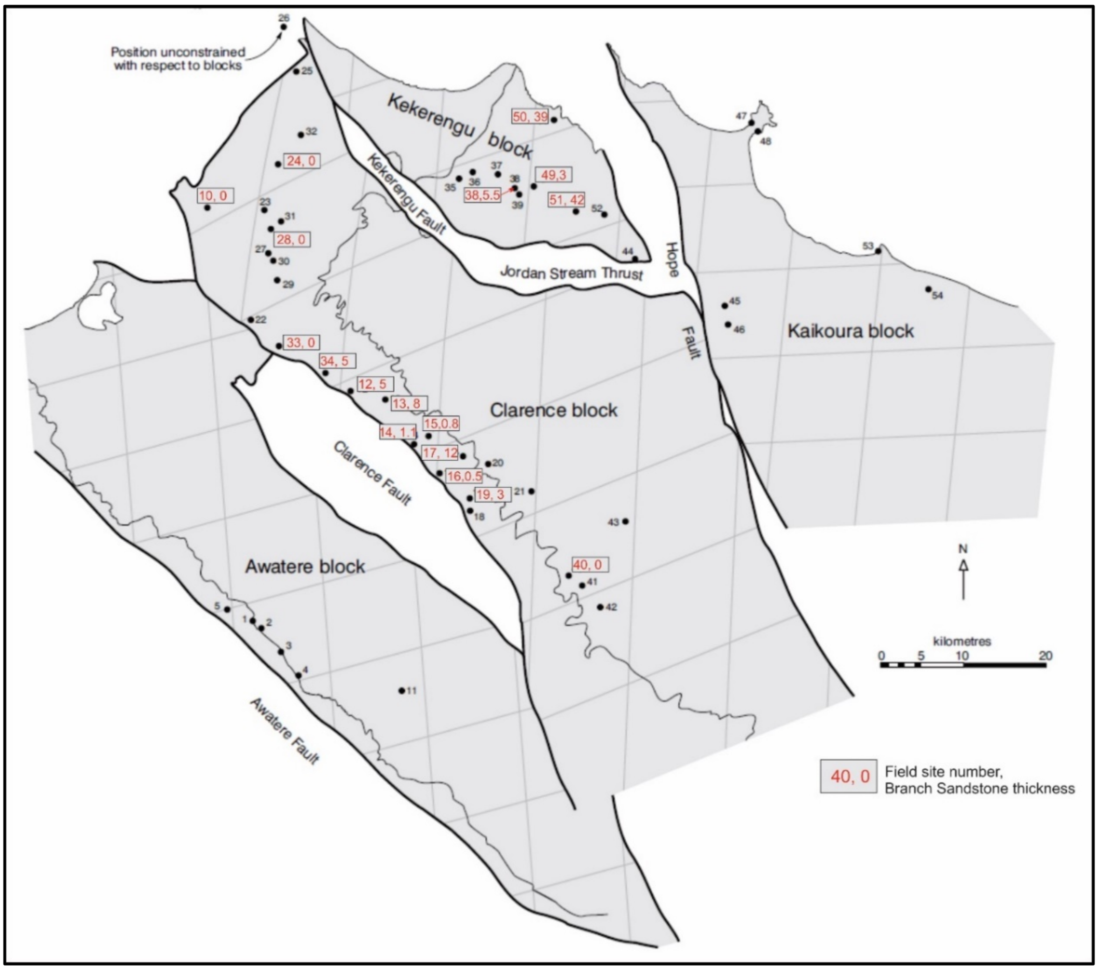

Figure 20. Palinspastic reconstruction of Crampton (2003), showing thickness of Branch Sandstone at various outcrop locations in the Marlborough region. Summary of thicknesses is shown in Table 2, along with references.

Table 2. Summary of measured sections compiled from CCP data. Crampton (2003) location no. refers to section reference on Figure 18, Figure 19, and Figure 20. Present day distribution of sections is shown in Figure 21.

Measured section name	Map sheet	CCP column no.	Crampton (2003) location no.	Grid ref y (Field et al., 1997)	Grid ref x (Field et al., 1997)	Easting (NZTM)	Northing (NZTM)	Branch Sandstone thickness	Measured section reference
Isolation Creek	P29	21	10	9163	2257	1681610.62	5360880.33	0	Schioler et al., 1996
Branch Stream Middle	O30	7	12	6940	0920	1659384.61	5347518.01	5	Strong et al., 1984
Dart Stream	O30	2	13	6740	0470	1657384.42	5343019.75	8	Morris, 1984
Muzzle Stream Paleogene	O30	10	14	6140	0240	1651385.94	5340721.43	1.1	Morris, 1984
Dead Horse Gullly & Muzzle Stream	O30	9	15	6200	0110	1651985.52	5339421.76	0.8	Morris, 1987
Bluff Stream, Upper	O30	3	16	5760	9990	1647586.76	5338222.82	0.5	Morris, 1984
Bluff Stream, lower	O30	1	17	5900	9730	1648985.83	5335623.48	12	Morris, 1984
Bluff River	O30	5	19	5400	9570	1643987.25	5334024.77	3	Morris, 1984
Benmore Stream, upper reaches	P30	14	24	9200	1860	1681979.77	5356911.4	0	Laird, 1991
Woodside Creek	P30	5	25	9750	1880	1687478.31	5357110.38	0	Laird, 1991
Whernside, south flanks	P30	7	28	8640	1810	1676381.23	5356412.51	0	Laird, 1991
Mead Stream, main branch	P30	6	33	7622	1606	1666203.78	5354374.8	0	Morris, 1987
Dee Stream	P30	8	34	7110	1130	1661084.46	5349617.08	5	Morris, 1987
Limestone & Wharekiri Streams	P30	10	38	7690	9180	1666878.96	5330122.39	5.5	Laird et al., 1981
Seymour Stream, southern limb	O31	8	40	4240	8590	1632389.66	5324229.82	0	Morris, 1985
Wallow Stream	O31	5	42	3880	8310	1628790.48	5321431.32	10+	Laird & Thrasher, 1990
Kaikoura Peninsula - Southside	O31	1	48	6610	6470	1656077.6	5303033.48	0	Browne, 1981
Kaikoura Peninsula - north side	O31	11	47	6740	6560	1657377.3	5303932.94	11	Morris, 1984
Headwaters of Limestone stream	P31	3	49	7660	8950	1666578.6	5327823.2	2	Laird, 1984
Mororimu Stream - Waipapa Bay	P31	2	50	8130	8860	1671276.95	5326922.65	38	Morris, 1984
Jordan Stream - Puhi Puhi River	P31	4	51	7240	8490	1662379.09	5323225.47	42	Morris, 1985

Thickness data are also plotted along three transects in Figure 22, Figure 23, and Figure 24 in an attempt to distinguish any geographic trend in Branch Sandstone distribution. Overall, these figures indicate that Branch Sandstone thickness is variable, but is lowest in the Clarence valley and greatest to the paleo-northeast. The modern day location of these transects is shown in Figure 21.

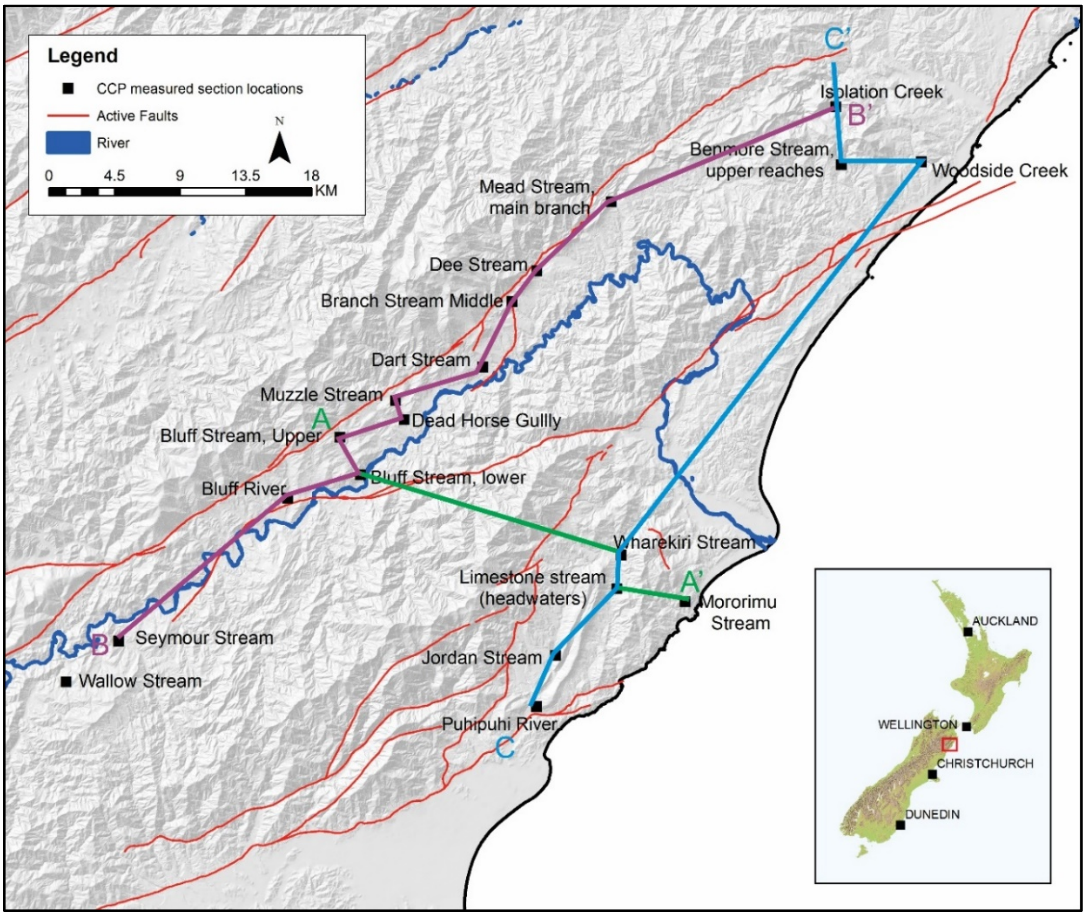

Figure 21. Modern geographic distribution of thickness transects shown in Figs 22-24.

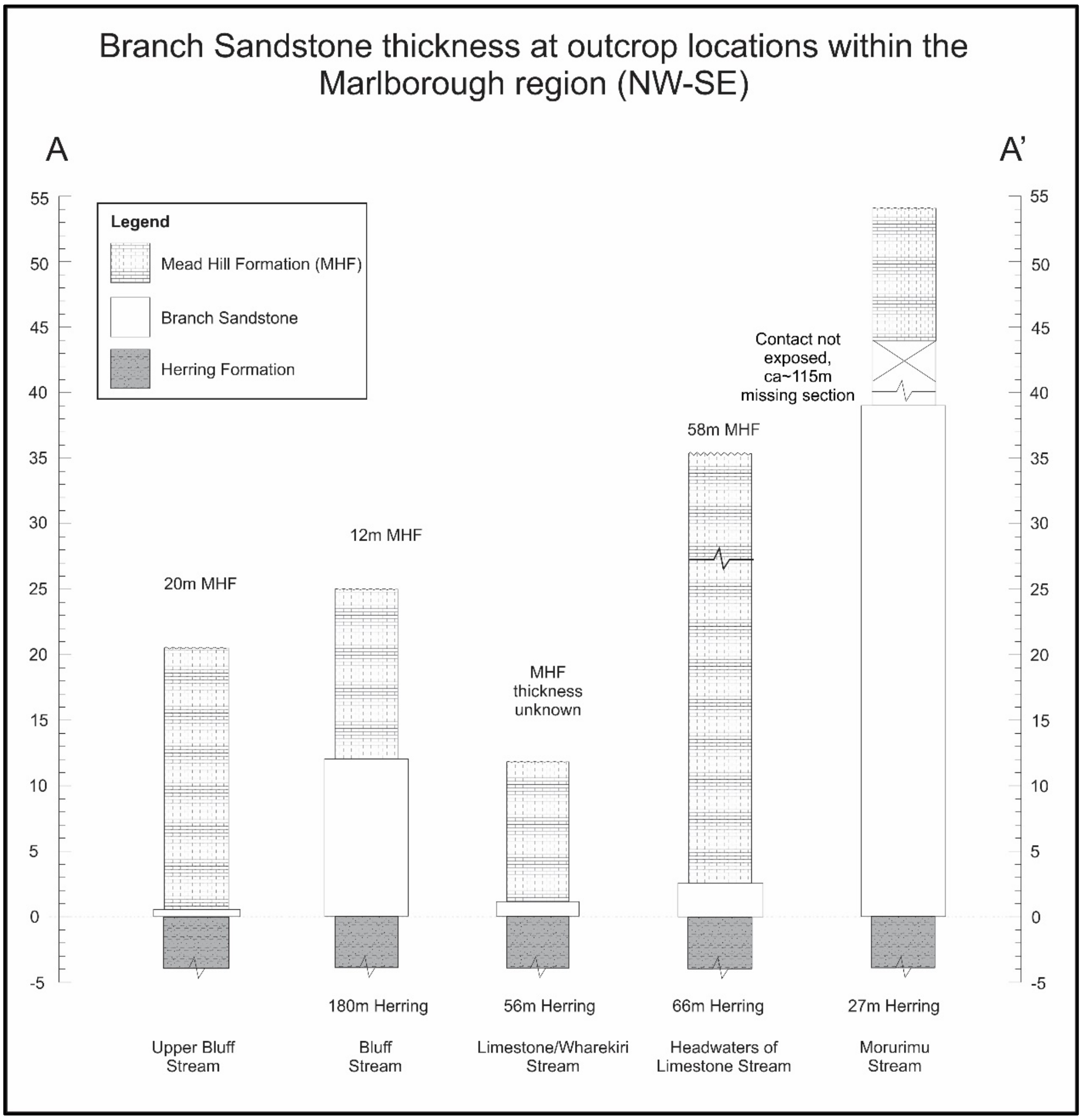

Figure 22. Branch Sandstone thickness, Clarence and Kekerengu blocks.

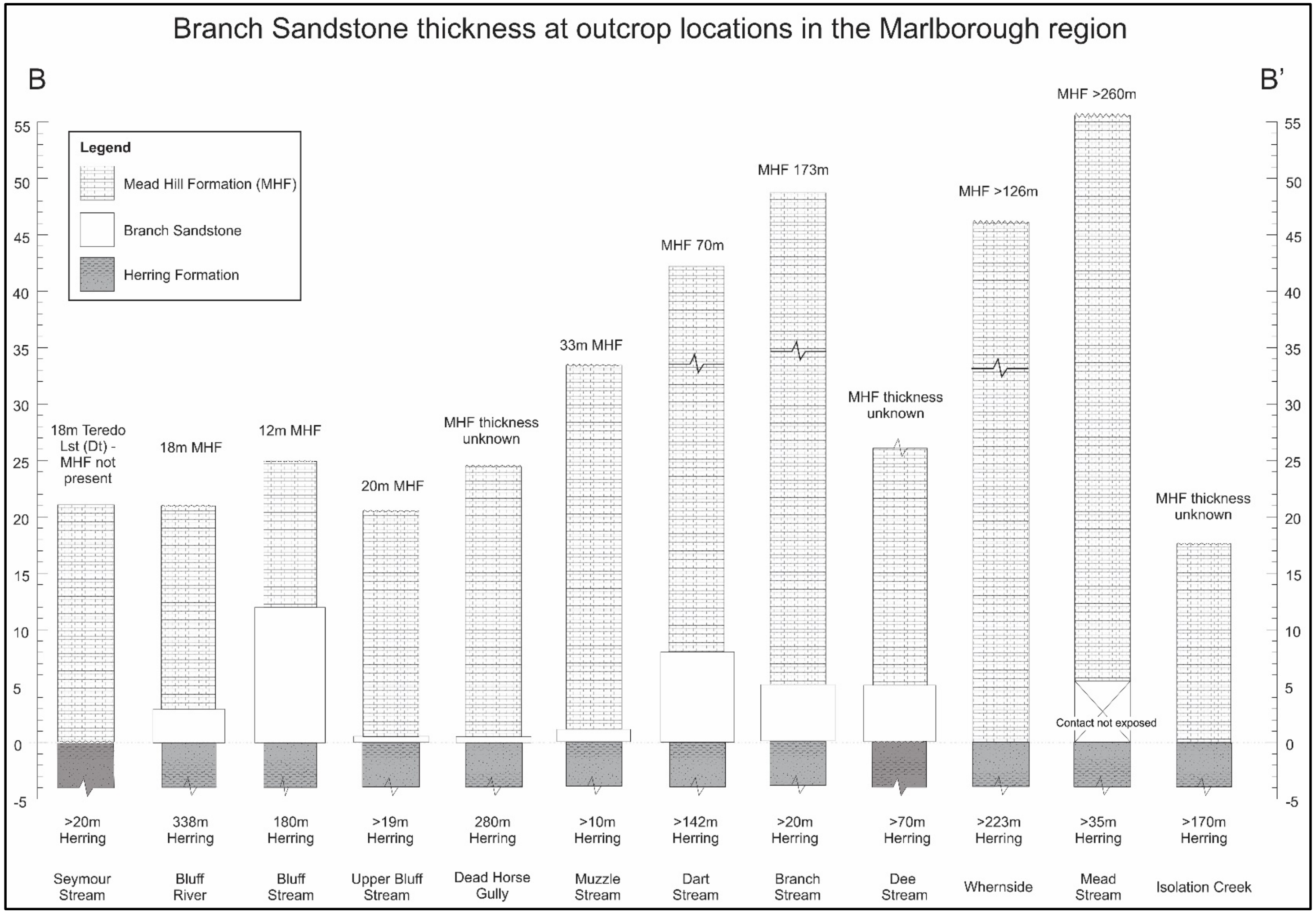

Figure 23. Branch Sandstone thickness Clarence Fault Block.

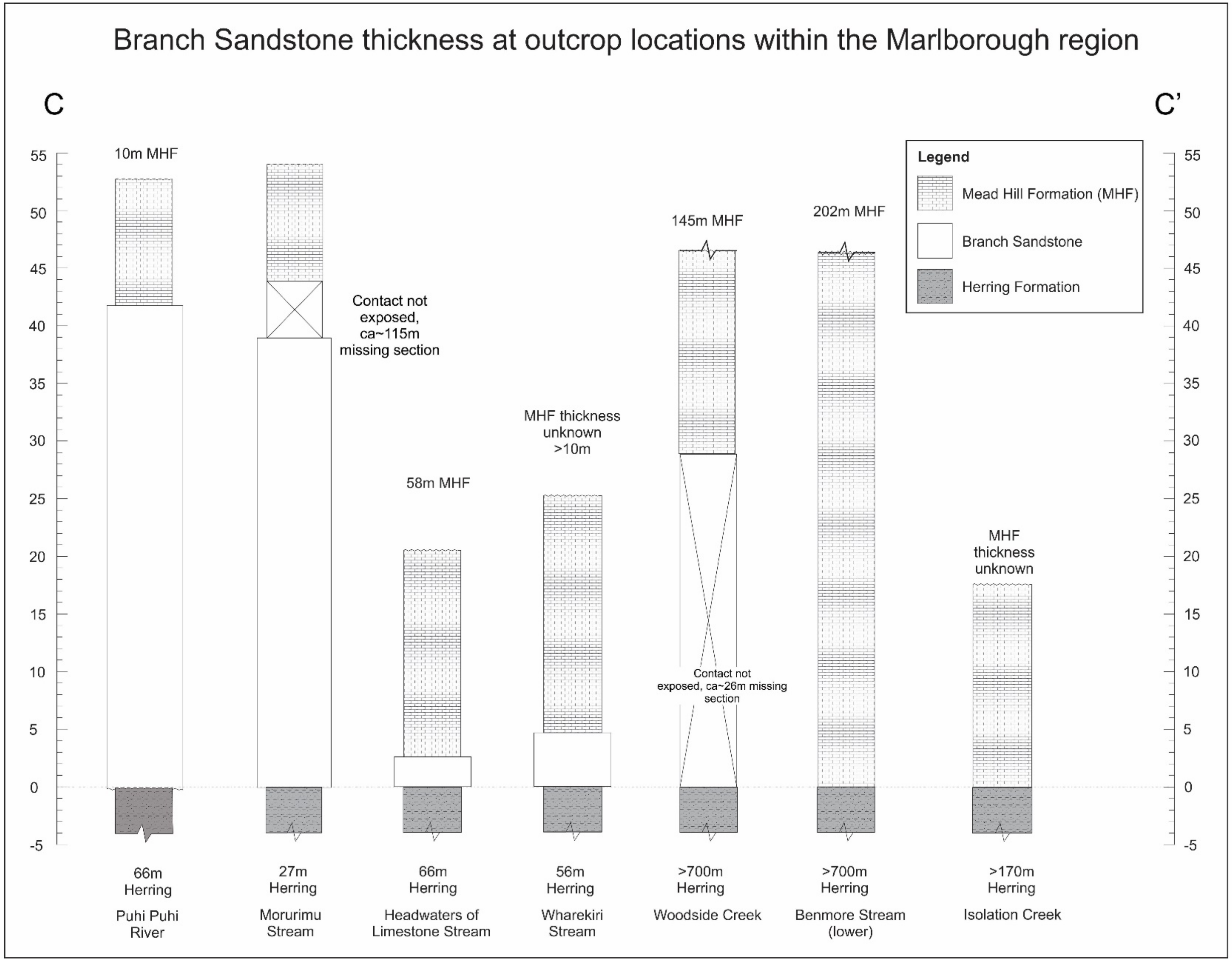

Figure 24. Branch Sandstone thickness, Clarence and Kekerengu fault blocks.

4 Biostratigraphy

4.1 Introduction and aims

To understand the depositional history of the sections documented herein, age control is required. A number of studies have previously analysed the biostratigraphy of the Mead Hill, Whangai and Herring Formations. For example, the latest Cretaceous to Paleocene succession of Clarence valley is relatively well studied with respect to biostratigraphy, due to the Cretaceous-Paleogene boundary being well exposed in the region (Hollis et al., 2003; Schiøler & Wilson, 1998; Strong et al., 1995; Willumsen, 2003; Willumsen, 2011). Despite this, no detailed biostratigraphy has been presented for Branch, Angora and Tangaruhe Stream sections. Preliminary analyses by Dr Poul Schiøler in 2001 revealed the presence of fossil dinoflagellate cyst floras in the section at Branch Stream. Likewise, the work of Crampton et al. (2006) has shown their presence at Angora and Tangaruhe Streams. Conversely investigations have shown that Branch Sandstone is devoid of other age diagnostic fossils such as foraminifera, radiolaria and macrofossils (Reay, 1993). This present research therefore uses assemblages of fossil dinoflagellate cysts (dinocysts) to provide age control for each of the sections.

This chapter first briefly describes previous studies of Late Cretaceous dinoflagellate biostratigraphy in relevant parts of New Zealand. Then, secondly, results from Branch, Angora and Tangaruhe Streams are presented. This is followed by a zonation for each section developed during this study. Finally, preliminary ages are presented and discussed with respect to results from previous research. Dinoflagellate assemblages, along with other organic content are reviewed in the next chapter, in order to assist paleoenvironmental interpretation.

4.2 Previous studies of Upper Cretaceous dinocyst assemblages

Studies of Late Cretaceous – early Paleocene dinoflagellate biostratigraphy are common from sites along the East Coast of New Zealand, which reflects the broad biostratigraphic utility of dinoflagellates and their widespread occurrence. Dinocysts were first identified in New Zealand sediments by Couper (1960). From then onwards, a succession of detailed systematic studies of dinocysts from the Late Cretaceous and Paleogene of New Zealand were carried out by Dr G. J. Wilson and his colleagues (e.g. Strong et al., 1995; Wilson, 1967b, 1978, 1984a; Wilson et al., 1989).

Wilson (1984a) devised an early dinocyst zonation for the Upper Cretaceous – Eocene in New Zealand. Wilson's zonal scheme for the Upper Cretaceous was later refined through palynological analysis of Piripauan-Haumurian aged sediments of north Canterbury and south Marlborough (Roncaglia et al. 1999; Roncaglia & Schiøler, 1997; Schiøler & Wilson, 1998). As a result of this work, the Haumurian stage presently incorporates six dinoflagellate zones (Crampton et al., 2000). The zonation scheme of Roncaglia et al. (1999) is followed herein (Figure 25).

Published studies of dinocyst assemblages from the uppermost Herring Formation in Marlborough are not available, although a number of research projects have analysed parts of the formation and correlative units. Schiøler and Wilson (1998) documented the dinoflagellate biostratigraphy of Upper Cretaceous sediments in south Marlborough, including the lower portion of the Herring Formation in sites located to the north-east of the present study area. This work indicated that the base of the Herring Formation, at Ben More Stream, was Santonian in age (Late Piripauan) and occurred at the boundary between the *Odontochitina porifera* and *Isabelidinium cretaceum* Interval Zones of Schiøler and Wilson (1998).

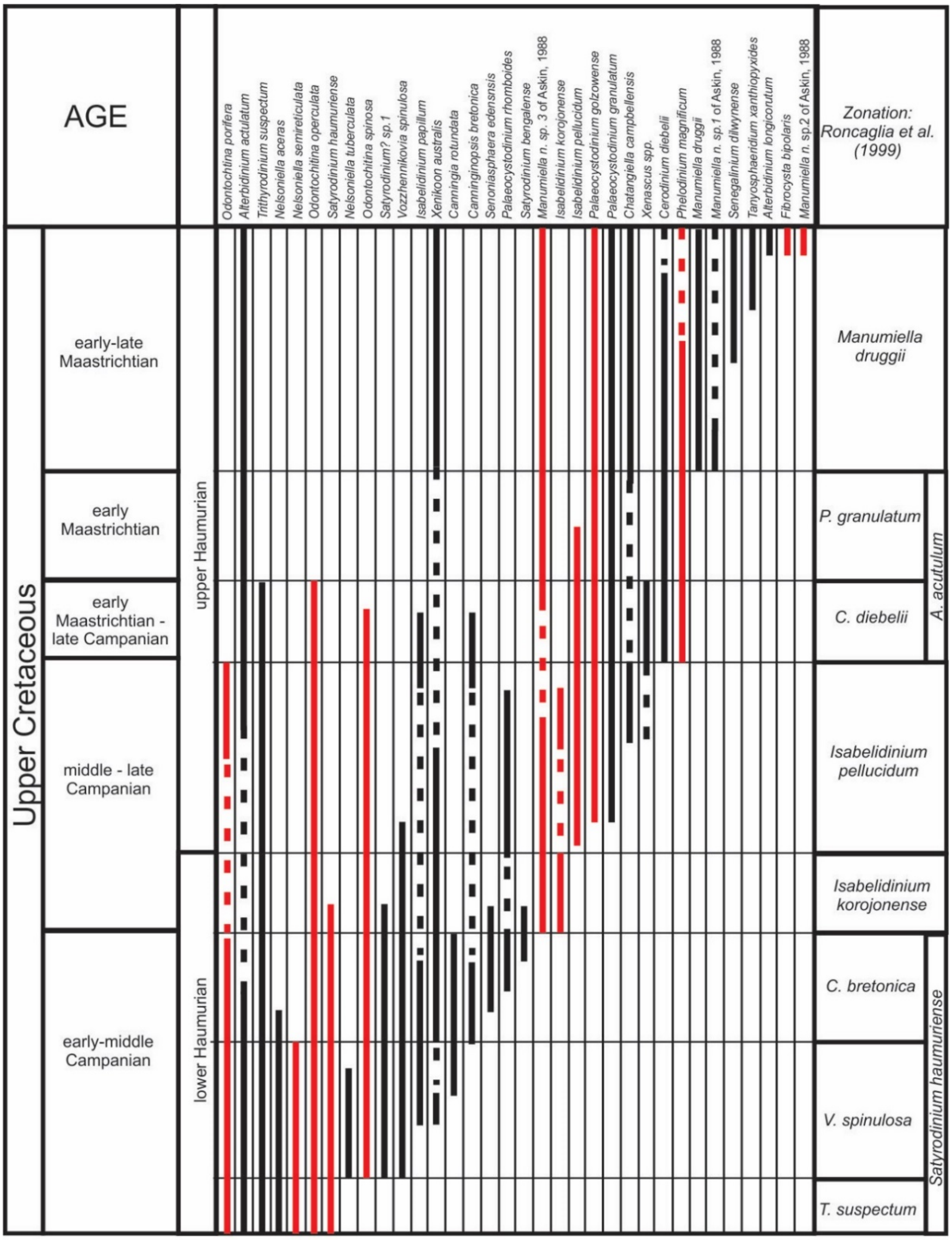

Figure 25. Zonation of Roncaglia et al. (1999) for the Haumurian stage. Important taxa referenced in this study are highlighted in red.

Schiøler et al. (2002) analysed Herring Formation from a section in the upper reaches of Benmore Stream, where over 200m of the unit is present. The upper contact of Herring Formation is not exposed at this locality, however palynological analysis places the upper part of the exposure in the *Isabelidinium korojonense* dinoflagellate Interval Zone, which spans the early Campanian age (upper Lower Haumurian stage) (Schiøler et al., 2002).

Strong et al. (1995) sampled the Mead Hill Formation in Mead Stream as part of a wider biostratigraphic study of the Muzzle Group. This work incorporated the study of dinocysts, foraminifera and radiolarians, and dated the lower Mead Hill Formation to the Maastrichtian, within the *Manumiella druggii* Interval Zone. At Mead Stream, however, the base of the Mead Hill Formation has been removed by faulting. An extrapolation, based on minimum sedimentation rates, led Strong et al. (1995) to assign an age of 72Ma to the base of the Mead Hill Formation.

Willumsen (2003, 2011) analysed the dinoflagellate biostratigraphy of the Cretaceous-Paleogene boundary at multiple East Coast localities, including Branch Stream. Although Willumsen's (2003) work at Branch Stream did not extend to the contact between Mead Hill Formation and Branch Sandstone, her work confirmed that deposition of part of the Mead Hill Formation occurred during the *Manumiella druggii* Interval Zone.

Crampton et al. (2006) used dinoflagellate biostratigraphy to evaluate several sections from the East Coast of the North Island and from Marlborough and north Canterbury. Sampling was undertaken at the Angora and Tangaruhe Stream sections analysed for this research, though at much coarser resolution (ca. 5m sampling intervals). Their analysis indicated that the lower Whangai Formation was of lower-upper Maastrichtian age at both localities. Additionally, based on dinocyst assemblages, the Tangaruhe Formation was considered to be Santonian to early Campanian in age (Crampton et al., 2006).

4.3 Methods

Bulk, fist-sized samples, collected from each field site were selected for processing. At Angora and Branch Streams, samples from the main sandstone units were taken at intervals of around one metre, with samples taken at ~10cm intervals in the vicinity of lithological boundaries. At Tangaruhe Stream, three samples were selected from either side of the contact between the Tangaruhe and Whangai formations over a total interval of around two metres.

Samples were processed by the author at Victoria University, using standard palynological techniques (e.g. Batten, 1999). To remove all mineral constituents, the samples were digested in hydrochloric and hydrofluoric acids. Due to concerns regarding the loss of organic material, no oxidisation step was applied. Samples were separated using sodium polytungstate (specific gravity ~2.1) and the resultant residue was sieved through a 6µm mesh and the >6µm fraction was slide mounted.

For biostratigraphic analysis, 200 dinocysts (where present) were counted in each sample, across a maximum of two slides, under a transmitted light microscope. Regularly spaced transects were made across each slide, until the target of 200 individuals was achieved. Following such counts slides were systematically scanned for any further important index species. Despite this, dinocyst abundance was low in most samples and all individuals were therefore counted. Where more than a quarter of an individual was present, and recognisable, this was counted as one individual. Dinocysts were identified using examples from scientific literature and via personal communication with Dr Poul Schiøler. Many cysts were poorly preserved and, in some cases, could only be identified to genus level. Count sheets, a taxonomic list and plates are available in Appendix 2.

4.4 Dinoflagellate biostratigraphy

4.4.1 General characteristics

The samples analysed reveal moderate-low diversity dinocyst assemblages at Branch, Angora and Tangaruhe Streams. In the sandstone intervals of primary interest, dinocyst abundance was low, meaning that 200 individuals could not be counted across two slides from each sample. Overall, preservation ranged from poor to moderate, resulting in a high number of unidentifiable individual cysts. Samples from some parts of the Branch Stream section were particularly problematic, with a number of slides contaminated with remnant mineral constituents. Samples from Tangaruhe Stream contained greater abundances of cysts overall, although preservation still ranged from poor to moderate.

4.4.2 Branch Stream section

In total, 12 samples were processed for biostratigraphy from the Branch Stream section, two each from the Herring and Mead Hill Formations and eight from the Branch Sandstone. Two samples, taken from the Branch Sandstone, were barren of dinocysts. Due to poor preservation and the low quality of some slides produced within the Branch Sandstone interval, a secondary set of slides was also examined to provide assurance. This pre-existing set of slides was collected from the same section, and was provided by Dr Poul Schiøler.

Dinocysts were relatively abundant in the samples extracted from the Herring Formation, below the lower contact of the Branch Sandstone. These samples contain numerous specimens assignable to the genus *Odontochitina*, including *Odontochitina porifera, Odontochitina spinosa* and, most commonly, *Odontochitina operculata*. Additionally, the late Cretaceous index species, *Isabelidinium* *pellucidum,* is common in this interval, as is the peridinoid species *Chatangiella packhamii*.

The Branch Sandstone contains a very restricted assemblage of dinocysts, indicating that the assemblage is potentially facies controlled. This inference is supported by the observation that dinocysts are common to abundant in the underlying Herring Formation and the overlying Mead Hill Formation. The dinocysts retrieved from the Branch Sandstone are sparse, poorly preserved, and dominated by *Manumiella seymourensis* and species of *Impagidinium.* In the slides produced during the course of this research, *Odontochitina operculata, Isabelidinium pellucidum and Chatangiella packhamii* specimens occur very rarely within the Branch Sandstone, in abundances that might have been consistent with their reworking from older strata. Examination of the additional set of slides, however, confirmed the presence of *Isabelidinium pellucidum*, as well as *Odontochitina operculata* and *Odontochitina spinosa,* in abundances that preclude reworking.

Mead Hill Formation exhibits a more diverse assemblage of dinocysts, containing abundant individuals. Preservation quality fluctuates dramatically, many *Impagidinium* specimens are moderately well preserved, whereas some peridinoid dinocysts are very badly degraded. In samples retrieved from the Mead Hill Formation, *Impagidinium* is the most abundant genus. *Manumiella seymourensis*, *Palaeocystodinium golzowense* and rare specimens of *Manumiella seelandica* and *Fibrocysta bipolaris* are other notable species observed in the uppermost part of the section.

4.4.3 Biostratigraphy – Branch Sandstone section

Given poor preservation and a scarcity of chronostratigraphically useful specimens, the age assignment given to the Branch Sandstone herein remains tentative. The age assessment is based on the distribution of the following species: *Isabelidinium pellucidum, Odontochitina operculata, Odontochitina porifera, Manumiella seymourensis, Manumiella seelandica* and *Fibrocysta bipolaris.* The stratigraphic ranges of these species are discussed below and a summary of biostratigraphic events is shown in Figure 26.

Isabelidinium pellucidum is common at the base of the section, within the Herring Formation, and occurs sporadically within the Branch Sandstone. The species is not observed above the Branch Sandstone-Meadhill Formation contact. In New Zealand, the lowest occurrence of *Isabelidinium pellucidum* marks the base of the Upper Haumurian Substage (Crampton et al., 2000) and defines the base of the *Isabelidinium pellucidum* Interval Zone of Roncaglia et al. (1999). The species has its latest occurrence in the *Cerodinium diebelii* Subzone and is not present within the Maastrichtian (Roncaglia et al., 1999).

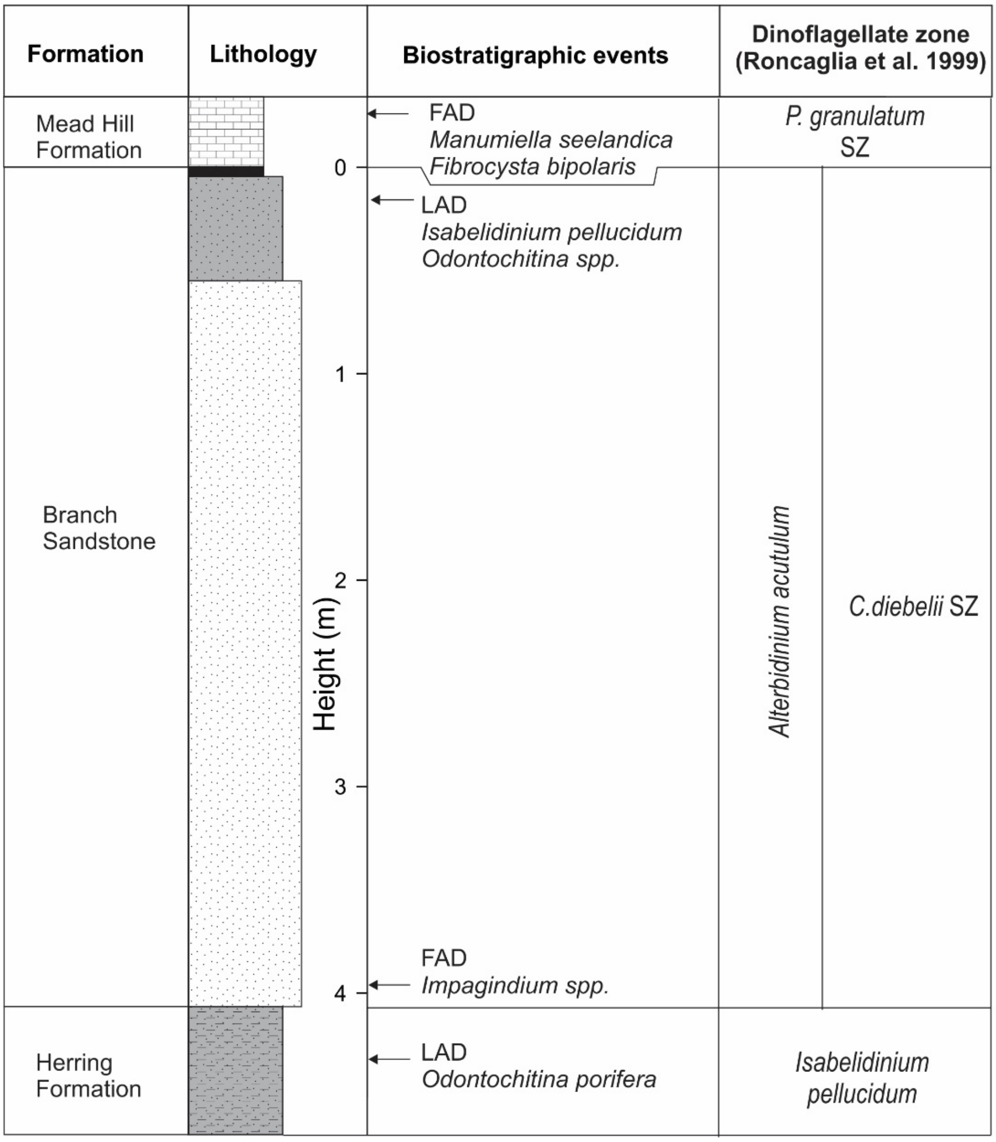

Figure 26. Biostratigraphic events within the Branch Stream section.

In New Zealand, the range of *Odontochitina* species spans a large portion of the Upper Cretaceous, including the entire Santonian and Campanian stages (Roncaglia et al., 1999; Wilson, 1984a). The latest occurrence of the genus is marked by the disappearance of *Odontochitina operculata* and correlated with the top of the *Cerodinium diebelii* Interval Subzone of Roncaglia et al. (1999). The latest occurrence of *Odontochitina porifera* occurs earlier, at the base of the *Cerodinium diebelii* Subzone.

Manumiella seymourensis is variably abundant throughout the entire section. Askin (1988) first documented the species as *Manumiella sp. 3* in a study of Cretaceous – Paleogene sediments from Seymour Island in Antarctica. *Manumiella sp. 3* was defined as the marker species for Askin's (1988) palynomorph zone 2, which was interpreted to range from the late Campanian, into the Maastrichtian. This species is noted as being characteristically common in the *Paleocystodinium granulatum* Interval Subzone of Roncaglia et al. (1999), however, in New Zealand, it is inferred to occur throughout the entire Upper Haumurian (mid-Campanian – end Maastrichtian).

Rare specimens of the genus *Odontochitina* are present above the Branch Sandstone-Mead Hill Formation boundary; however, these are considered reworked on the basis of scarcity and preservation. This observation is supported by examination of the control set of slides, in which the genus *Odontochitina* does not appear within the Mead Hill Formation.

Very rare *Manumiella seelandica* specimens are observed in the stratigraphically highest sample from this section. In New Zealand, this species first occurs in the late Maastrichtian, in the *Manumiella druggii* Interval Zone (Roncaglia et al., 1999; Willumsen, 2003). It is also noteworthy that *Fibrocysta bipolaris* is present in samples from the lower Mead Hill Formation in the control set of slides. This species has a first occurrence approximately equivalent to *M. seelandica*, in the upper part of the *Manumiella druggii* Interval Zone (Roncaglia et al., 1999).

Based on the occurrences of the species outlined above an age assignment has been made, following the scheme of Roncaglia et al. (1999). Given the low abundance of individual dinocysts and the low dinocyst diversity displayed in the section this age assignment must be considered provisional.

As shown in Figure 26, the base of the section, corresponding to the Herring Formation has been assigned to the *Isabelidinium pellucidum* Interval Zone, based on the presence of species including *Isabelidinium pellucidum, Odontochitina operculata* and *Odontochitina porifera*. The Branch Sandstone has been attributed to the *Cerodinium diebelii* Interval Subzone due to the presence of *Isabelidinium pellucidum*, *Odontochitina operculata, Palaeocystodinium golzowense*, and the absence of *Odontochitina porifera*, although not all species are consistently present in the formation. Based on the zonation of Roncaglia et al. (1999), uppermost Herring Formation is middle to late Campanian (Upper Haumurian) in age at Branch Stream. The Branch Sandstone is, at a minimum, Early Maastrichtian-Late Campanian in age.

The Mead Hill Formation has been placed within the *Palaeocystodinium granulatum* Interval Subzone based on the presence of *Manumiella seymourensis and Palaeocystodinium golzowense* and the absence of *Isabelidinium pellucidum* and *Odontochitina spp*. Accordingly, the base of the Mead Hill Formation at Branch Stream is assigned an early Maastrichtian age. This age determination is considered a maximum age due to the presence of *Manumiella seelandica* in the primary set of slides, as well as *Fibrocysta bipolaris* in the secondary set. These species first occur in the *Manumiella druggii* interval zone of Roncaglia et al. (1999), which encompasses the Late Maastrichtian (uppermost Haumurian). The marker taxon for the zone (*Manumiella druggii*), however, was not encountered in this interval in either set of slides and the occurrences of *Manumiella seelandica* and *Fibrocysta bipolaris* were rare.

4.4.4 Angora Stream assemblages

In total, 12 samples were processed for biostratigraphy from the Angora Stream section, two each from the Whangai and Glenburn formations and eight from sandstone A. Two samples from sandstone A were barren of identifiable dinocysts, whereas in other samples, dinocysts were rare to abundant.

The two stratigraphically lowest samples in this section are extracted from mud-rich facies of the Glenburn Formation. Both samples contain numerous *Odontochitina spinosa* and *Odontochitina porifera*, whereas *Isabelidinium pellucidum* is extremely abundant in AST-005, immediately below the Glenburn Formation sandstone facies.

Within sandstone A, dinocysts are rare and poorly preserved. The two stratigraphically lowest samples (AST-007 and AST-008) contain several species similar to the underlying interval, including *Odontochitina spinosa, Odontochitina porifera, Isabelidinium pellucidum* and *Palaeocystodinium golzowense*, though in greatly reduced numbers. Notably however, *Conosphaeridium abbreviatum* is present at the very base of the sandstone, along with *Cymososphaeridium benmorense* and *Glaphyrocysta marlboroughensis*. Dinocysts become extremely rare through most of the sandstone A interval before increasing in abundance immediately below the Glenburn-Whangai contact. In the uppermost samples, taken from the Whangai Formation, *Odontochitina spinosa, Odontochitina porifera, Isabelidinium pellucidum* and *Palaeocystodinium golzowense* are present in variable abundance.

4.4.5 Biostratigraphy – Angora Stream

Dinocysts are sparse in the sandstone A interval, and thus the assignment made below must again be considered tentative. Age assignment is made using similar Late Cretaceous marker taxa to those from the Branch Sandstone, including *Isabelidinium pellucidum*, *Odontochitina porifera*, *Odontochitina spinosa* and

Palaeocystodinium golzowense (Figure 27). The temporal distribution of these species is outlined above.

Isabelidinium pellucidum, Odontochitina spinosa, *Odontochitina porifera* and *Palaeocystodinium golzowense* occur throughout the sampled section, despite not being present in all samples. Based on the presence of *Isabelidinium pellucidum, Odontochitina porifera, Odontochitina spinosa, Palaeocystodinium golzowense* in the lower and upper parts of the section, the entire interval is tentatively assigned to the *Isabelidinium pellucidum* Interval Zone of Roncaglia et al. (1999).

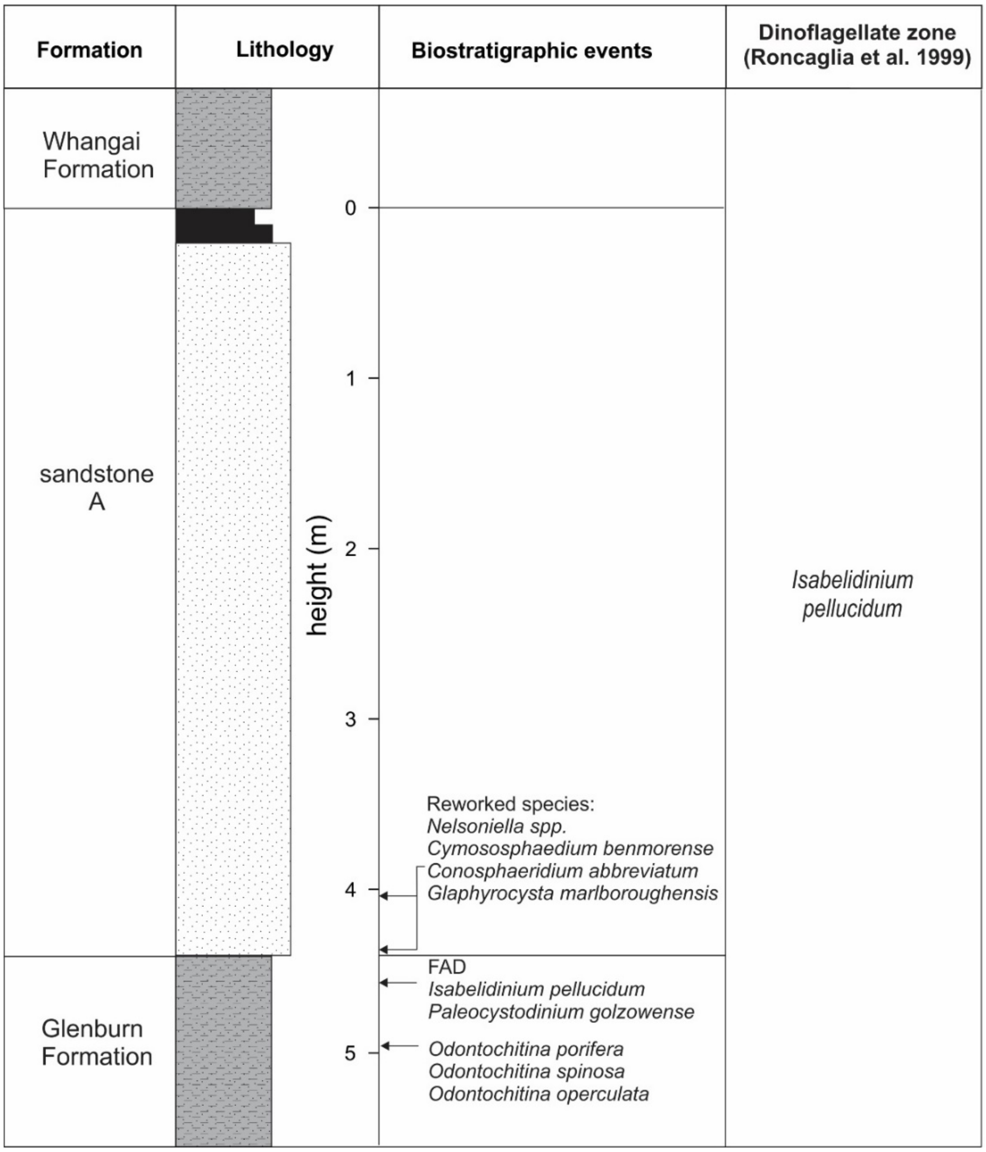

Figure 27. Biostratigraphic events within the Angora Stream section.

The base of sandstone A at Angora Stream, however, contains a notably different dinoflagellate assemblage to the succession it overlies. According to Schiøler and Wilson (1998), *Conosphaeridium abbreviatum, Cymososphaeridium benmorense* and *Glaphyrocysta marlboroughensis* are Piripauan-restricted species, whereas the genus *Nelsoniella* is typically present in the Lower Haumurian Substage (Roncaglia et al., 1999). These species co-occur in the sandstone with sparse specimens of *Isabelidinium pellucidum*, however, which are considered in-situ, due to their common occurrence elsewhere in the section. The presence of numerous older species at the base of the sandstone A is probably indicative of redeposition of older sediments, given the enclosing succession indicates a much younger age.

Based on the zonation of Roncaglia et al. (1999), the uppermost Glenburn Formation and lower Whangai Formation at Angora Stream are middle to late Campanian (upper Haumurian) in age.

4.4.6 Tangaruhe Stream section

In total, six samples were processed for biostratigraphy from the Tangaruhe Stream section, three each from the Whangai and Tangaruhe formations. Fewer samples were processed in comparison to the other sections, reflecting the absence of a sandstone interval at the Tangaruhe locality. The primary aim at this locality was therefore to sample the contact between the Tangaruhe and Whangai Formations, in order to identify any depositional hiatus or unconformity.

Dinocysts were comparatively abundant in the Tangaruhe Stream section. Preservation of dinocysts ranged from poor to good, although most samples contained a high number of unidentifiable dinocysts.

The three stratigraphically lowest samples, collected from the Tangaruhe Formation, contain a moderately diverse assemblage. The most abundant species from these samples include *Satyrodinium haumuriense, Nelsoniella semireticulata* and *Odontochitina porifera*. The three uppermost samples were collected from the Whangai Formation, and these contain a markedly different assemblage. The most abundant species through this interval are *Isabelidinium pellucidum* and *Palaeocystodinium golzowense*. Notably, TST-008, the sample taken immediately above the contact, contains frequent *Impagidinium* spp. specimens, which are not present in any other sample from this section.

4.4.7 Biostratigraphy – Tangaruhe Stream

Age assignments at Tangaruhe Stream are based on several Late Cretaceous taxa encountered therein (Figure 28). The temporal distribution of *Satyrodinium haumuriense, Nelsoniella semireticulata* and *Phelodonium magnificum* are discussed below, whereas *Odontochitina porifera, Isabelidinium pellucidum* and *Palaeocystodinium golzowense* have been covered earlier in this section.

The first occurrence of *Satyrodinium haumuriense* is considered an early Campanian event in New Zealand and Australia (Helby et al., 1987; Roncaglia et al., 1999). Elsewhere, in the Indian and Southern Oceans, the first occurrence is thought to coincide with the Lower Maastrichtian and Upper Campanian respectively (Mao & Mohr, 1992; Mohr & Mao, 1997). According to Roncaglia et al. (1999), *Nelsoniella semireticulata* has a latest occurrence at the base of the *Vozzhennikovia spinulosa* interval subzone, sometime around the middle Campanian.

Based on the presence of *Satyrodinium haumuriense* and *Nelsoniella semireticulata*, the top Tangaruhe Formation at Tangaruhe Stream is assigned to the *Satyrodinium haumuriense* Interval Zone of Roncaglia et al. (1999). Whereas the occurrence of *Satyrodinium haumuriense* ranges into the *Isabelidinium korojonense* Interval Zone, the presence of *Nelsoniella semireticulata* indicates that the succession must sit with in the *Vozzhennikovia spinulosa* subzone, at a minimum. Based on this assignment, the lower part of the Tangaruhe section is early-middle Campanian aged (Lower Haumurian).

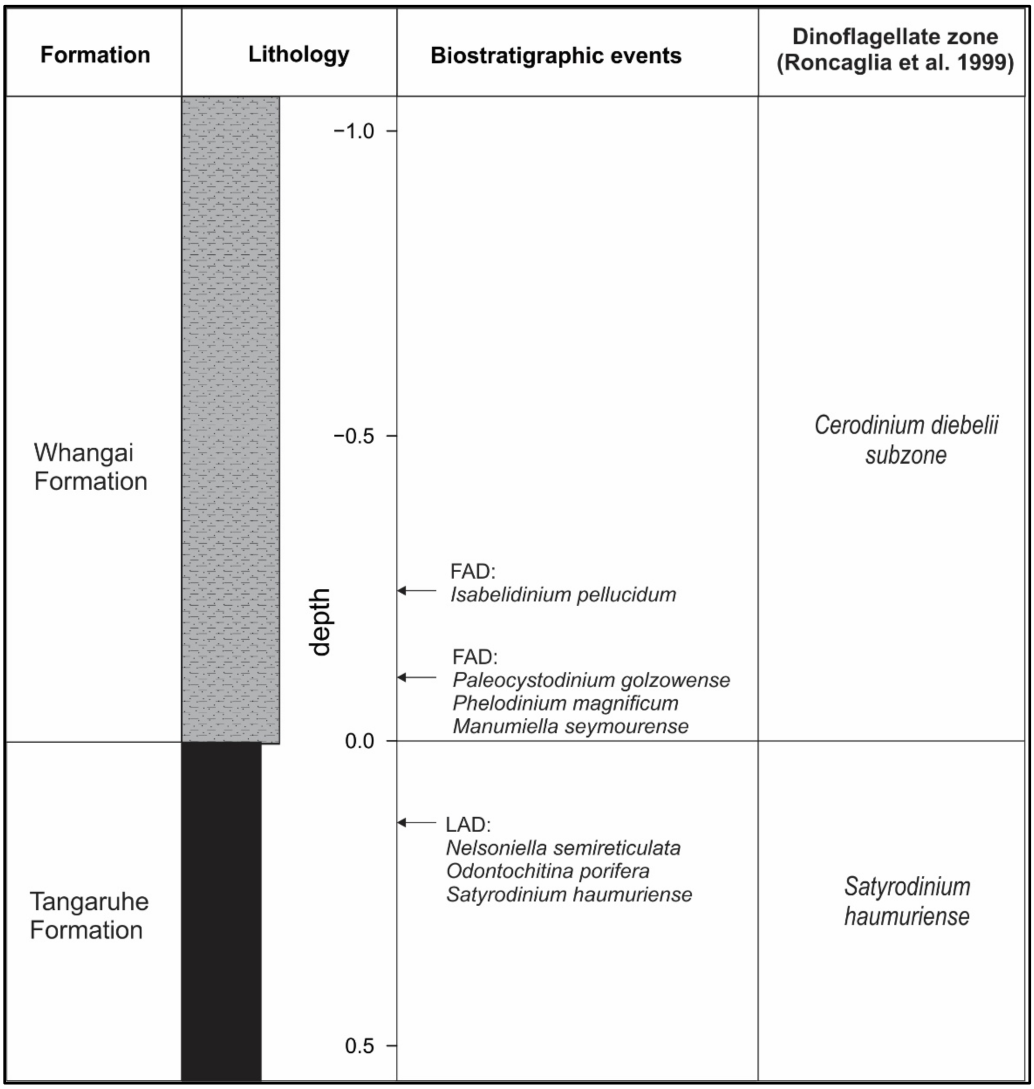

Figure 28. Biostratigraphic events within the Tangaruhe Stream section.

Above the Whangai-Tangaruhe contact, the widespread presence of *Isabelidinium pellucidum* indicates the lower Whangai Formation sits, at a maximum, within the *Isabelidinium pellucidum* Subzone. *Odontochitina spinosa* occurs rarely in the uppermost sample, whereas *Phelodinium magnifcum* occurs rarely in all samples above the contact. According to Roncaglia et al. (1999), the earliest occurrence of *Phelodinium magnificum* takes place at the base of the *Cerodinium diebelii* Interval Zone. Based on the presence of *Isabelidinium pellucidum*, *Odontochitina spinosa,* and *Phelodinium magnificum*, the base Whangai Formation at Tangaruhe Stream is attributed to the *Cerodinium diebelii* Interval Subzone of Roncaglia et al. (1999).

Accordingly, the formation is interpreted to be Late Campanian – Early Maastrichtian (Upper Haumurian) in age.

4.5 Discussion

Despite the poor preservation and generally low recoveries of dinocysts at Branch and Angora Streams a number of age assignments can be suggested (Figure 29).

Deposition of Branch Sandstone is interpreted to have occurred in the Late Campanian to Early Maastrichtian stages (Upper Haumurian). Deposition of sandstone A at Angora Stream is inferred to have taken place slightly earlier, in the middle to late Campanian period (Upper Haumurian). In addition, a distinct stratigraphic discontinuity has been documented at Tangaruhe Stream, encompassing much of the middle-late Campanian.

At Branch Stream, biostratigraphy suggests a break in deposition at the base of Branch Sandstone, corresponding to a pronounced change in lithology. A depositional break is also interpreted at the top of the Branch Sandstone, though this is less well constrained. The assignment of the base Mead Hill Formation to the *Palaeocystodinium granulatum* Interval Subzone of Roncaglia et al. (1999) is based on the absence of marker species for other zones, such as *Manumiella druggii*, *Isabelidinium pellucidum* and *Cerodinium diebelii*, as well as *Odontochitina* spp. It is possible that this absence could reflect fluctuating paleoenvironmental conditions, however; the presence of both *Manumiella seymourensis* and *Paleocystodinium golzowense* is consistent with the *Paleocystodinium granulatum* Interval Subzone interpretation. Additionally, this assignation is in keeping with the work of Strong et al. (1995), who assigned an age of 72Ma to the base Mead Hill Formation at Mead Stream.

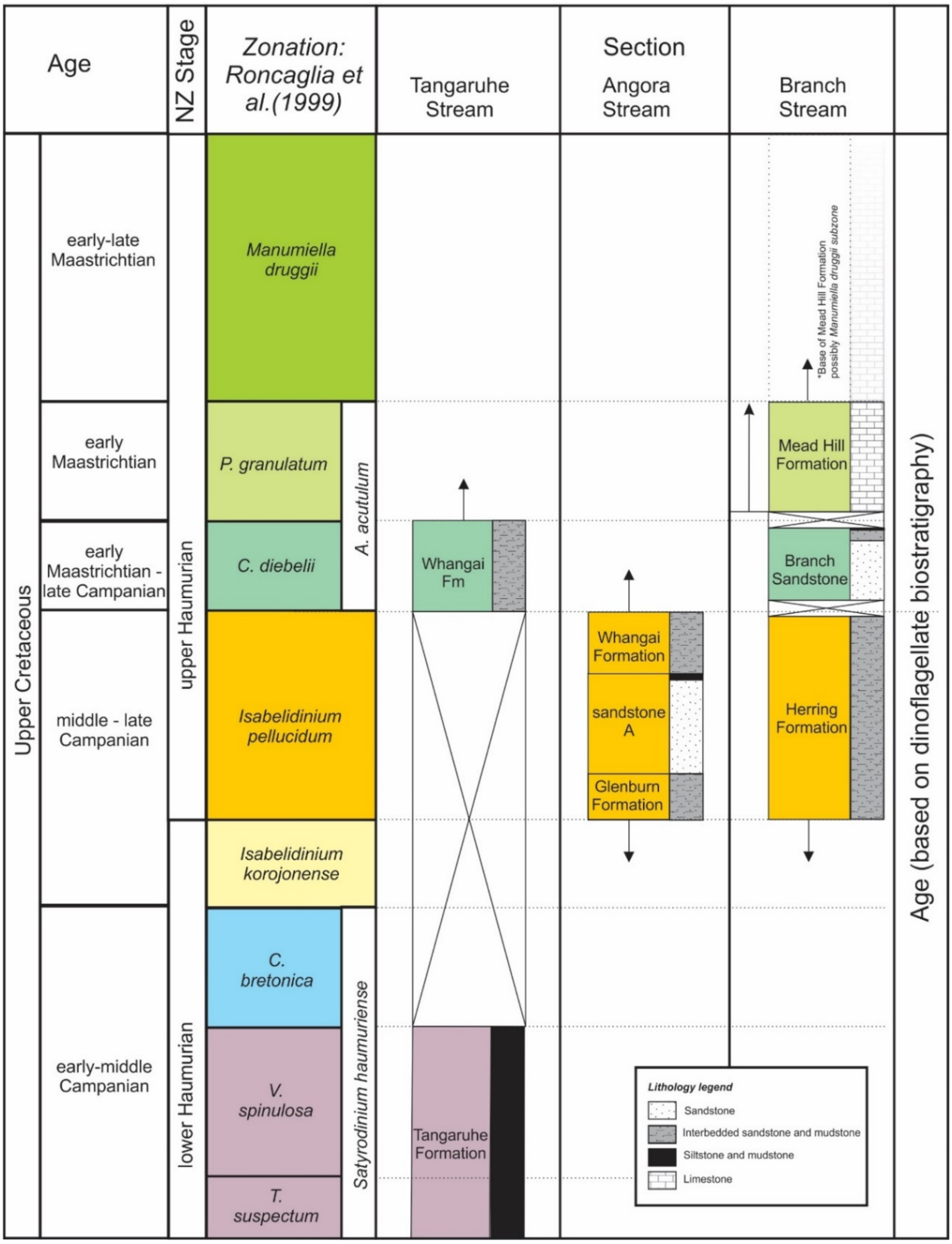

Figure 29. Summary of biostratigraphic results at Branch, Angora and Tangaruhe Stream.

At Angora Stream, sandstone A contains an extremely low abundance of dinoflagellate cysts. The underlying Glenburn Formation contains moderate to high abundances of *Isabelidinium pellucidum* Interval Zone marker taxa. Similarly, Whangai Formation has been assigned to the *Isabelidinium pellucidum* zone, therefore the entire section has been assigned to the *Isabelidinium pellucidum* *zone*. An older dinocyst assemblage is encountered at the base of the sandstone A and probably indicates reworking of older sediments.

The placement of the Angora Stream section within the *Isabelidinium pellucidum* Interval Zone differs from findings from other studies. Crampton et al. (2006) assigned the base Whangai Formation to the lower-upper Maastrichtian at Angora Stream, which diverges from the middle-late Campanian age given here. The presence of *Odontochitina porifera* in the base Whangai in this study, however, makes a late Campanian diagnosis more likely.

The Tangaruhe Steam section contains a moderate diversity of dinoflagellate cysts and overall cyst abundance is greater than in the other sections sampled in this study. Analysis places the lower part of the section, corresponding to the Tangaruhe Formation, in the *Satyrodinium haumuriense* Interval Zone of Roncaglia et al. (1999). The upper part of the section, which comprises Whangai Formation appears to sit within the *Cerodinium diebelii* Interval Subzone. On this basis, the change in species assemblages are indicative of either a lengthy period of non-deposition, or a substantial amount of erosion. This unconformity was documented by Crampton et al. (2006), and the results of the dinoflagellate biostratigraphy produced herein confirm their findings. The dinoflagellate zonation for Tangaruhe Formation presented herein also broadly agrees with the findings of Adams (1985), who concluded the formation was Piripauan to Lower Haumurian in age based on macrofossils and dinoflagellate assemblages.

5 Palynofacies

5.1 Introduction and aims

Palynofacies analysis involves the study of all acid-resistant organic material derived from a sedimentary rock unit. The study of the wider organic matter assemblages in different lithofacies provides a useful method for interpreting the depositional history of rock formations. As described by Tyson (1995), numerous studies have indicated that the composition of organic constituents in rock will vary in response to fluctuations in relative sea level. Palynofacies analysis therefore provides a supporting method for determining paleoshoreline positions, rather than basing interpretation on lithofacies alone (Clowes et al, 2016; McCarthy et al, 2003).

In this study, palynofacies analysis is intended to augment paleoenvironmental interpretations based on sedimentological data presented in Chapter 3. This chapter first describes the categories of organic matter demarcated from the sections presented herein. Second, the results of counts from the Branch, Angora and Tangaruhe stream sections are presented. Finally, the assemblages are interpreted with respect to paleoenvironmental factors such as shoreline proximity and oxygenation.

5.2 Methods

The slides prepared for biostratigraphic analysis (Chapter 4) were re-examined for palynodebris. Counting followed the procedure outlined in Clowes et al. (2016). 300 particles were counted in each sample and classified into seven major categories (Table 3). Data were then normalised and assembled into the following groups: terrestrial palynomorphs, marine palynomorphs, indeterminate palynomorphs, amorphous organic matter (AOM) and phytoclasts (black, brown and other). Raw and normalised count data are available in Appendix 3.

Table 3. Summary of palynodebris categories, after Clowes et al. (2016).

Group (Clowes et al. 2016)	Category (Clowes et al. 2016	Subgroup (this project)
Amorphous Organic Matter (AOM)	Amorphous organic matter	AOM
Palynomorphs	Monolete spores	Terrestrial palynomorphs
	Trilete spores	
	Saccate gymnosperm pollen	
	Other gymnosperm pollen	
	Mangrove pollen	
	Other angiosperm pollen	
	Freshwater algae	
	Peridinoid dinoflagellate cysts	Marine palynomorphs
	Gonyaulacoid dinoflagellate cysts	
	Indeterminate and other dinoflagellate cysts	
	Acritarchs and other marine 'algae'	
	Foraminiferal test linings	
	Other zoomorphs	
	Interderminate and unknown palynomorphs	Interdeterminate palynomorphs
Phytoclasts	Brown structured phytoclasts	Brown phytoclasts
	Degraded phytoclasts	
	Opaque equidimensional phytoclasts	Black phytoclasts
	Opaque elongate phytoclasts	
	Opaque 'other' phytoclasts	
	Resin/Humic gel	Other phytoclasts
	Fungal remains	
	Cellular membranes	
	Non-cellular membranes	

Investigation of the varying abundance of specific dinoflagellate groups can similarly be used as a paleoenvironmental proxy (e.g. Carvalho et al., 2016; Carvalho et al., 2013; Habib, et al., 1992; Li & Habib, 1996; Tyson, 1995). Because of poor preservation and low dinocyst recovery, analysis here focusses on *Impagidinium spp.*, which are readily identifiable even when poorly preserved.

5.3 Explanation of palynofacies categories

5.3.1 Amorphous Organic Matter

Amorphous Organic Matter (AOM) is defined as structureless organic material that frequently contains numerous inclusions (Pacton et al., 2011; Tyson, 1995). AOM is derived from degraded microplankton, bacterially-produced amorphous material, plant tissues and resins, or diagenetically altered macrophyte tissues (Pacton et al., 2011; Tyson, 1995). High relative proportions of AOM are commonly interpreted to reflect either reducing environments, or distal paleoenvironments removed from inputs of terrestrial material (Carvalho et al., 2013; Tyson, 1995). Significantly, the abundance of AOM typically increases in a proximal-distal direction (Schiøler et al., 2002; Tyson, 1995).

5.3.2 Palynomorphs

Counts of the palynomorph group are presented as 'terrestrial palynomorphs' and 'marine palynomorphs'. The terrestrial palynomorph group includes all spores and pollen, as well as freshwater algae. Tyson (1995) previously included fungal detritus within a sporomorph subgroup also incorporating spores and pollen; however, as the approach of Clowes et al. (2016) is adopted here, fungal remains are grouped under the phytoclast category.

Pollen is generated by gymnosperm and angiosperm plants, whilst spores are produced by pteridophyte plants (Carvalho et al., 2006). Due to their origin, the abundance of terrestrial-derived palynomorphs is expected to decrease in an offshore direction (Schiøler et al., 2002; Tyson, 1995). In this study, freshwater algae were not observed in any samples, and the relative abundance of the terrestrial palynomorph group was low in all sections.

The marine palynomorph group incorporates all dinoflagellates cysts, acritarchs, other marine algae, foraminiferal test linings and zoomorphs. The relative abundance of this group is greatest in shelfal marine settings, and declines in nearshore, as well as slope and bathyal conditions. Additionally, marine palynomorph distribution is influenced by many factors such as oceanic conditions, currents and freshwater input (Schiøler et al., 2002; Tyson, 1995). Fossil dinoflagellate cysts represent the majority of marine palynomorphs encountered among this group.

5.3.3 Phytoclasts

Nine different phytoclast categories are defined by Clowes et al. (2016), which, for simplicity, are here grouped into three categories; brown phytoclasts, black phytoclasts and other phytoclasts (Table 3). The components that make up most of the assemblage are the brown and black phytoclasts, overall comprising a large proportion of the total palynodebris.

Brown and black phytoclasts are largely derived from the tissues of terrestrial plants (Carvalho et al., 2006). Black phytoclasts are defined by their opacity, and an inability to discern translucency across 90% of the particle (Clowes et al., 2016). The opacity of particles is suggested to be the result of long distance transport under oxidising conditions, hence the proportion of black phytoclasts is expected to increase in an offshore direction (Carvalho et al., 2016; Tyson, 1995). Conversely, brown phytoclasts are interpreted as having undergone less transport (Carvalho et al., 2016). It follows that brown phytoclasts are more abundant in a nearshore direction, so in high relative proportions can represent proximity to shoreline (Tyson, 1995).

Brown phytoclasts are defined by the presence of remnant structures, such as linear thickenings or tracheids, or by their non-opaque nature, where remnant structures are degraded. The other phytoclast category consists of cellular and non-cellular membranes, fungal remains and resin. In this study, the other phytoclast category is dominated by leaf cuticles.

A ratio of black/brown phytoclasts is presented for each of the sections, and may be indicative of proximal-distal trend.

5.3.4 Impagidinium group

The *Impagidinium* group comprises dinoflagellate taxa from the genera *Impagidinium* and *Pterodinium*. Studies of recent sediments have indicated that

Impagidinium predominantly occurs in outer neritic to oceanic marine settings (e.g. Crouch et al., 2010; Matthiessen, 1995; Wall et al., 1977).

5.3.5 Interpretation of palynofacies results

The distribution of organic material in each sample is presented in two formats for each section. First, the normalised distribution of the subgroups shown in Table 3 are plotted in graph format, alongside lithology and grain-size.

Second, samples from each section are presented on a Tyson (1993) plot, which gives an indication of depositional environment, based on the relative abundance of the phytoclast, palynomorph and AOM groups. For reference, the Tyson plot is illustrated in Figure 30.

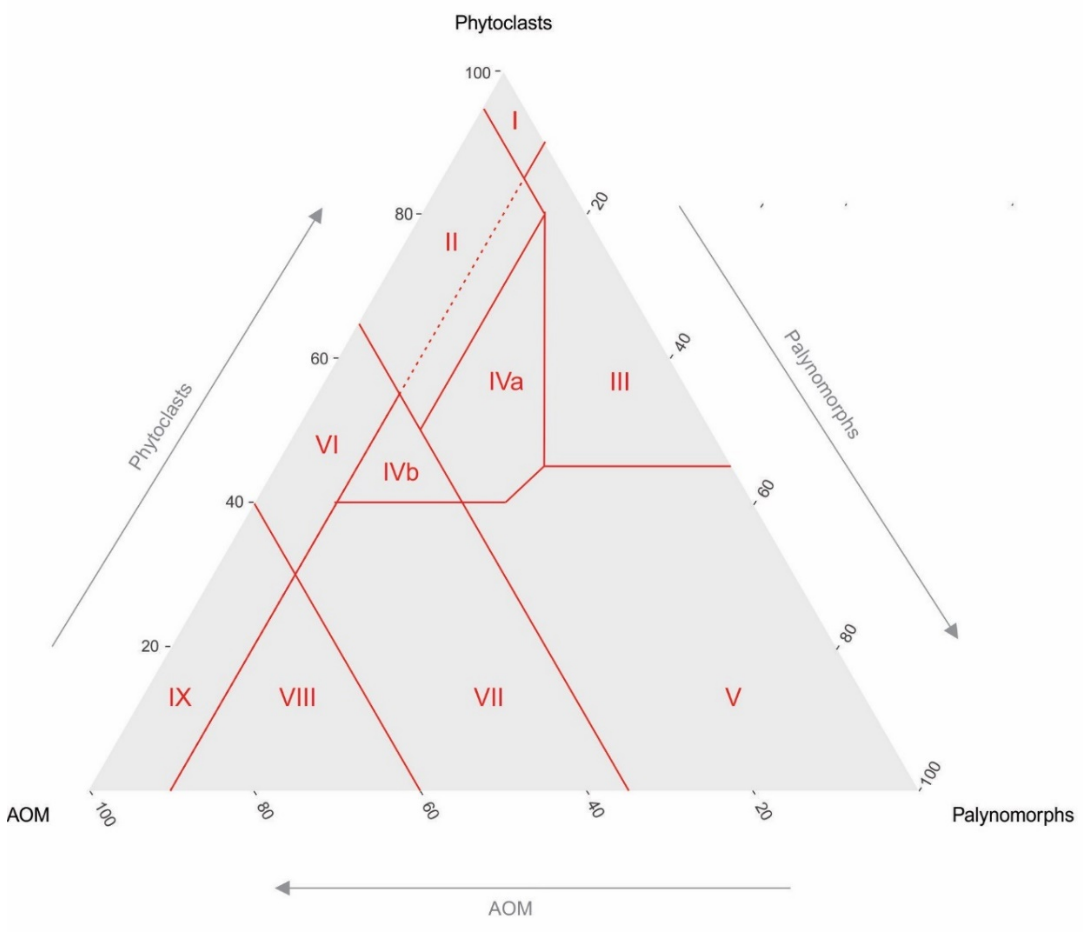

I: Highly proximal shelf or basin	IV: Shelf to basin transition	VII: Distal dysoxic-anoxic 'shelf'
II: Marginal dysoxic-anoxic basin	V: Mud-dominated oxic shelf ('distal shelf')	VIII: Distal dysoxic-oxic shelf
III: Heterolithic oxic shelf ('proximal shelf')	VI: Proximal suboxic-anoxic shelf	IX: Distal suboxic-anoxic basin

Figure 30. Ternary diagram from Tyson (1993), which distinguishes different paleoenvironments based on the relative abundance of AOM, Phytoclasts and Palynomorphs.

5.4 Branch Stream results

Figure 31 shows the distribution of various palynodebris subgroups from Branch Stream. Amorphous organic matter, along with brown and black phytoclasts dominate the assemblages from this section. Palynomorphs are relatively sparse overall.

Description

Samples from the Herring Formation contain only a minor component of AOM. Brown and black phytoclasts comprise the majority of organic material and the black:brown ratio is strongly positive immediately below the contact with Branch Sandstone. In the lowest sample from the section, marine palynomorphs are relatively abundant, but terrestrial palynomorphs are rare. At the base of the Branch Sandstone, a rapid increase in AOM to up to 30% of the total assemblage is observed. Greater numbers of terrestrial palynomorphs are recorded and the black-brown ratio decreases to 0.3 at 3.7m. At 3.7m a spike in other phytoclasts occurs, driven largely by an increase in cellular membranes.

In the interval from 1.7m to the top of the Branch Sandstone, AOM increases and the abundance of black phytoclasts declines. The proportion of other phytoclasts and brown phytoclasts barely fluctuates, with the exception of a spike in brown phytoclasts at 0.5m. The abundance of the palynomorph group increases within the interval.

Above the Branch Sandstone-Mead Hill Formation contact, brown phytoclast content increases markedly, resulting in a negative black:brown $\log_{10}$ ratio. Additionally, a spike in terrestrial palynomorphs occurs, and a fall in amorphous organic material.

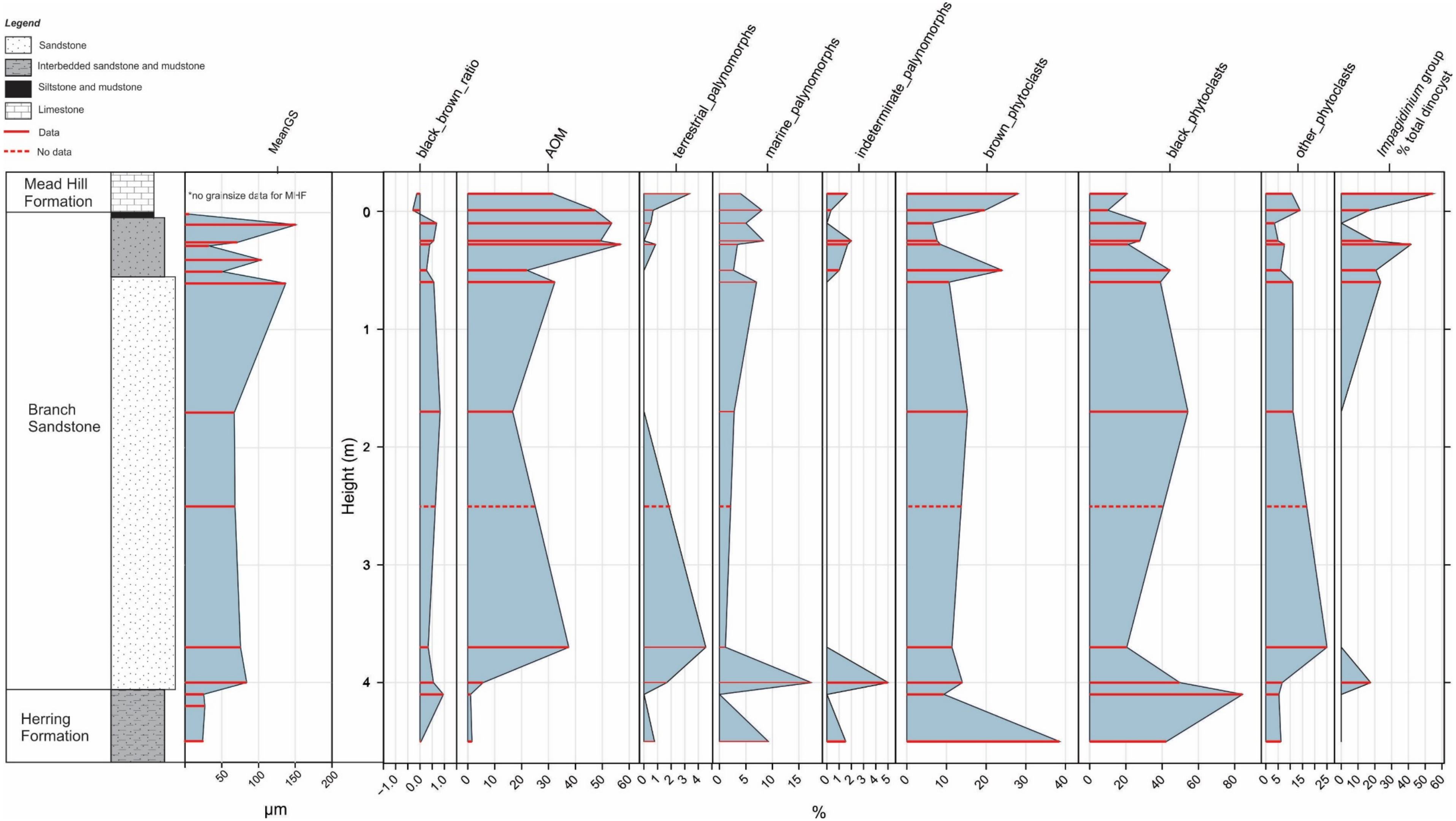

Figure 31. Grouped palynodebris from Branch Stream.

Interpretation

Plotting samples from Branch Stream on the Tyson (1993) diagram shows a large amount of scatter. Herring Formation samples plot close to the apex of the diagram, in fields I and III. Based on these values, Herring Formation is interpreted to have been deposited in a highly proximal to proximal shelf environment.

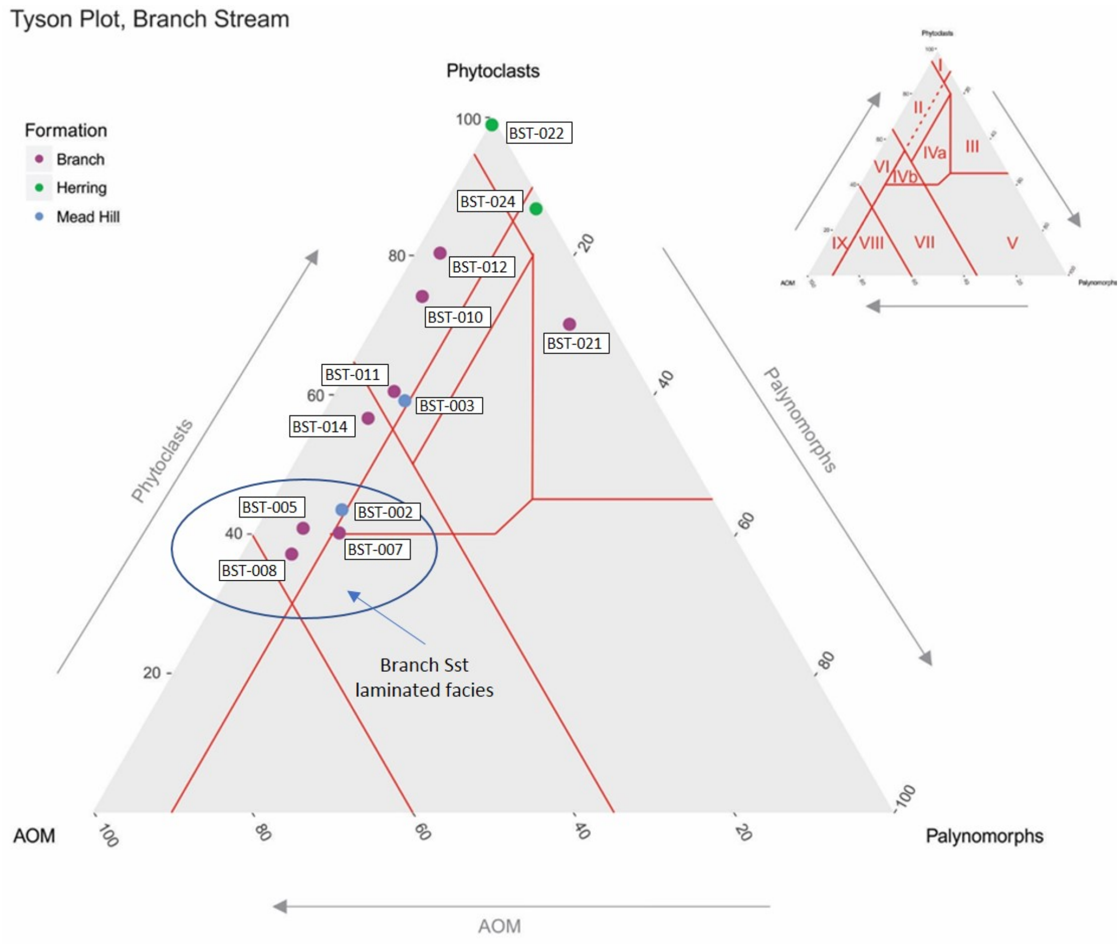

Figure 32. Palynofacies samples from Branch Stream plotted on Tyson (1993) ternary diagram.

With the exception of two outliers, samples from the Branch Sandstone (purple) plot in fields II and VI of the ternary diagram. These fields are defined as marginal dysoxic and anoxic basin, and proximal suboxic-anoxic shelf. Based on the distribution of the samples, marine conditions likely fluctuated somewhat.

Notably, samples from the uppermost Branch Sandstone plot in the lower section of field VI, whilst samples each side of the Branch Sandstone-Mead Hill Formation contact plot in, and adjacent to field IV. This field is representative of the shelf-basin transition. This may suggest a minor shallowing toward the top of the Branch Sandstone, followed by deepening coincident with deposition of the Mead Hill Formation. The abundance of the *Impagidium* group throughout the upper interval, however, indicates a relatively oceanic setting overall.

5.5 Angora Stream results

Figure 33 shows the distribution of various palynodebris subgroups from Angora Stream. The assemblage is dominated by black phytoclasts, although brown phytoclasts and other phytoclasts are common. Palynomorphs are relatively sparse overall, but comprise a larger percentage of all organic matter in comparison with Branch Stream.

Description

Within the Glenburn Formation, AOM constitutes only a minor fraction of the total assemblage. Marine palynomorphs are relatively abundant, whilst terrestrial palynomorph content is negligible. Directly below the contact of the sandstone A, black phytoclast content is relatively low, and the black to brown ratio approximates zero. The other phytoclast group largely consists of cellular membranes, and comprises around 10-15% of the total assemblage.

In the interval from the base of sandstone A to 1.25m, AOM broadly increases upsection. Terrestrial palynomorphs comprise only a minor fraction of the total assemblage, but also appear to increase upward. Brown phytoclast content increases upward, whereas black phytoclast abundance declines. A peak in other phytoclasts, largely comprising cellular membranes, occurs at 1.25m.

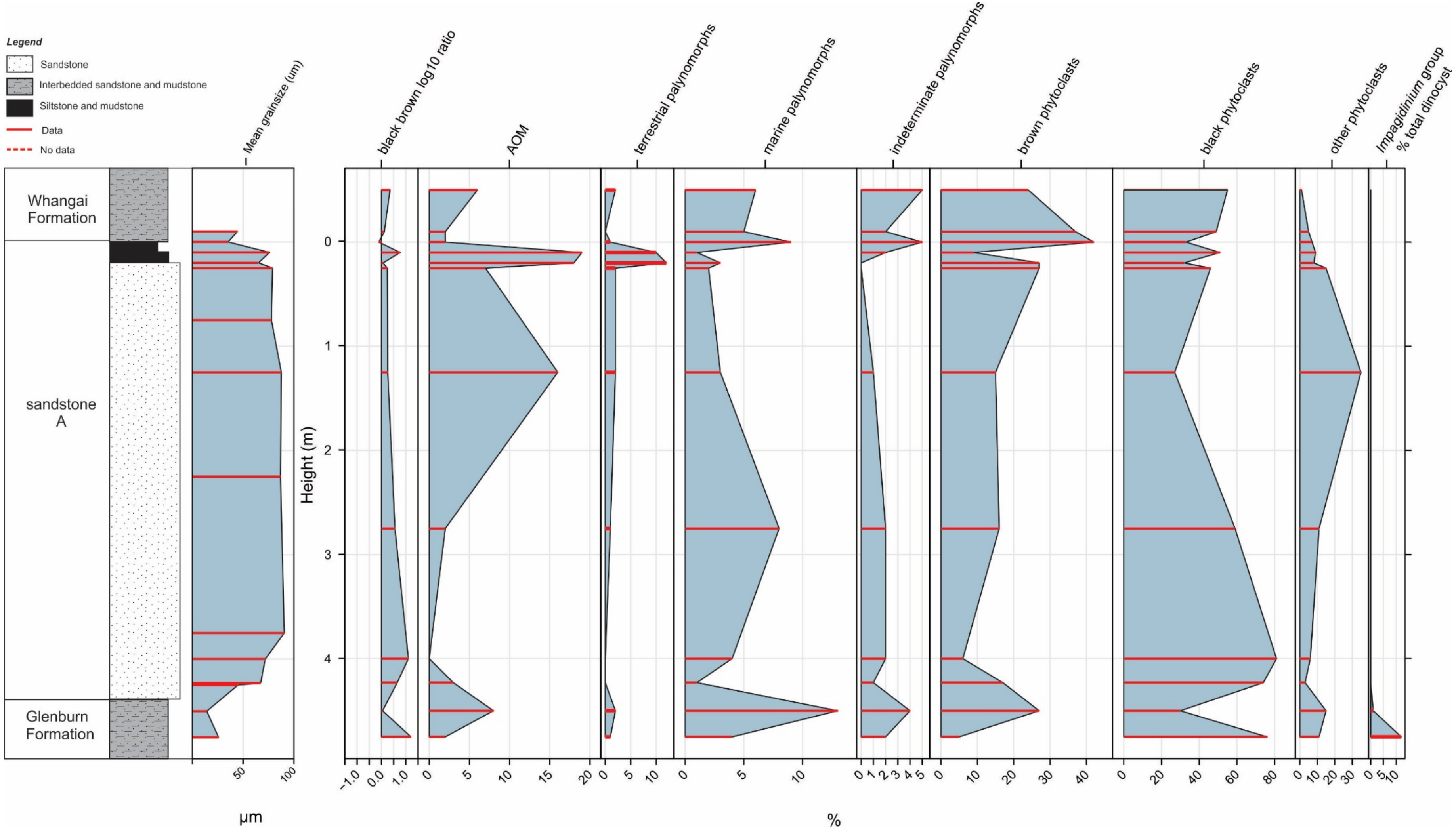

Figure 33. Plot showing distribution of palynofacies categories from Angora Stream.

A pronounced spike in both AOM and terrestrial palynomorphs occurs immediately below the sandstone A-Whangai Formation contact. Brown phytoclast content decreases and there is a fall in marine palynomorph abundance. Black phytoclast content fluctuates though the small sampling interval, however maintains a relatively constant increasing trend from 1.25m to the top of the section. Conversely, other phytoclasts decline in abundance through the contact and in the lower Whangai Formation.

Above the Whangai-sandstone A contact, the percentage of AOM is low. Marine palynomorphs are relatively abundant, whilst terrestrial palynomorphs are comparatively rare. The black to brown phytoclast ratio remains positive, apart from a negative excursion immediately above the contact.

Interpretation

The distribution of samples from Angora Stream with respect to Tyson's (1993) ternary diagram is shown in Figure 34. In this format, it is notable that phytoclasts form an overwhelming proportion of the total organic matter at Angora Stream. Samples from the Glenburn Formation plot within fields I and III. The high proportion of terrestrially derived material in the Glenburn Formation is suggestive of deposition in a highly proximal shelf or basin to proximal shelf environment. Specimens from the *Impagidinium* group are relatively common at the base of the section, however, giving some indication of oceanic conditions.

There is considerable variation in samples from sandstone A, which plot in fields I, II, III and IV. These fields correspond to environments ranging from proximal shelf to marginal basin. Because of this scatter, it is difficult to establish a paleoenvironmental interpretation for sandstone A unit based on organic material alone, however, it is notable that a high proportion of all material is terrestrially derived.

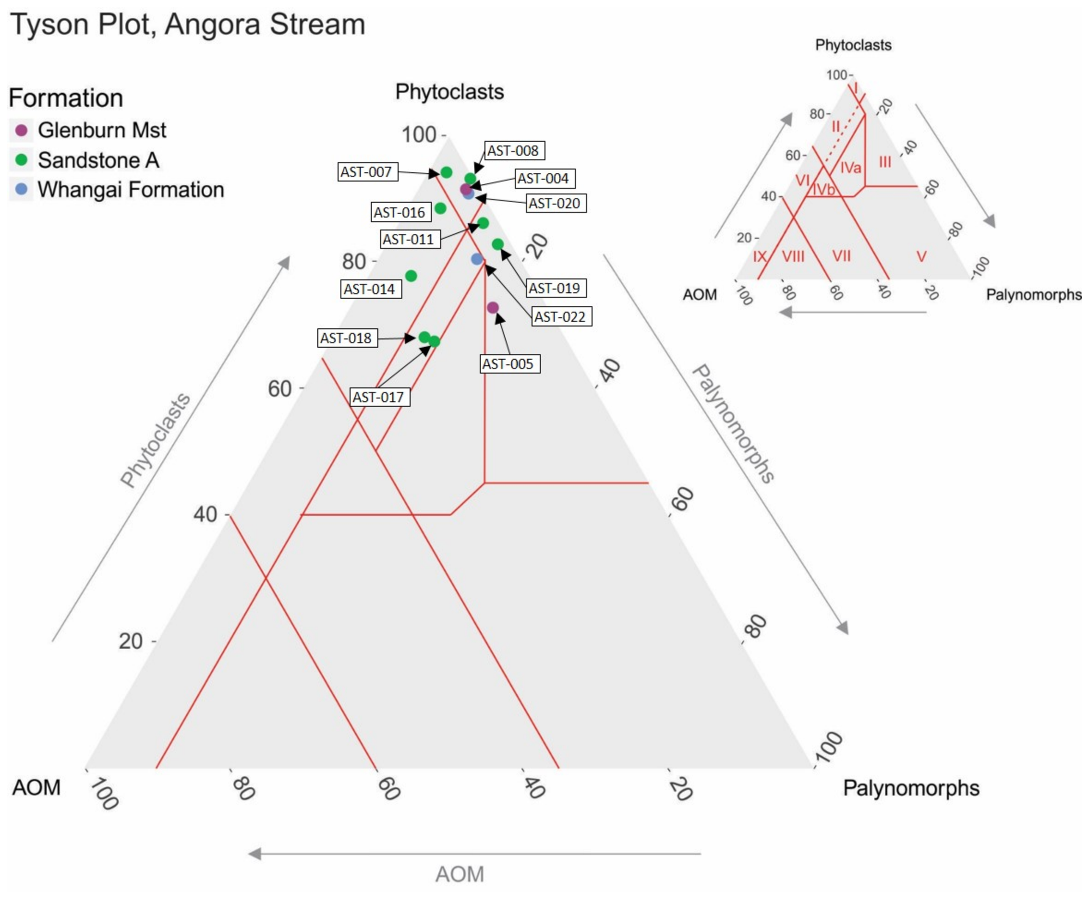

Figure 34. Palynofacies samples from Angora Stream plotted on Tyson (1993) ternary diagram

A declining black to brown phytoclast ratio possibly indicates a shallowing toward the top of the sandstone facies. This is supported by an influx in terrestrial palynomorphs immediately below the upper contact of the sandstone A. This event, however, also coincides with increasing mudstone content and a reduction in mean grain-size, so could be facies related. The absence of the *Impagidinium* group in sandstone A is non-instructive, as dinoflagellate abundance was low in the majority of the unit.

Whangai Formation samples plot within fields I and II of the Tyson ternary plot, which corresponds with proximal-marginal basin conditions. Deepening is indicated by increased marine palynomorph content, although again the effects of lithologic control cannot be ruled out. The black-brown phytoclast ratio becomes increasingly positive above the contact, though further samples are required to confirm this trend.

5.6 Tangaruhe Stream results

Figure 35 shows the distribution of various palynodebris subgroups from Tangaruhe Stream. The assemblage is dominated by black phytoclasts and AOM. The section contains the greatest abundance of marine palynomorphs overall, and the fewest terrestrial palynomorphs.

Description

Within the lower half of the section, coinciding with the Tangaruhe Formation, AOM is moderately abundant. The proportion of AOM increases upsection, toward the Tangaruhe-Whangai contact. Marine palynomorphs equate to around 5% of the total assemblage below the contact, while terrestrial palynomorph content is negligible. Brown phytoclast content broadly decreases upward, whilst black phytoclast abundance remains relatively constant at ~60%.

A marked change in palynodebris composition occurs across the Tangaruhe-Whangai Formation contact. Above the contact, the abundance of black and brown phytoclasts broadly halves. AOM is far more prevalent, comprising up to 60% of the total organic fraction. Marine palynomorphs are most abundant in this interval, comprising ~13% of all palynodebris at -0.25m. Terrestrial and indeterminate palynomorphs, as well as other phytoclasts, are a negligible proportion of organic material within the Whangai Formation.

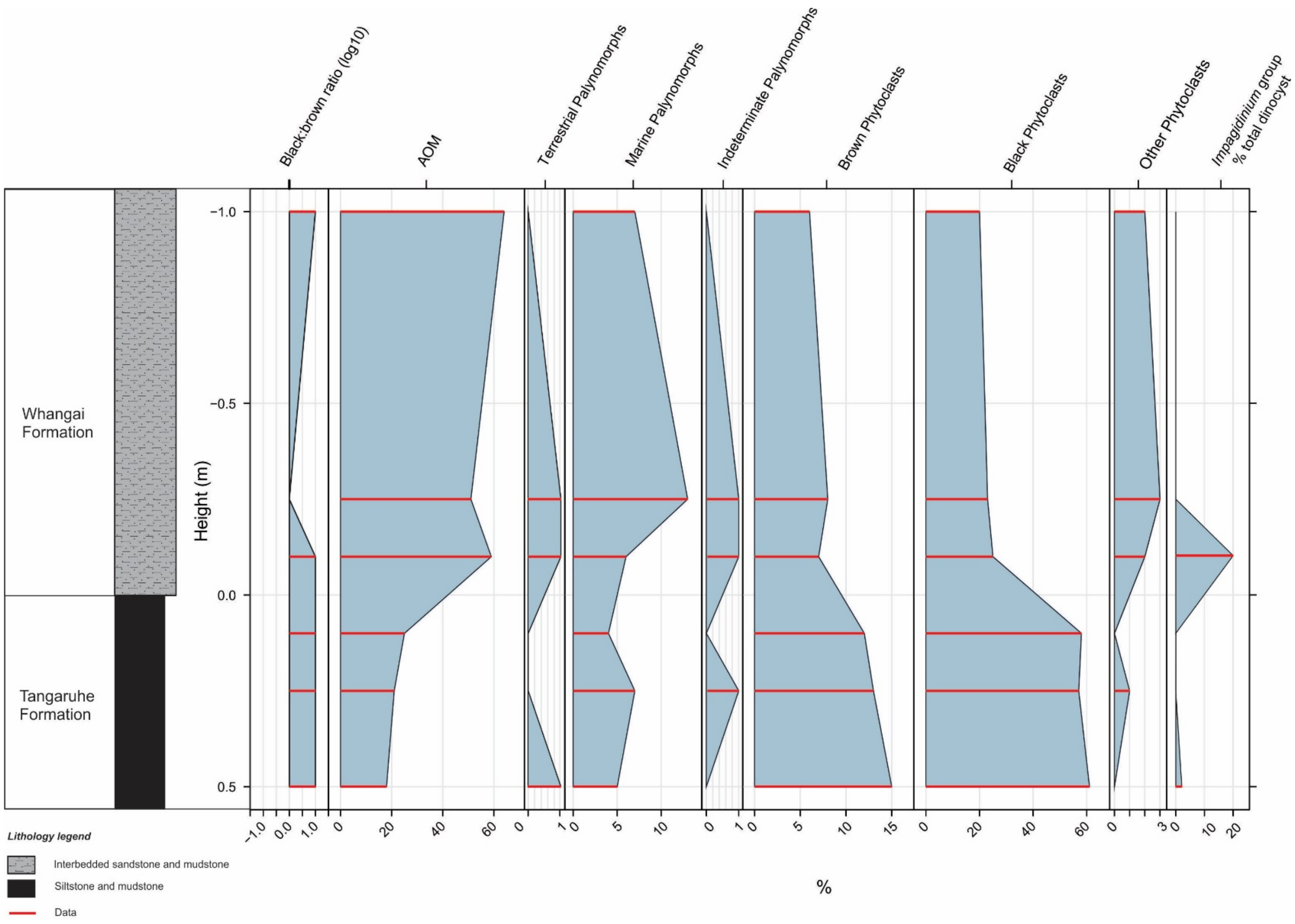

Figure 35. Tangaruhe Stream palynofacies plot.

Interpretation

The ternary diagram of Tyson (1993) indicates that, at Tangaruhe Stream, the Tangaruhe Formation and overlying Whangai Formation have been deposited in relatively distal marine environments.

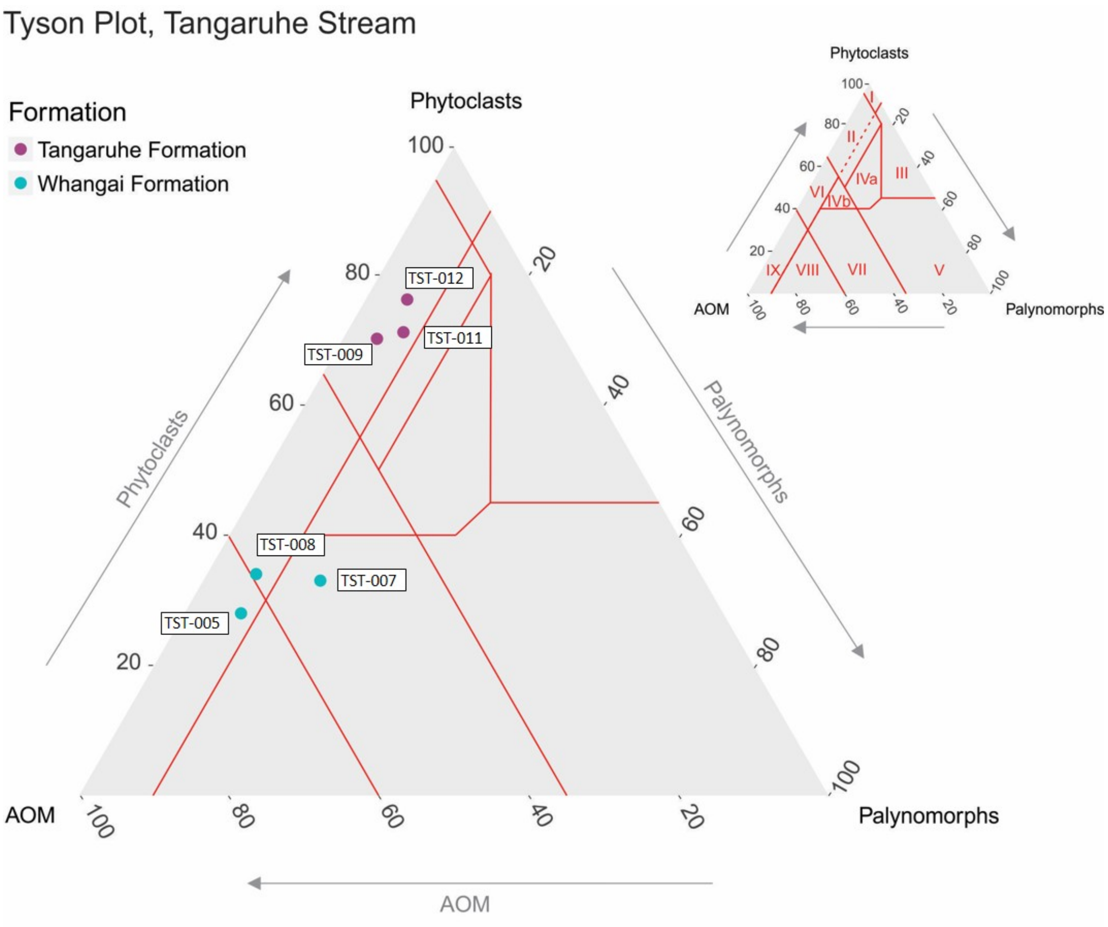

Figure 36. Palynofacies samples from Tangaruhe Stream plotted on Tyson (1995) ternary diagram.

Samples from the Tangaruhe Formation plot within the marginal dysoxic-anoxic basin field (Figure 35). This interpretation is supported by data shown in Figure 36, which indicates a high relative abundance of marine palynomorphs with respect to terrestrial palynomorphs, and a strongly positive black:brown phytoclast ratio. Both these indicators are interpreted to signify that the depositional environment was relatively distal from a source of terrestrial inputs.

Based on the Tyson diagram, samples from the Whangai Formation within multiple fields (VI, VII & IX). These samples are reasonably well clustered, however, and indicate a change from relatively oxic conditions during the period in which the Tangaruhe Formation was deposited, to largely anoxic conditions. Based on palynofacies data Whangai Formation is suggested to have been deposited in a distal, but likely shelfal environment.

6 Discussion

This chapter integrates results from this thesis with regional data to interpret depositional environments at each field location. The depositional environments of Branch Sandstone and sandstone A are discussed in the context of under- and overlying formations, and findings from Tangaruhe Stream are summarised. Finally, relationships between the three sections are interpreted and compared with the eustatic sea level curve of Haq (2014).

6.1 Southeast Marlborough

6.1.1 Depositional environment

Branch Sandstone is interpreted as a marine deposit, based on the dinocyst assemblage recovered from the formation. Further, deposition of Branch Sandstone is suggested to have occurred in a shelfal setting, based on evidence presented in Chapters 3, 4 and 5. A shelfal marine interpretation is consistent with findings from laser particle grain-size analysis, which shows that the Branch Sandstone is a very fine to fine grained sandstone containing a significant silt fraction. Very fine sandstones containing significant proportions of silt have been documented to occur in the lower shoreface to offshore transition portions of the continental shelf (e.g. McCubbin, 1982, Dunbar & Barrett, 2005).

With respect to grain-size alone, however, the deposit could represent a restricted marine environment, such as an estuarine or lagoonal setting. Multiple lines of evidence make such an interpretation unlikely. First, the presence of the dinoflagellate genus *Impagidinium* is indicative of open marine settings. Second, assemblages of organic matter from Branch Sandstone contain a significant proportion of marine-derived material. Finally, there is no specific sedimentological or paleontological evidence for estuarine/lagoonal deposition – sedimentary structures are absent, as are macrofossils.

At Branch Stream, however, most of Branch Sandstone is heavily bioturbated, so the paucity of sedimentary structures may not be a primary depositional feature. Nevertheless, extensive bioturbation throughout the massive portion of the unit may suggest that the sandstone is unlikely be the product of a density current or mass emplacement event. Additionally, there is no biostratigraphic evidence for redeposition of older sediments, although, it is recognised that dinoflagellates are generally rare in the major sandstone interval. Finally, the unit coarsens upward in grain-size, which is inconsistent with deposition in a mass emplacement event. Sandstone beds of turbidites, for example, commonly display an upward decrease in grain-size or are ungraded (Shanmugam, 1997; Shanmugam & Moiola, 1988; Walker, 1992). The level of bioturbation present in Branch Sandstone, is also supportive of a shelfal marine interpretation, where sub-environments such as the lower shoreface and offshore transition commonly exhibit extensive bioturbation (e.g. McCubbin, 1982 and references therein).

Palynofacies data presented in Chapter 5 suggest that the lower part of Branch Sandstone, corresponding with massive facies, was deposited in a marginal dysoxic basin. Organic assemblages from the upper part of the Branch Sandstone, corresponding with a laminated facies, suggest deposition in a proximal suboxic-anoxic shelf environment. Overall, therefore palynofacies data are consistent with a shelfal marine interpretation, and a general upward shallowing trend within the Branch Sandstone is supported by an upward increase in grain-size at Branch Stream.

Whether Branch Sandstone accumulated over a short period in response to changes in sedimentation rates, or whether it was deposited over a lengthy period is uncertain. The dinoflagellate biostratigraphy presented in this research can only constrain the period of deposition to a single dinoflagellate interval zone. Regional biostratigraphic studies are likely to result in more clarity, for example, detailed dinoflagellate biostratigraphy through the Mororimu Stream section may indicate that Branch Sandstone at that locality was deposited across a significantly expanded time interval (see section 6.1.2).

6.1.2 Relationships with enclosing formations

Figure 37 shows the chronostratigraphy of the Branch Stream section based on the biostratigraphy presented in Chapter 4. Stratigraphy is displayed as a function of proximity to shoreline, primarily based on data presented in this thesis, but drawing on information from regional studies (e.g. Crampton et al., 2003; Laird, 1992; Morris, 1987; Reay, 1993; Reay & Strong, 1992).

Herring Formation is interpreted as the most proximal deposit of the three formations encountered in the Branch Stream section. This inference is based predominantly on palynofacies data, which show that over 90% of all organic matter in samples from Herring Formation was terrestrially derived. The Herring Formation immediately below Branch Sandstone at Branch Stream comprises massive silt rich facies, although further downsection, and at other localities displays some sedimentological characteristics that would be consistent with deposition in a restricted marine environment, such as an embayment, lagoon or estuary (e.g. flaser bedding in Figure 10b).

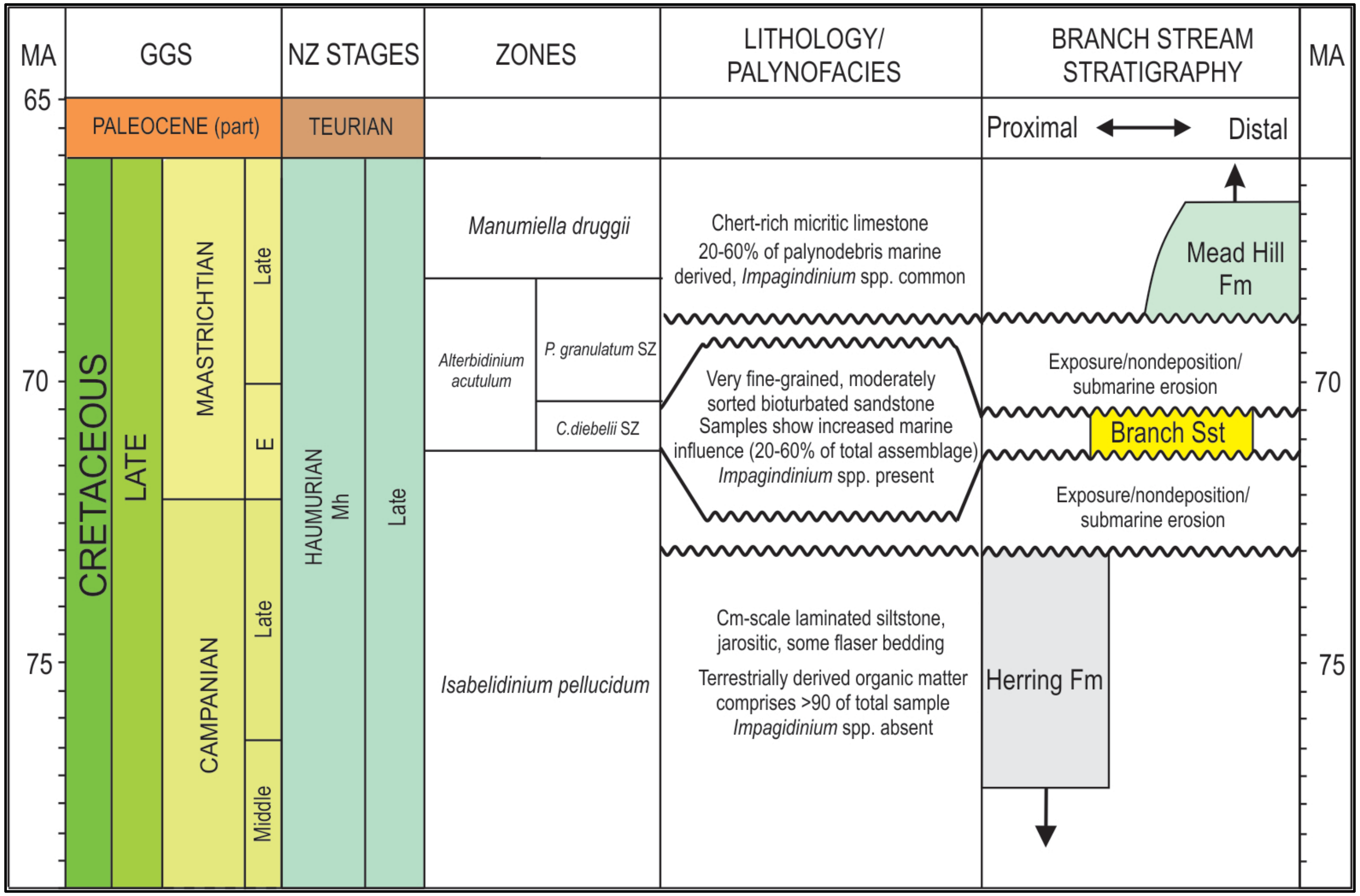

Figure 37. Summary of stratigraphy and palynofacies of the Branch Stream section.

In the middle Clarence valley area, Herring Formation has previously been described as being deposited in dysaerobic inner shelf conditions (Crampton et al., 2003; Laird, 1992; Morris, 1987). Whilst this is probable for much of the Herring Formation, the preferred interpretation herein, is that uppermost Herring Formation was deposited in a marginal marine setting at Branch Stream. At Mororimu Stream, biostratigraphic evidence from other research is broadly supportive of this assertion: a sample from the uppermost Herring Formation (1m below the Branch Sandstone) indicates a highly proximal marine environment (sample P31/f64; data from Dr J.I. Raine, 1990, and Dr G.J. Wilson, 1989, retrieved from the New Zealand Fossil Record File, https://fred.org.nz/fred/). This sample from Mororimu Stream is dominated by terrestrial material and contains a moderately rich assemblage of spores and pollen.

The biostratigraphic component of the present study indicated that Branch Sandstone disconformably overlies Herring Formation at Branch Stream. This is consistent with lithological evidence from field studies at other localities, including Wharekiri Stream, where the lower contact is sharp and heavily burrowed (Figure 38), and Bluff Stream where the base Branch Sandstone comprises a poorly sorted matrix supported pebble conglomerate (Laird, 1992; Reay, 1993).

Figure 38. Heavily burrowed base of Branch Sandstone at Wharekiri Stream. Photo courtesy of James Crampton.

A change in paleoenvironmental conditions is therefore interpreted at the Herring-Branch boundary resulting in a period of either erosion, or non-deposition, which was followed by an influx of more sand-rich sediment.

The significance and temporal extent of the disconformity at the base of Branch Sandstone is currently unclear. At localities other than Branch Stream, the Herring-Branch Sandstone contact shows some characteristics indicative of a transgressive surface, such as the burrowed surface documented at Wharekiri Stream and the pebble lag at Bluff Stream.

Branch Sandstone overlies the disconformity and is interpreted to have been deposited in a more distal environment that the Herring Formation. This is consistent with palynofacies data which show a greater marine influence in the Branch Sandstone, as well as the presence of *Impagidinium* spp. The basinward shift in facies implied by a transition from coastal facies (Herring Formation) to marine facies (Branch Sandstone) is also indicative of marine transgression.

Some shallowing of the marine environment at the top of the Branch Sandstone is indicated by the palynofacies data presented in Chapter 5, and is consistent with overall upward coarsening in grain-size indicated by laser particle analysis. It should be noted, however, that the relative abundance of all marine derived organic matter increases noticeably at the top of Branch Sandstone, so the evidence for upward shallowing in the Branch Sandstone is not conclusive.

Branch Sandstone is disconformably overlain by Mead Hill Formation at Branch Stream. The length of time not represented in deposits from this section is poorly constrained, and could range from a period of a <1myr to ca ~5myr. An ongoing fall in relative sea level, consistent with shallowing observed in uppermost Branch Sandstone, may have resulted in subaerial exposure and a period of non-deposition and/or erosion.

At its base, Mead Hill Formation is inferred to have been deposited at similar depths to the Branch Sandstone, but the relative depth of deposition increases upward. The organic matter assemblage and abundance of *Impagindinium* spp. from Mead Hill Formation samples is consistent with this interpretation. Deposition of the basal Mead Hill Formation has elsewhere been interpreted as occurring in mid- to inner shelf conditions, based on foraminifera (Reay & Strong, 1992; Strong et al., 1995). Foraminifera are indicative of an upward deepening trend, and water depths are thought to have reached bathyal conditions by the end of the Cretaceous (Strong et al., 1995). A clear change in paleoenvironmental conditions occurred in association with deposition of the basal Mead Hill Formation, as indicated by a sharp reduction in clastic content and marked shift in lithofacies. This may suggest that, during marine transgression, sediment was trapped further back on the shelf.

Based on data presented in Figure 37, the Branch Sandstone and Mead Hill Formation at Branch Stream represent a transgressive succession of facies, indicative of progressive deepening, although these are punctuated by depositional hiatuses. This model is broadly consistent with the depositional model proposed by Reay and Strong (1992), as illustrated in Figure 39.

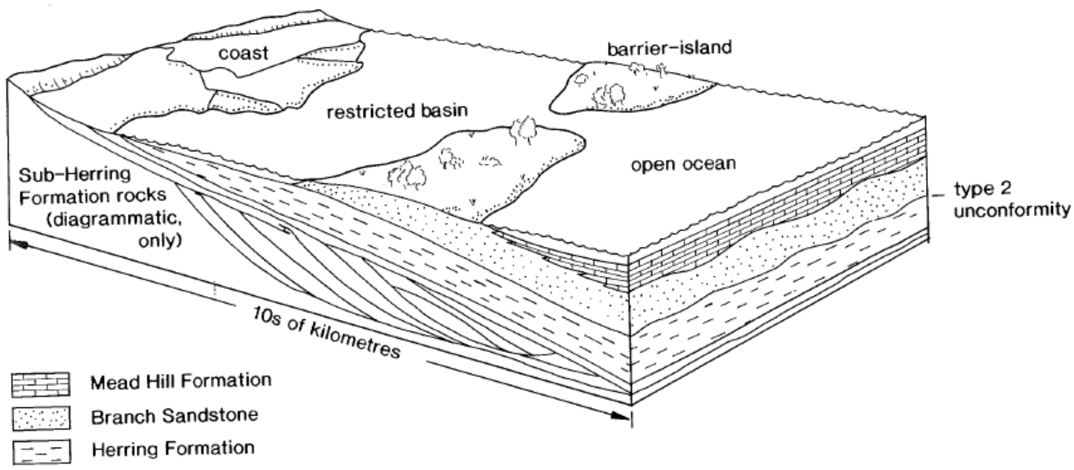

Figure 39. Depositional model for Branch Sandstone from Reay and Strong (1992).

Reay and Strong's (1992) model suggests a restricted marine origin for Herring Formation, such as an estuary or lagoon. Branch Sandstone is described as an emergent barrier island sandstone, which migrated landward along with the shoreline during ongoing marine transgression. It is uncertain, however, if the regional extent of the Branch Sandstone is consistent with a barrier bar origin. Additional uncertainty results from the lack of coarse grained, well-sorted shoreface deposits within the overall sedimentary succession, though it is possible these have been removed by erosion. During transgression, for example, barriers are expected to move landward, and upper shoreface and beach deposits associated with the original bars are eroded and redeposited elsewhere (Figure 40).

Image removed for copyright reasons.

Figure 40. Transgression of barrier sandstone by shoreface retreat (Boggs, 2006).

It is plausible, therefore, that Branch Sandstone was deposited as a barrier island system, although equally, the formation could simply comprise a lower shoreface-shelfal sand. Regional data presented in Chapter 3 shows no consistent trend in the thickness of Branch Sandstone in Marlborough, although the thickest exposures occur in a separate fault block to the east (paleo-north), at Puhi Puhi River and Mororimu Stream.

The cause of the observed changes in thickness is uncertain, but could include localised tectonic activity, pre-existing topography, depositional topography, distance from sediment source, erosion of the upper portions of some sections or some combination of these factors. At Branch Stream, the disconformity at the top of Branch Sandstone may indicate the removal of some unknown thickness of sediment. Conversely, at localities such as Mororimu Stream and Puhi Puhi River, chert and dolomite are interbedded with upper Branch Sandstone, perhaps indicating a gradational contact. Erosion related variability in thickness of Branch Sandstone can therefore not be ruled out. Despite this, sites immediately adjacent to Mororimu Stream and Puhi Puhi River exhibit rapid changes in thickness, for example a change from 42m to 3m over a distance of 5km.

Tectonic influences on Branch Sandstone thickness cannot be ruled out for two reasons. First, Nicol (1993) documented evidence for extensional tectonic activity in North Canterbury during the period in which Branch Sandstone was deposited. Second, the Herring Formation contains numerous siliciclastic dykes, which comprise sandstone that has been injected upward. Clastic dykes are believed to form in response to a number of factors, which include, but are not limited to, tectonic stress and seismicity (Jolly & Lonergan, 2002).

Overall, the Branch Stream section comprises a transgressive succession of facies, punctuated by depositional hiatuses. Uppermost Herring Formation is interpreted to have been deposited in highly proximal conditions, and is overlain by an unconformity that is thought to coincide with a fall in relative sea level. At this time the Branch Stream section is thought to have been subaerially exposed, resulting in erosion/non-deposition, whilst the locus of marine deposition shifted basinward. Following this, marine transgression, consistent with overall basin subsidence, resulted in the locus of sedimentation moving back to the site of Branch Stream. A minor fall in sea level is indicated by shallowing at the top of Branch Sandstone, and an unconformity, potentially due to subaerial exposure. Around this time, clastic sediment input into the basin appears to have been shut off, resulting in development of the carbonate facies of Mead Hill Formation.

6.2 Angora Stream

6.2.1 Depositional environment

Based on evidence presented in Chapters 3 and 4, sandstone A at Angora Stream is interpreted to be the product of a sediment gravity flow, most likely deposited at bathyal depths. Despite this interpretation, palynofacies data presented in Chapter 5 may be more consistent with deposition in a proximal shelfal setting.

Sandstone A is interpreted to lie within a conformable succession, surrounded by silt-rich facies of the Glenburn and Whangai Formations. Deposition by density current is consistent with findings from laser particle grain-size analysis, which shows that sandstone A is a fine to very fine sandstone that subtly fines upward. Additional evidence for a submarine fan or turbidite interpretation is provided by both lithological studies and biostratigraphy. First, sandstone A has very fine scale planar lamination at the base, and in the upper parts of the sandstone. Additionally, the unit becomes increasingly micaceous toward the top, which could indicate some density sorting, with mica being deposited in falling energy conditions.

The presence of sedimentological characteristics such as lamination, sediment grading and density sorting is consistent with sedimentological models of submarine fans (Howell & Normark, 1982; Shanmugam & Moiola, 1988). Furthermore, the abundance of allochthonous dinoflagellate assemblages toward the base of the sandstone indicates an influx of reworked sediments, which is consistent with a rapid depositional event.

Whilst submarine fans may accumulate in a range of water depths, deposition of Glenburn Formation at bathyal depths has previously been suggested by Crampton (1997) and Leckie et al. (1992). Importantly, samples taken from below the sandstone A contact, contain a foraminifera assemblage indicative of bathyal depths (Leckie et al., 1992). A literal reading of the Tyson (1993) plot, however, indicates that the entire Angora Stream section was deposited in a proximal, probably shelfal environment which is inconsistent with a bathyal interpretation. Further, classification of the palynofacies data into binary marine and terrestrial categories shows that over 75% of the material in every sample has a terrestrial origin. It is also worth noting that leaf cuticle material, which often has a strong association with fluvio-deltaic and proximal depositional settings (Tyson, 1995 and references therein) is abundant in multiple samples.

Palynofacies data could therefore point to a depositional setting highly proximal to a terrestrial source of organic material. Despite this, studies of modern and ancient submarine fan and turbidite successions from deep sea settings, have indicated that these deposits are often enriched in leaf cuticle material, as this material bypasses the shelf and is funnelled to distal oceanic settings (Boulter & Riddick, 1986; McArthur et al., 2017; Schnyder et al., 2017; Stanley, 1986). Given recent interpretations of greater Glenburn Formation suggest the unit is derived from sediment gravity flows deposited at bathyal depths (Crampton, 1997; Leckie et al., 1992), a similar depositional setting is assigned to sandstone A in this study.

6.2.2 Relationships with enclosing formations

The entire section from Angora Stream is interpreted to sit within the *Isabelidinium pellucidum* interval zone and thus no significant depositional hiatus or unconformity is recognised (Figure 41). Sandstone A is interpreted as the product of a density current, whilst the finer grained facies immediately below probably represent background conditions. Some degree of oceanicity is indicated by the presence of *Impagidinium* spp at the base of the section, which is consistent with an open marine setting. Further, as discussed above, foraminifera recovered from Angora Stream, at around 2m below the sandstone facies discussed herein, are indicative of bathyal depths (Leckie et al., 1995).

Based on the above, there is little information, other than the obvious facies changes to indicate a sudden change in depositional environment coincident with development of the sandstone facies at Angora Stream. The sandstone facies of the uppermost Glenburn Formation are therefore considered to represent ongoing deposition by sediment gravity flows in outer-shelf to bathyal marine conditions.

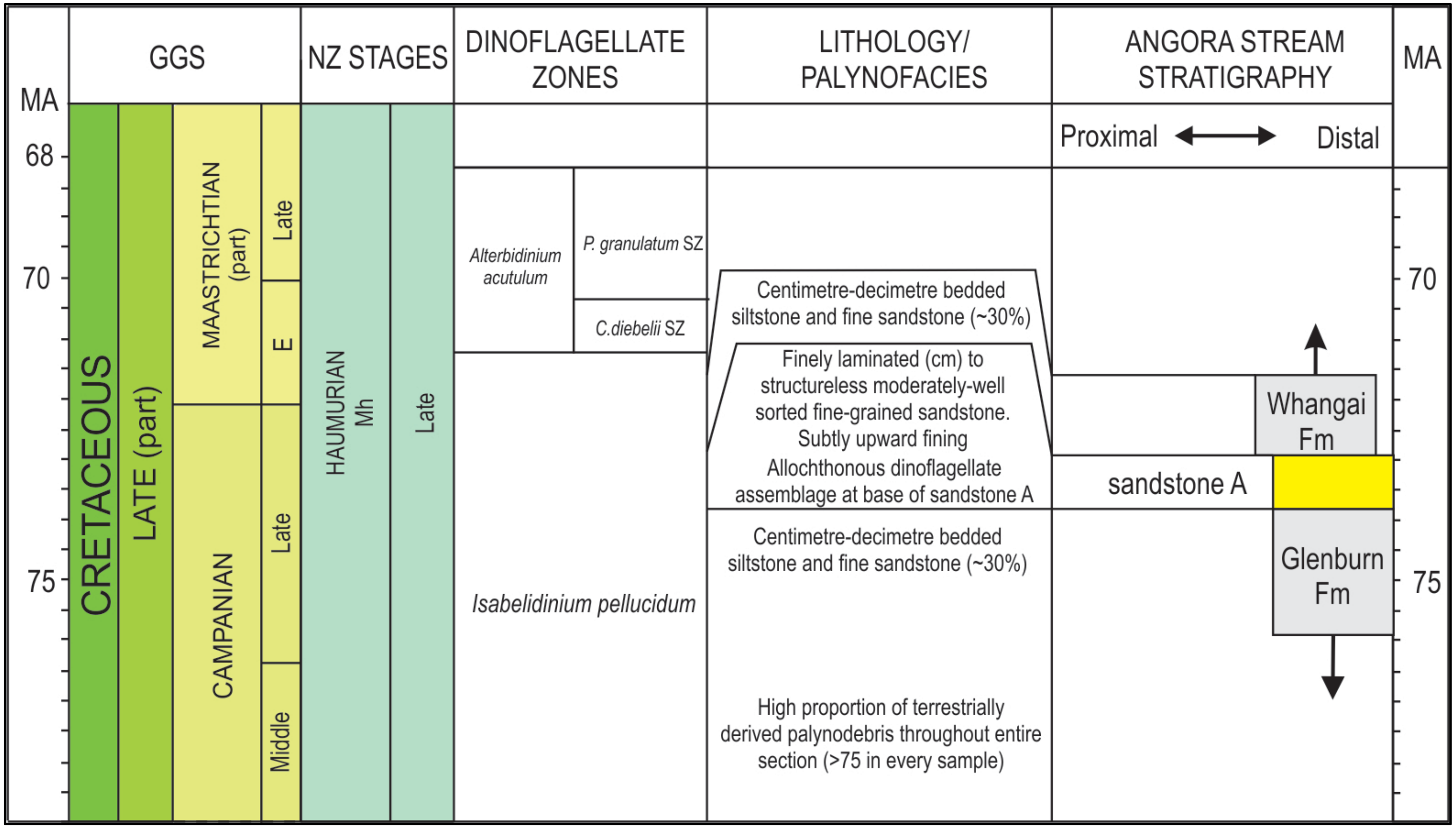

Figure 41. Stratigraphy and palynofacies of the Angora Stream section.

The overlying Whangai Formation comprises interbedded very fine sand and silt, displays planar lamination, and localised cross-stratification at a centimetre scale. The uppermost sample from the section contains relatively abundant dinocysts, consistent with a deposition in marine setting. Palynofacies analysis again indicates a mostly terrestrial source for Whangai Formation samples from Angora Stream. Whangai Formation is interpreted to have been deposited conformably on Glenburn Formation at Angora Stream, based on biostratigraphy.

There is no evidence to suggest a substantial change in water depth occurred at this locality and hence the lower Whangai Formation at Angora Stream is inferred to have similar origins to the upper Glenburn Formation. This is consistent with the findings of Leckie et al. (1995), who suggested that the lower Whangai Formation at Angora Stream was deposited in outer shelf to bathyal water depths, based on foraminifera.

6.3 Tangaruhe Stream

The primary aim at Tangaruhe Stream was to sample the contact between Tangaruhe and Whangai Formation, and establish any time equivalency with the other sections studied for this thesis. Biostratigraphy results indicate that multiple dinoflagellate interval zones are absent through the contact, suggesting either a lengthy period of non-deposition, or more probably, subaerial exposure and erosion (Figure 42).

Palynofacies analysis herein has suggested that the uppermost Tangaruhe Formation at Tanguruhe Stream was deposited in a marginal suboxic-anoxic basin. Studies of foraminifera assemblages from the formation have indicated deposition at depths exceeding 200m in an anoxic basin (Adams, 1985, C. P. Strong, pers. comm. 1989, in Crampton, 1997) so are broadly consistent with findings from organic matter assemblages. Basal Tangaruhe Formation facies (not encountered in this study) contain partial Bouma sequences and are interpreted as the product sediment gravity flows (Crampton, 1997). Upper Tangaruhe Formation, however, dominantly comprises mudstone and siltstone, that probably accumulated in a low energy environment (Crampton, 1997).

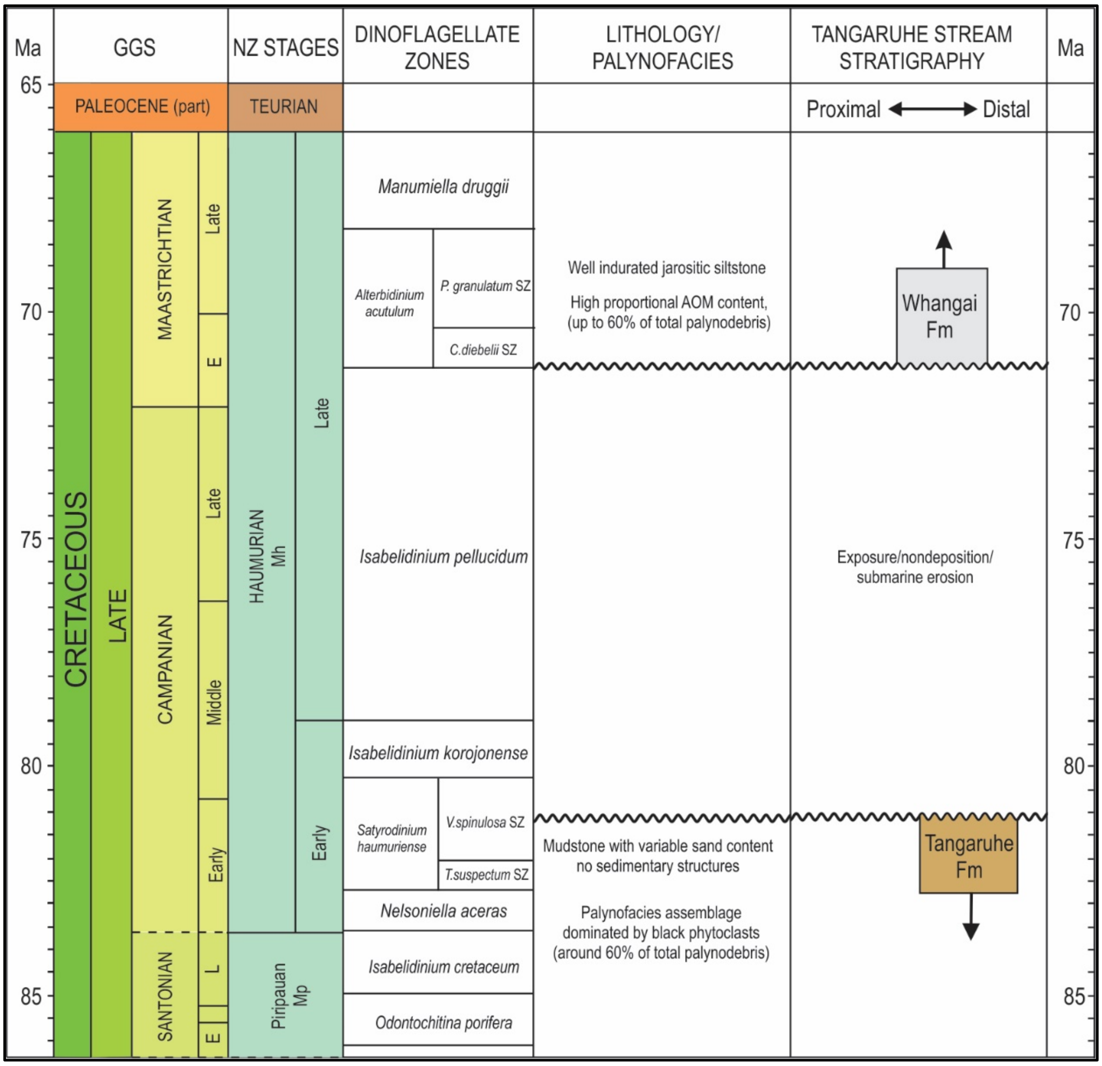

Figure 42. Stratigraphy and palynofacies of the Tangaruhe Stream section.

Palynofacies analysis indicates a slightly more proximal setting for the basal Whangai Formation at Tangaruhe Stream. Based on the lengthy hiatus between the Tangaruhe and Whangai Formations, a period of subaerial exposure seems likely. Submarine erosion remains a possibility, although this seems less likely, given that the lithologies of the upper Tangaruhe and lower Whangai formations are more indicative of low energy environs.

6.4 Relationships between sections

A chronostratigraphic synthesis of the three sections investigated in this thesis is shown in Figure 43. The dinoflagellate zonation is from Roncaglia et al. (1999) and the eustatic sea level curve is from Haq (2014). Based on the evidence discussed above, the age and approximate depositional settings of the three sections studied are summarised.

With existing biostratigraphic constraints, the development of a disconformity at the top of the Herring Formation at Branch Stream could coincide with several of Haq's (2014) sea level events, including KCa 4, 5, 6, 7 and KMa1. Deposition of the uppermost Glenburn Formation at Angora Stream, may also have occurred at a similar time, although, as the *Isabelidinium pellucidum* interval zone spans a period of approximately eight million years it is highly speculative to suggest that the events are temporally related. Branch Sandstone has been attributed to the *Cerodinium diebelii* interval subzone, thus the sea level events most likely to relate to the Branch Stream unconformity are KMa1 and KCa7, based on temporal proximity. According to Haq (2014), the KCa7 sea level event is of moderate amplitude (ranging from 25-75m), and is supported by oxygen-isotope data. The KMa1 event is of lower amplitude (<25m), but has been recognised in New Zealand (Haq, 2014). The New Zealand expression of KMa1 was documented by Crampton et al. (2006), based on quantitative analysis of dinoflagellate biostratigraphy from East Coast Basin successions.

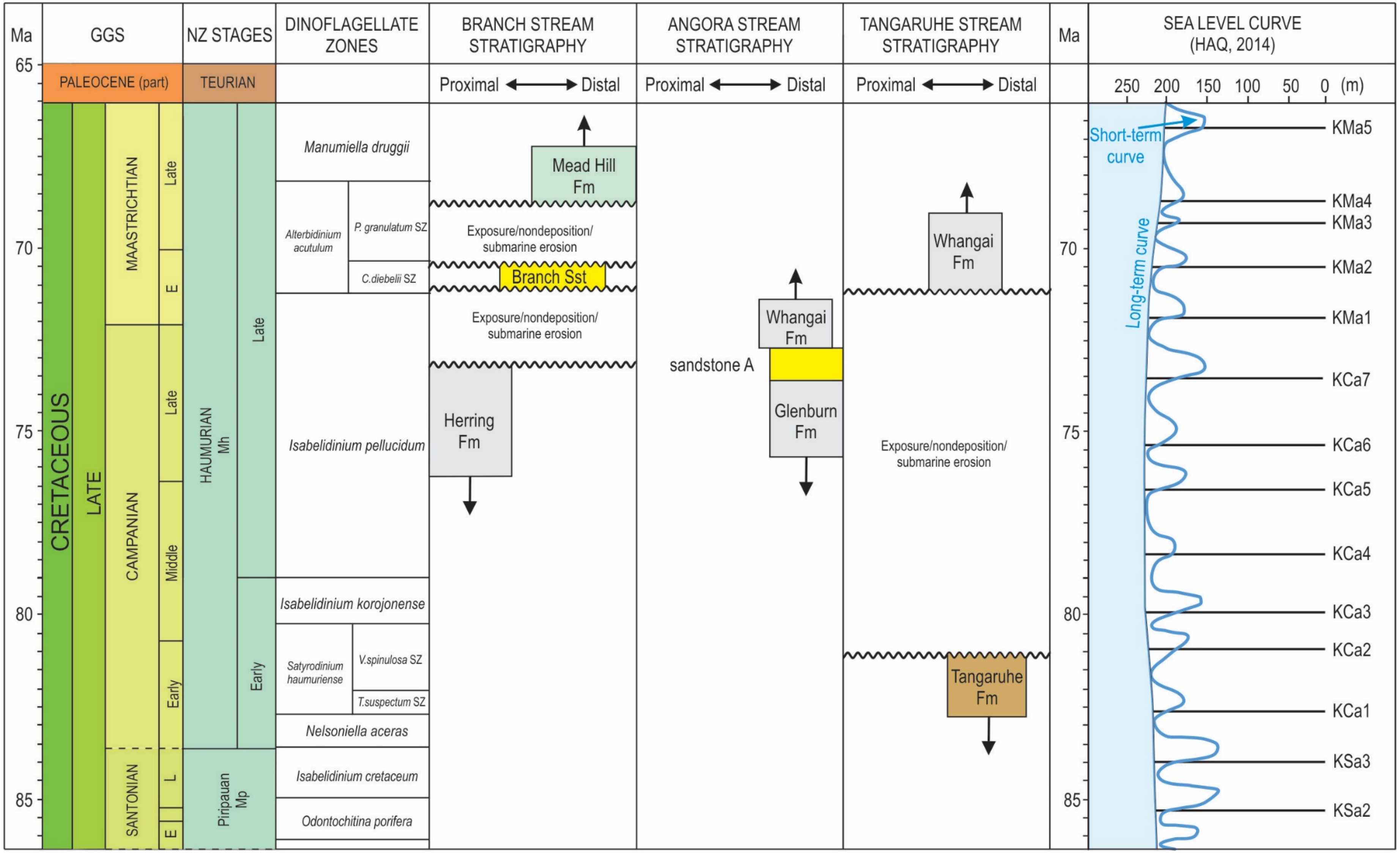

Figure 43. Approximate chronostratigraphy of Branch, Angora and Tangaruhe Stream sections, with dinoflagellate zonation (Roncaglia et al. (1999) and eustatic sea level curve from Haq (2014).

Interestingly, the ~72 Ma event identified by Crampton et al. (2006) was recognised in a section from Isolation Creek. The Isolation Creek section is located ~30km northeast of Branch Stream and does not contain Branch Sandstone; Mead Hill Formation directly overlies Herring Formation. The ~72Ma event at Isolation Creek occurs ~55m below the base Mead Hill Formation and corresponds with an intra-formational unconformity or condensed horizon within Herring Formation (Crampton et al., 2006). This suggests that the event at Isolation Creek may correlate with the unconformity displayed in the top of the Herring Formation at Branch Stream.

Crampton et al. (2003) suggested that Branch Stream occupied a more proximal locality than Isolation Creek during the late Cretaceous (Section 3.4, Figure 18). Here, it is suggested that the KMa1 fall in relative sea level resulted in subaerial exposure and non-deposition at Branch Stream, whereas the Isolation Creek section was not subaerially exposed due to its more distal location. This indicates that the uppermost Herring Formation is diachronous and encompasses a variety of depositional environments and that the Branch Sandstone comprises a paleogeographically restricted deposit, which developed in proximal regions, in response to relative sea level fluctuation.

A similar pattern may be evident at Angora Stream, however, the broad age assignation of this section makes this more uncertain. The paleo-locality of the Branch Stream section is relatively proximal, thus the changes in paleoenvironment due to fluctuations in relative sea level are expected to be pronounced and conspicuous in the sedimentary record. A relatively distal depositional environment is interpreted at Angora Stream, thus a regional fall in relative sea level is likely to be less prominent in the sedimentary record and will not coincide with periods of erosion due to sub aerial exposure.

The development of basin floor and slope fan deposits, including turbidites, is commonly associated with lowstand events (Posamentier & Vail, 1988; Shanmugam & Moiola, 1982). As shown in Figure 44, a fall in relative sea level can result in fluvial incision on the shelf and canyon incision into the slope, thus sediments transported along these pathways bypass the shelf and slope before being deposited on the basin floor (Posamentier & Vail, 1988; Van Wagoner et al., 1988).

Image removed for copyright reasons.

Figure 44. Development of lowstand fan systems during fall in relative sea level (from Posamentier & Vail, 1988).

It is conceivable, therefore, that the depositional sequence at Angora Stream has therefore developed in response to a lowstand event, which may coincide with the KMa1 event in Marlborough. On the other hand, the occurrence of sediment gravity flows is not exclusively restricted to times of falling sea level or lowstands, and there could be other equally plausible explanations for their development at Angora Stream. Further work examining the age, nature, variability and lateral extent of the upper Glenburn Formation on the East Coast of the North Island would go some way to providing a more conclusive interpretation.

At Tangaruhe Stream, an unconformity between the Tanguruhe and Whangai Formations is shown to extend from the *Satyrodinium haumuriense* Interval Zone to the *Cerodinium diebelii* Interval Subzone. As Branch Sandstone is interpreted to have been deposited above a disconformity spanning part of the *Isabelidinium pellucidum* Interval Zone, some equivalency is indicated between the two sections.

The temporal extent of the unconformity at Tangaruhe Stream means that it cannot be tied to one specific sea level event. Due to the resumption of deposition within the *Cerodinium diebelii* Interval Subzone, however, the most likely candidates are KMa1 and KCa7.

The extent of erosion associated with the Tangaruhe-Whangai Formation contact in Tangaruhe Stream is unknown, but the temporal extent of the unconformity clearly encompasses a relatively long interval of time, particularly when compared to the unconformity at the base of the Branch Sandstone. A number of factors may have contributed to the temporal extent of the disconformity at Tangaruhe Stream, and these are considered below.

Given that the upper Tangaruhe Formation has elsewhere been described as forming in a low energy, offshore environment, it is possible that sedimentation rates were relatively low. This is consistent with the prevailing tectonic regime in the East Coast Basin during the Late Cretaceous, which was one of passive margin subsidence. Given low sedimentation rates, it is plausible that a relatively large expanse of time could be removed in a single erosive event/period of subaerial exposure related to a fall in relative sea level during the Late Campanian.

Alternatively, successive erosive events may have cut down into the Tangaruhe Formation and removed any intervening depositional sequences. This scenario is seen as less likely, as previous estimates have indicated that Tangaruhe Formation was deposited at paleo-water depths exceeding 200m. At such depths, fluctuating periods of subaerial exposure and prolonged intervals of non-deposition seem extremely unlikely, even during periods of relative sea level fall. Deep marine currents could alternatively account for the erosion interpreted at Tangaruhe Stream, but sedimentological evidence is more in keeping with a low energy environment, and no current indicators have been logged.

Based on the age of the uppermost Tangaruhe Formation at Tangaruhe Stream (~ 80My), it is also possible that tectonic reorganisation related to Tasman Sea spreading affected that locality. For example, localised uplift due to extension-related normal faulting or folding may have resulted in subaerial exposure and erosion of the Tangaruhe Stream area. Tectonic activity in the Whangai Range region has previously been inferred for Motuan times, whilst the base of Tangaruhe Formation overlies Springhill Formation with angular unconformity (Crampton, 1989). Given the evidence for tectonism in the period leading up to deposition of Tangaruhe Formation, ongoing activity cannot be discounted.

The simplest, most parsimonious explanation for the disconformity at Tangaruhe Stream is that a pronounced fall in relative sea level during the Late Campanian or early Maastrichtian resulted in subaerial exposure and removal of part of the upper Tangaruhe Formation. Whether this was the result of tectonic activity or eustatic sea level changes is unclear. Following renewed marine transgression, sedimentation resumed with deposition of the Whangai Formation. Despite this, there is little sedimentological evidence that the unconformity relates to a transgressive surface. Further regional mapping, as well as sedimentological and paleontological analysis of the upper Tangaruhe Formation is required to understand the mechanisms leading to the development of the unconformity.

6.5 Summary

Whilst acknowledging that changes in sedimentation are driven by complex interactions between tectonic regime, sediment supply and oceanographic conditions, it is also possible that a single eustatic sea level event is manifest at each of the field sites documented in this research. Due to the presence of corresponding interpreted regressive events in the uppermost Herring Formation at Branch Stream and Isolation Creek, the lithological changes at each section are interpreted to relate to Haq's (2014) KMa1 event. Further, it is plausible that relative sea level fall at both Angora Stream and Tangaruhe Stream relates to the same event, although the resolution of the biostratigraphic analysis documented herein presents significant uncertainty.

7 Conclusions

The purpose of this thesis was to understand the depositional setting of the Branch Sandstone at Branch Stream, as well as correlatives in the East Coast Basin of the North Island. Further, this research has sought to understand the regional implications of changes in sedimentation at the three sections studied. To achieve this, detailed measured sections of key intervals were logged at Branch Stream, Angora Stream and Tangaruhe Stream. Sedimentological and palynofacies data were used to interpret depositional environment, whilst age control was developed for each section using dinoflagellate biostratigraphy. Finally, all data have been examined with respect to the global eustatic sea level curve of Haq (2014).

The primary findings from this thesis are as follows:

- At Branch Stream, the Branch Sandstone overlies Herring Formation with disconformable contact. The uppermost Herring Formation was deposited during the *Isabelidinium pellucidum* Interval Zone. The Herring Formation is inferred to have been deposited in a more proximal location to Branch Sandstone, possibly in a restricted marine setting such as a lagoon or estuary.
- Branch Sandstone at Branch Stream comprises a shelfal body of sandstone, which was deposited during the *Cerodinium diebelii* Interval Zone.
- Mead Hill Formation overlies Branch Sandstone with disconformable contact and was deposited during the *Paleocystodinium granulatum* Interval Zone in a shelfal setting.
- At Branch Stream, higher frequency tectonic or eustatic sea-level changes can be distinguished within an overall passive margin sedimentary sequence, where overall sedimentation reflects thermal subsidence following rifting of the Tasman Sea.
- At Angora Stream, the uppermost Glenburn Formation, sandstone A and lower Whangai Formation were deposited within the *Isabelidinium*

pellucidum Interval Zone. These rock formations are interpreted as the product of sediment gravity flows, deposited at bathyal depths.

- At Tangaruhe Stream, a disconformity between the Tangaruhe and Whangai Formations spans a period of ca. 10 million years. The lower Whangai Formation is interpreted to lie within the *Cerodinium diebelii* Interval Zone.
- A fall in relative sea level fall is interpreted to have occurred at each section at broadly corresponding times during the Late Cretaceous. Given the geographic span of the sections, the sea-level fall may reflect a regional signal that is eustatic in origin.

Based on the conclusions above, a number of recommendations for further work are set out below:

- Further dinoflagellate biostratigraphy through other Branch Stream sections to better constrain the duration and extent of unconformities associated with the base and top of Branch Sandstone. This will assist in refining the period of deposition of Branch Sandstone, and will test the validity of the depositional model presented in this thesis. At the time of writing, possibility of access to other sections of Branch Sandstone is unknown, following damage during the November 2016 Kaikoura earthquake.
- Regional palynofacies analysis in the Marlborough study area. The suggestion that the uppermost Herring Formation was deposited in a highly proximal setting was unexpected, given that the formation is often referred to as an outer shelf deposit. Further palynofacies work is expected to give more comprehensive insights into the transition between Herring Formation and Branch Sandstone, and will improve understanding regarding the depositional environment of the uppermost Herring Formation.
- Analysis of proximal sedimentary sections of similar ages from the North Island sector of the East Coast Basin (if these exist). The impact of relative sea level fluctuations is expected to be most pronounced in shelfal sedimentary sections, and therefore analysis of similar sections in the North Island may highlight similar events to those seen indicated at Branch Stream. This is expected to further test the validity of the hypothesis that a

Late Cretaceous fall in eustatic sea level event impacted sedimentation in the East Coast Basin.

8 Bibliography

Adams, A. G. (1985). Late Cretaceous fauna and sediments of souther Hawkes Bay - New Zealand. *Unpublished PhD thesis lodged in the library, University of Auckland, New Zealand*.

Askin, R. A. (1988). Campanian to Paleocene palynological succession of Seymour and adjacent islands, northeastern Antarctic Peninsula. In R. M. Feldmann & M. O. Woodburne (Eds.), *Geology and paleontology of Seymour Island, Antarctic Peninsula*. Boulder, Colorado: Geological Society of America.

Atta-Peters, D., & Salami, M. B. (2006). Aptian–Maastrichtian palynomorphs from the offshore Tano Basin, western Ghana. *Journal of African Earth Sciences, 46*(4), 379-394. doi:https://doi.org/10.1016/j.jafrearsci.2006.07.002

Backhouse, J. (2006). Albian (Lower Cretaceous) Dinoflagellate cyst biostratigraphy of the Lower Gearle Siltstone, Southern Carnarvon Basin, Western Australia. *Palynology, 30*(1), 43-68. doi:10.1080/01916122.2006.9989618

Ballance, P. F. (1993). The paleo-Pacific, post subduction, passive margin thermal relaxation sequence (Late Cretaceous-Paleogene) of the drifting New Zealand continent. In P. F. Ballance (Ed.), *South Pacific Sedimentary Basins* (Vol. 2, pp. 93-110). Amsterdam, Netherlands: Elsevier Science Publishers.

Barnes, P. M., de Lépinay, B. M., Collot, J.-Y., Delteil, J., & Audru, J.-C. (1998). Strain partitioning in the transition area between oblique subduction and continental collision, Hikurangi margin, New Zealand. *Tectonics, 17*(4), 534-557. doi:10.1029/98TC00974

Batten, D. J. (1999). Small palynomorphs. In T. P. Jones & N. P. Rowe (Eds.), *Fossil plants and spores : modern techniques* (pp. 15-19). London: Geological Society.

Beanland, S., Melhuish, A., Nicol, A., & Ravens, J. (1998). Structure and deformational history of the inner forearc region, Hikurangi subduction margin, New Zealand. *New Zealand Journal of Geology and Geophysics, 41*(4), 325-342. doi:10.1080/00288306.1998.9514814

Bijl, P. K., Sluijs, A., & Brinkhuis, H. (2013). A magneto- and chemostratigraphically calibrated dinoflagellate cyst zonation of the early Palaeogene South Pacific Ocean. *Earth-Science Reviews, 124*, 1-31. doi:10.1016/j.earscirev.2013.04.010

Boggs, S. (2010). *Principles of sedimentology and stratigraphy* (5th ed., International ed.). Upper Saddle River, N.J. ; Harlow: Pearson Education.

Boulter, M. C., & Riddick, A. (1986). Classification and analysis of palynodebris from the Palaeocene sediments of the Forties Field. *Sedimentology, 33*(6), 871-886. doi:10.1111/j.1365-3091.1986.tb00988.x

Boyes, A. F., Field, B. D., Jones, C. M., King, P. R., Lugowki, A., & Ogg, J. (2011). *New Zealand Stratlink - East Coast Basin chronostratigraphic transects.* GNS Data Series 6b. Lower Hutt, New Zealand

Bradshaw, J. D. (1989). Cretaceous geotectonic patterns in the New Zealand Region. *Tectonics, 8*(4), 803-820. doi:10.1029/TC008i004p00803

Carvalho, M. d. A., Bengtson, P., & Lana, C. C. (2016). Late Aptian (Cretaceous) paleoceanography of the South Atlantic Ocean inferred from dinocyst communities of the Sergipe Basin, Brazil. *Paleoceanography, 31*(1), 2-26. doi:10.1002/2014PA002772

Carvalho, M. d. A., Mendonça Filho, J. G., & Menezes, T. R. (2006). Palynofacies and sequence stratigraphy of the Aptian–Albian of the Sergipe Basin, Brazil. *Sedimentary Geology, 192*(1), 57-74. doi:https://doi.org/10.1016/j.sedgeo.2006.03.017

Carvalho, M. d. A., Ramos, R. R. C., Crud, M. B., Witovisk, L., Kellner, A. W. A., Silva, H. d. P., . . . Romano, P. S. R. (2013). Palynofacies as indicators of paleoenvironmental changes in a Cretaceous succession from the Larsen Basin, James Ross Island, Antarctica. *Sedimentary Geology, 295*(Supplement C), 53-66. doi:https://doi.org/10.1016/j.sedgeo.2013.08.002

Clowes, C. D., Crouch, E. M., Prebble, J., & Roncaglia, L. (2016). Development and multi-operator calibration of a standardised palynofacies analysis technique. *GNS Science Report 2016/19.* 49p.

Cookson, I. C., & Eisenack, A. (1958). Microplankton from Australian and New Guinea Upper Mesozoic sediments. *Proceedings of the Royal Society of Victoria, v. 70*(1), 19-79.

Cookson, I. C., & Eisenack, A. (1960). Microplankton from Australian Cretaceous Sediments. *Micropaleontology, 6*(1), 1-18. doi:10.2307/1484313

Couper, R. A. (1960). New Zealand mesozoic and cainozoic plant microfossils. In S. New Zealand Geological (Ed.). Wellington, N.Z.: Wellington, N.Z. : Government Printer.

Crampton, J. S. (1989). An inferred Motuan sedimentary melange in southern Hawkes Bay. *New Zealand Geological Survey Record, 40*, 3-12.

Crampton, J. S. (1997). The Cretaceous stratigraphy of the Southern Hawkes Bay – Wairarapa region. *Institute of Geological and Nuclear Sciences Report, 97(08), 92*

Crampton, J. S., Laird, M. G., Nicol, A., Townsend, D., & Van Dissen, R. (2003). Palinspastic reconstructions of southeastern Marlborough, New Zealand, for mid-Cretaceous-Eocene times. *New Zealand Journal of Geology and Geophysics, 46*(2), 153-175. doi:10.1080/00288306.2003.9515002

Crampton, J. S., Mumme, T., Raine, I., Roncaglia, L., Schi∅ler, P., Strong, P., . . . Wilson, G. J. (2000). Revision of the Piripauan and Haumurian local stages and correlation of the Santonian-Maastrichtian (Late Cretaceous) in New Zealand. *New Zealand Journal of Geology and Geophysics, 43*(3), 309-333. doi:10.1080/00288306.2000.9514890

Crampton, J. S., Schiøler, P., & Roncaglia, L. (2006). Detection of Late Cretaceous eustatic signatures using quantitative biostratigraphy. *Geological Society of America. Geological Society of America Bulletin, 118*(7), 975.

Crouch, E. M., Mildenhall, D. C., & Neil, H. L. (2010). Distribution of organic-walled marine and terrestrial palynomorphs in surface sediments, offshore eastern New Zealand. *Marine Geology, 270*(1), 235-256. doi:https://doi.org/10.1016/j.margeo.2009.11.004

Deflandre, G., & Cookson, I. C. (1955). Fossil Microplankton from Australian Late Mesozoic and Tertiary Sediments. *Marine and Freshwater Research, 6*(2), 242-314.

Dunbar, G. B., & Barrett, P. J. (2005). Estimating palaeobathymetry of wave-graded continental shelves from sediment texture. *Sedimentology, 52*(2), 253-269. doi:10.1111/j.1365-3091.2004.00695.x

Eade, J. V. (1963). *The geology of the Mount Adams area, Southern Wairarapa : submitted for the Degree of Master of Science in Geology at the Victoria University of Wellington / by J.V. Eade.* Thesis (M.Sc.) Victoria University of Wellington, 1963.

Eade, J. V. (1966). Stratigraphy and structure of Mount Adams Area, Eastern Wairarapa. *Transactions of the Royal Societey of New Zealand, Geology, 4*(4), 103-117.

Fensome, R. A., Williams, G. L., & MacRae, R. A. (2009). Late Cretaceous and Cenozoic fossil dinoflagellates and other palynomorphs from the scotian margin, offshore eastern Canada. *Journal of Systematic Palaeontology, 7*(1), 1-79. doi:10.1017/S1477201908002538

Fensome, R. A.,Williams, G. L & MacRae, R. A.. (2017). The Lentin and Williams index of fossil dinoflagellages 2017 Edition. *AASP Contributions Series Number 48.* American Association of Stratigraphic Palynologists Foundation.

Field, B. D., Uruski, C. I., Beu, A., Browne, G., Crampton, J. S., Funnell, R., . . . Strong, P. (1997). *Cretaceous-Cenozoic geology and petroleum systems of the East Coast* *region, New Zealand*. Lower Hutt, N.Z.: Lower Hutt, N.Z. : Institute of Geological & Nuclear Sciences.

Habib, D., Moshkovitz, S., & Kramer, C. (1992). Dinoflagellate and calcareous nannofossil response to sea-level change in Cretaceous-Tertiary boundary sections. *Geology, 20*(2), 165.

Haq, B. U. (2014). Cretaceous eustasy revisited. *Global and Planetary Change, 113*, 44-58. doi:https://doi.org/10.1016/j.gloplacha.2013.12.007

Helby, R., Morgan, R., & Partridge, A. D. (1987). A palynological zonation of the Australian Mesozoic. In P. A. Jell (Ed.), *Studies in Australian Mesozoic palynology*. Sydney: Association of Australasian Palaeontologists.

Hollis, C. J. (2003). The Cretaceous/Tertiary boundary event in New Zealand: Profiling mass extinction. *New Zealand Journal of Geology and Geophysics, 46*(2), 307-321. doi:10.1080/00288306.2003.9515011

Hollis, C. J., Crampton, J. S., Morgans, H. E. G., & Reid, C. M. (2013). Cretaceous-Paleogene Stratigraphy of North-Eastern South Island: North Canterbury, Kaikoura, South Eastern Marlborough. In C. M. Reid & S. J. Hampton (Eds.), *Field Trip Guides, Geosciences 2013 Conference* (Vol. Miscellaneous Publication 136B, pp. 51). Christchurch, New Zealand: Geoscience Society of New Zealand.

Hollis, C. J., Rodgers, K. A., Strong, C. P., Field, B. D., & Rogers, K. M. (2003). Paleoenvironmental changes across the Cretaceous/Tertiary boundary in the northern Clarence valley, southeastern Marlborough, New Zealand. *New Zealand Journal of Geology and Geophysics, 46*(2), 209-234. doi:10.1080/00288306.2003.9515005

Hollis, C. J., & Strong, C. P. (2003). Biostratigraphic review of the Cretaceous/Tertiary boundary transition, mid-Waipara River section, North Canterbury, New Zealand. *New Zealand Journal of Geology and Geophysics, 46*(2), 243-253. doi:10.1080/00288306.2003.9515007

Howell, D. G., & Normark, W. R. (1982). Sedimentology of Submarine Fans. In P. A. Scholle & D. Spearing (Eds.), *Sandstone Depositional Environments* (pp. 365-404). Tulsa, Oklahoma: American Association of Petroleum Geologists.

Hutton, F. W. (1877). Report on the geology of the north-east portion of the South Island, from Cook Straits to the Rakaia. *Reports of geological explorations, 10*.

Johnston, M. R. (1971). Geology of the Tinui district: *Thesis Submitted for the Degree of Doctor of Philosophy in Geology at Victoria University of Wellington.*

Johnston, M. R. (1980). Geology of the Tinui-Awatoitoi district. Wellington:DSIR *New Zealand Geological Survey bulletin 94.* 62p.

Jolly, R. J. H., & Lonergan, L. (2002). Mechanisms and controls on the formation of sand intrusions. *Journal of the Geological Society, 159*(5), 605-617. doi:10.1144/0016-764902-025

King, P. R. (2000). *New Zealand's changing configuration in the last 100 million years: plate tectonics, basin development, and depositional setting.* Paper presented at the 2000 New Zealand Petroleum Conference Proceedings.

King, P. R., Naish, T. R., Browne, G. H., Field, B. D., & Edbrooke, S. W. (1999). Cretaceous to recent sedimentary patterns in New Zealand. *Institute of Gelogical & Nuclear Sciences Folio Series, 1*, 1-35.

Kingma, J. T. (1960). Outline of the Cretaceo-tertiary sedimentation in the eastern basin of New Zealand. *New Zealand Journal of Geology and Geophysics, 3*(2), 222-234. doi:10.1080/00288306.1960.10423595

Laing, A. C. M. (1961). *The geology and petroleum prospects of the Dannevirke area*. *Unpublished New Zealand Geological Survey open file petroleum report*, *318.*

Laird, M. G. (1992). *Cretaceous stratigraphy and evolution of the Marlborough segment of the East Coast region.* Paper presented at the New Zealand Oil Exploration Conference, Wellington, NZ.

Laird, M. G., & Bradshaw, J. D. (2004). The Break-up of a Long-term Relationship: the Cretaceous Separation of New Zealand from Gondwana. *Gondwana Research, 7*(1), 273-286. doi:http://dx.doi.org/10.1016/S1342-937X(05)70325-7

Leckie, D. A., Morgans, H., Wilson, G. J., & Edwards, A. R. (1995). Mid-Paleocene dropstones in the Whangai Formation, New Zealand—evidence of mid-Paleocene cold climate? *Sedimentary Geology, 97*(3), 119-129. doi:http://dx.doi.org/10.1016/0037-0738(95)00016-2

Leckie, D. A., Morgans, H. E. G., Wilson, G. J., & Uruski, C. I. (1992). Stratigraphic framework and source-rock potential of Maastrichtian to Paleocene marine shale, East Coast, North Island, New Zealand : hydrocarbon prospects. *Institute of Geological & Nuclear Sciences Report 92/5.* 31p.

Lee, J. M., & Begg, J. G. (2002). *Geology of the Wairarapa Area. Institute of Geological & Nuclear Sciences 1:250 000 geological map 11* (p. 66 + 1 sheet). Lower Hutt, New Zealand: Institute of Geological & Nuclear Sciences Limited.

Lensen, G. J. (1978). Stratigraphy: Marlborough. In R. P. Suggate, G. R. Stevens, & M. T. Te Punga (Eds.), *The Geology of New Zealand* (Vol. 2, pp. 383-390). Wellington: Government Printer.

Lewis, K. B., & Pettinga, J. R. (1993). The Emerging, Imbricate Frontal Wedge of the Hikurangi Margin. In P. F. Ballance (Ed.), *South Pacific Sedimentary Basins* (Vol. 2, pp. 222-250). Amsterdam, Netherlands: Elsevier Science Publishers.

Li, H., & Habib, D. (1996). Dinoflagellate Stratigraphy and Its Response to Sea Level Change in Cenomanian-Turonian Sections of the Western Interior of the United States. *PALAIOS, 11*(1), 15-30. doi:10.2307/3515113

Lillie, A. R. (1953). The geology of the Dannevirke Subdivision. *New Zealand Geological Survey bulletin 46.* 156p.

Mao, S., & Mohr, B. A. (1992). Late Cretaceous dinoflagellate cysts (? Santonian-Maestrichtian) from the southern Indian Ocean (hole 748C). In Proceedings of the Ocean Drilling Program, Scientific Results (Vol. 120, pp. 307-341).

Marshall, N. G. (1990). Campanian dinoflagellates from southeastern Australia. *Alcheringa: An Australasian Journal of Palaeontology, 14*, 1-38.

Matthiessen, J. (1995). Distribution patterns of dinoflagellate cysts and other organic-walled microfossils in recent Norwegian-Greenland Sea sediments. *Marine Micropaleontology, 24*(3), 307-334. doi:https://doi.org/10.1016/0377-8398(94)00016-G

McArthur, A. D., Gamberi, F., Kneller, B. C., Wakefield, M. I., Souza, P. A., & Kuchle, J. (2017). Palynofacies classification of submarine fan depositional environments: Outcrop examples from the Marnoso-Arenacea Formation, Italy. *Marine and Petroleum Geology, 88*, 181-199. doi:https://doi.org/10.1016/j.marpetgeo.2017.08.018

McCarthy, F., E. Gostlin, K., Mudie, P., & A. Hopkins, J. (2003). *Terrestrial and marine palynomorphs as sea-level proxies: An example from Quaternary sediments on the New Jersey Margin, USA*. In H. C. Olson & M. Leckie (Ed.), *Micropaleontologic proxies for sea-level change and stratigraphic continuities: SEPM Special Publication 75.* pp 119-129.

McCubbin, D. G. (1982). Barrier-Island and Strand Plain Facies. In P. A. Scholle & D. Spearing (Eds.), *Sandstone depositional environments* (pp. 247-280). Tulsa, Oklahoma: American Association of Petroleum Geologists.

Mohr, B. A. R., & Mao, S. (1997). Maastrichtian Dinocyst Floras from Maud Rise and Georgia Basin (Southern Ocean): Their Stratigraphic and Paleoenvironmental Implications. *Palynology, 21*, 41-65.

Moore, P. R. (1980). Late Cretaceous-Tertiary stratigraphy, structure, and tectonic history of the area between Whareama and Ngahape, eastern Wairarapa, New Zealand. *New Zealand Journal of Geology and Geophysics, 23*(2), 167-177. doi:10.1080/00288306.1980.10424204

Moore, P. R. (1986). A revised Cretaceous-Early Tertiary stratigraphic nomenclature for eastern North Island, New Zealand. *New Zealand Geological Survey Report, G104*

Moore, P. R. (1988a). Stratigraphy, composition, and environment of deposition of the Whangai Formation and associated Late Cretaceous-Paleocene rocks, eastern North Island, New Zealand. *New Zealand Geological Survey Bulletin, 100*.

Moore, P. R. (1988b). Structural Divisions of Eastern North Island. *New Zealand Geological Survey Record, 30*. 1-24.

Morris, J. C. (1987). *The stratigraphy of the Amuri limestone group, east Marlborough, New Zealand.* Unpublished PhD thesis. University of Canterbury.

Mortimer, N., Campbell, H. J., Tulloch, A. J., King, P. R., Stagpoole, V. M., Wood, R. A., . . . Collot, J. (2017). Zealandia: Earth's hidden continent. *GSA Today, 27*(3), 27-35.

Neef, G. (1995). Cretaceous and Cenozoic geology east of the Tinui Fault Complex in northeastern Wairarapa, New Zealand. *New Zealand Journal of Geology and Geophysics, 38*(3), 375-394. doi:10.1080/00288306.1995.9514664

Nicol, A. (1993). Haumurian (c. 66–80 Ma) half-graben development and deformation, mid Waipara, North Canterbury, New Zealand. *New Zealand Journal of Geology and Geophysics, 36*(1), 127-130. doi:10.1080/00288306.1993.9514560

Pacton, M., Gorin, G. E., & Vasconcelos, C. (2011). Amorphous organic matter — Experimental data on formation and the role of microbes. *Review of Palaeobotany and Palynology, 166*(3), 253-267. doi:https://doi.org/10.1016/j.revpalbo.2011.05.011

Posamentier, H. W., & Vail, P. R. (1988). Eustatic controls on clastic deposition II – Sequence and Systems Tract Models. In C. K. Wilgus, B. S. Hastings, G. Kendall, H. W. Posamentier, C. A. Ross, & J. C. Van Wagoner (Eds.), *Sea-level change: an integrated approach: SEPM Special Publication 42* (Vol. 42, pp. 125-154).

Rait, G., Chanier, F., & Waters, D. W. (1991). Landward- and seaward-directed thrusting accompanying the onset of subduction beneath New Zealand. *Geology, 19*(3), 230-233. doi:10.1130/0091-7613(1991)019<0230:LASDTA>2.3.CO;2

Rattenbury, M. S., Townsend, D. B., & Johnston, M. R. (2006). *Geology of the Kaikoura area.Institute of Geological & Nuclear Sciences 1:250 000 geological map 13.* 1 sheet + 70p. Lower Hutt, New Zealand: Institute of Geological & Nuclear Sciences Limited.

Rattenbury, M. S., & Isaac, M. J. (2012). The QMAP 1: 250 000 geological map of New Zealand project. New Zealand Journal of Geology and Geophysics, 55(4), 393-405.

Reay, M. B. (1993). *Geology of the middle part of the Clarence valley*. *Institute of Geological & Nuclear Sciences geological map 10* (1 sheet +144p). Lower Hutt, New Zealand: Institute of Geologial and Nuclear Sciences.

Reay, M. B., & Strong, C. P. (1992). The Branch Sandstone, Clarence Valley, and implications for latest Cretaceous paleoenvironments and geological history of Central Marlborough. *New Zealand Geological Survey Record 44:* 43-49.

Ridd, M. F. (1964). The geology of the northern Wairarapa, North Island, New Zealand. *Unpublished New Zealand Geological Survey open file petroleum report*, *329*.

Roberts, A. P. (1995). Tectonic rotation about the termination of a major strike-slip fault, Marlborough Fault System, New Zealand. *Geophysical Research Letters, 22*(3), 187-190. doi:10.1029/94GL02582

Roncaglia, L. (2000). A new dinoflagellate species from the Upper Cretaceous of New Zealand - a morphological intermediate between three genera. *Alcheringa: An Australasian Journal of Palaeontology, 24*(2), 135-146. doi:10.1080/03115510008619530

Roncaglia, L., Field, B. D., Raine, J. I., Schiøler, P., & Wilson, G. J. (1999). Dinoflagellate biostratigraphy of Piripauan-Haumurian (Upper Cretaceous) sections from northeast South Island, New Zealand. *Cretaceous Research, 20*(3), 271-314. doi:http://dx.doi.org/10.1006/cres.1999.0153

Roncaglia, L., & Schiøler, P. (1997). Dinoflagellate biostratigraphy of Piripauan-Haumurian sections in Southern Marlborough and northern Canterbury*, New Zealand*. Lower Hutt: Institute of Geological & Nuclear Sciences. Institute of Geological & Nuclear Sciences science report 97/09 50 p

Schiøler, P., Crampton, J. S., & Laird, M. G. (2002). Palynofacies and sea-level changes in the Middle Coniacian–Late Campanian (Late Cretaceous) of the East Coast Basin, New

Zealand. *Palaeogeography, Palaeoclimatology, Palaeoecology, 188*(3–4), 101-125. doi:http://dx.doi.org/10.1016/S0031-0182(02)00548-5

Schiøler, P., & Wilson, G. J. (1998). Dinoflagellate Biostratigraphy of the Middle Coniacian: Lower Campanian (Upper Cretaceous) in South Marlborough, New Zealand. *Micropaleontology, 44*(4), 313-349. doi:10.2307/1486039

Schiøler, P., & Wilson, G. J. (1998). Dinoflagellate Biostratigraphy of the Middle Coniacian: Lower Campanian (Upper Cretaceous) in South Marlborough, New Zealand. *Micropaleontology, 44*(4), 313-349. doi:10.2307/1486039

Schnyder, J., Stetten, E., Baudin, F., Pruski, A. M., & Martinez, P. (2017). Palynofacies reveal fresh terrestrial organic matter inputs in the terminal lobes of the Congo deep-sea fan. *Deep Sea Research Part II: Topical Studies in Oceanography, 142*, 91-108. doi:https://doi.org/10.1016/j.dsr2.2017.05.008

Shanmugam, G. (1997). The Bouma Sequence and the turbidite mind set. *Earth-Science Reviews, 42*(4), 201-229. doi:https://doi.org/10.1016/S0012-8252(97)81858-2

Shanmugam, G., & Moiola, R. J. (1982). Eustatic control of turbidites and winnowed turbidites. *Geology, 10*(5), 231-235. doi:10.1130/0091-7613(1982)10<231:ECOTAW>2.0.CO;2

Shanmugam, G., & Moiola, R. J. (1988). Submarine fans: characteristics, models, classification, and reservoir potential. *Earth-Science Reviews, 24*(6), 383-428.

Sluijs, A., Brinkhuis, H., Williams, G. L., & Fensome, R. A. (2009). Taxonomic revision of some Cretaceous–Cenozoic spiny organic-walled peridiniacean dinoflagellate cysts. *Review of Palaeobotany and Palynology, 154*(1), 34-53. doi:https://doi.org/10.1016/j.revpalbo.2008.11.006

Stanley, D. J. (1986). Turbidity current transport of organic-rich sediments: Alpine and Mediterranean examples. *Marine Geology, 70*(1), 85-101. doi:https://doi.org/10.1016/0025-3227(86)90090-3

Strong, C. P., Hollis, C. J., & Wilson, G. J. (1995). Foraminiferal, radiolarian, and dinoflagellate biostratigraphy of Late Cretaceous to Middle Eocene pelagic sediments (Muzzle Group), Mead Stream, Marlborough, New Zealand. *New Zealand Journal of Geology and Geophysics, 38*(2), 171-209. doi:10.1080/00288306.1995.9514649

Suggate, R. P. (1958). The Geology of the Clarence Valley from Gore Stream to Bluff Hill. *Transactions of the Royal Society of New Zealand, 85*(3), 397-408.

Thomson, J. A. (1919). The Geology of the Middle Clarence and Ure Valleys, East Marlborough, New Zealand. *Transactions of the New Zealand Institute, 51*, 289-349.

Thorn, V. C., Riding, J. B., & Francis, J. E. (2009). The Late Cretaceous dinoflagellate cyst Manumiella — Biostratigraphy, systematics, and palaeoecological signals in Antarctica. *Review of Palaeobotany and Palynology, 156*(3), 436-448. doi:http://dx.doi.org/10.1016/j.revpalbo.2009.04.009

Townsend, D. (2001). Neogene evolution of the Pacific—Australia plate boundary zone in NE Marlborough. South Island, New Zealand [Ph D thesis]: Victoria University of Wellington.

Tyson, R. V. (1993). Palynofacies analysis. In J. M. (Ed.), *Applied Micropalaeontology* (pp. 153-191). Netherlands: Springer.

Tyson, R. V. (1995). *Sedimentary organic matter : organic facies and palynofacies / R.V. Tyson*. London: Chapman & Hall. 615p.

Van Wagoner, J. C., Posamentier, H. W., Mitchum, R. M. J., Vail, P. R., Sarg, J. F., Loutit, T. S., & Hardenbol, J. (1988). An overview of the fundamentals of sequence stratigraphy and key definitions. In C. K. Wilgus, B. S. Hastings, G. Kendall, H. W. Posamentier, C. A. Ross, & J. C. Van Wagoner (Eds.), *Sea-level change: an integrated approach: SEPM Special Publication 42* (pp. 39-45).

Walker, R. G. (1992). Turbidites and submarine fans. In R. G. Walker & N. P. James (Eds.), *Facies models: response to sea level change* (pp. 239-264). Quebec: Geological Association of Cananda.

Wall, D., Dale, B., Lohmann, G. P., & Smith, W. K. (1977). The environmental and climatic distribution of dinoflagellate cysts in modern marine sediments from regions in the North and South Atlantic Oceans and adjacent seas. *Marine Micropaleontology, 2*, 121-200. doi:http://dx.doi.org/10.1016/0377-8398(77)90008-1

Walpole, L. M., & Burr, I. L. (1939). Report on a Reconnaisance Survey of the Dannevirke-Pongaroa-Aohanga District. *Unpublished New Zealand Geological Survey open file petroleum report*, *7.*

Walpole, L. M., Quennell, A. M., & Burr, I. L. (1938). Report on the Te Uri Stream and Tangaruhe Gorge Sections, Hawkes Bay District. *Unpublished New Zealand Geological Survey open file petroleum report*, *179.*

Webb, P. N. (1971). New Zealand late Cretaceous (Haumurian) Foraminifera and stratigraphy: A summary. *New Zealand Journal of Geology and Geophysics, 14*(4), 795-828. doi:10.1080/00288306.1971.10426335

Wellman, H. W. (1959). Divisions of the New zealand Cretaceous. *Transactions of the Royal Society of New Zealand, 87*, 99-163.

Willumsen, P. S. (2000). Late Cretaceous to early Paleocene palynological changes in midlatitude Southern Hemisphere, New Zealand. *GFF, 122*(1), 180-181. doi:10.1080/11035890001221180

Willumsen, P. S. (2003). *Marine palynology across the Cretaceous-Tertiary boundary in New Zealand : a thesis submitted to the Victoria University of Wellington in fulfilment of the requirements for the degree of Doctor of Philosophy in Geology.* Thesis (Ph.D.)--Victoria University of Wellington, 2003.

Willumsen, P. S. (2011). Maastrichtian to Paleocene dinocysts from the Clarence Valley, South Island, New Zealand. *Alcheringa: An Australasian Journal of Palaeontology, 35*(2), 199-240. doi:10.1080/03115518.2010.494484

Wilson, G. J. (1967a). Microplankton from the Garden Cove formation, Campbell Island. *New Zealand Journal of Botany, 5*(2), 223-240. doi:10.1080/0028825X.1967.10428743

Wilson, G. J. (1967b). Some new species of lower Tertiary Dinoflagellates from McMurdo sound, Antarctica. *New Zealand Journal of Botany, 5*(1), 57-83. doi:10.1080/0028825X.1967.10428735

Wilson, G. J. (1978). The dinoflagellate species Isabelia druggii (Stover) and I. seelandica (Lange): their association in the Teurian of Woodside Creek, Marlborough, New Zealand. *New Zealand Journal of Geology and Geophysics, 21*(1), 75-80. doi:10.1080/00288306.1978.10420723

Wilson, G. J. (1984a). New Zealand Late Jurassic to Eocene dinoflagellate biostratigraphy - a summary. *Newsletters on Stratigraphy, 13*, 104-117.

Wilson, G. J. (1984b). Some new dinoflagellate species from the New Zealand Haumurian and Piripauan stages (Santonian-Maastrichtian, Late Cretaceous). *New Zealand Journal of Botany, 22*(4), 549-556.

Wilson, G. J., Morgans, H. E. G., & Moore, P. R. (1989). Cretaceous-Tertiary boundary at Tawanui, southern Hawkés Bay, New Zealand. *New Zealand Geological Survey Record, 40*, 29-40.

Wood, S. E., & Askin, R. A. (1992). Dinoflagellate cysts from the Marambio Group (Upper Cretaceous) of Humps Island. *Antarctic Science, 4*(3), 327-336.

Wood, S. E., Riding, J. B., Fensome, R. A., & Williams, G. L. (2016). A review of the Sentusidinium complex of dinoflagellate cysts. *Review of Palaeobotany and*

Palynology, 234(Supplement C), 61-93.
doi:https://doi.org/10.1016/j.revpalbo.2016.08.008

Appendix 1: Grain-size data

Grainsize (µm)	Differential volume							
	BST004	BST005	BST007	BST008	BST009	BST010	BST011	BST012
0.3751	0.3737	0.0362	0.0322	0.0268	0.0076	0.0000	0.0051	0.0000
0.4118	0.6641	0.0644	0.0569	0.0474	0.0133	0.0000	0.0088	0.0000
0.4521	0.9748	0.0950	0.0843	0.0701	0.0200	0.0000	0.0135	0.0000
0.4963	1.3833	0.1362	0.1222	0.1036	0.0301	0.0000	0.0212	0.0000
0.5448	1.7179	0.1717	0.1572	0.1392	0.0421	0.0000	0.0315	0.0000
0.5980	2.0004	0.2041	0.1918	0.1798	0.0562	0.0001	0.0448	0.0000
0.6565	2.2451	0.2348	0.2287	0.2280	0.0735	0.0013	0.0620	0.0000
0.7207	2.4699	0.2656	0.2706	0.2877	0.0944	0.0087	0.0833	0.0005
0.7911	2.6506	0.2945	0.3175	0.3628	0.1207	0.0315	0.1104	0.0071
0.8685	2.7815	0.3208	0.3698	0.4563	0.1525	0.0736	0.1435	0.0382
0.9534	2.8754	0.3457	0.4312	0.5740	0.1911	0.1357	0.1837	0.1050
1.0466	2.9435	0.3692	0.5026	0.7173	0.2357	0.2160	0.2295	0.2056
1.1489	3.0088	0.3933	0.5879	0.8920	0.2872	0.3197	0.2815	0.3264
1.2612	3.0746	0.4173	0.6847	1.0956	0.3446	0.4428	0.3378	0.4677
1.3845	3.1492	0.4412	0.7922	1.3246	0.4062	0.5825	0.3968	0.6243
1.5199	3.2262	0.4639	0.9029	1.5655	0.4690	0.7291	0.4552	0.7833
1.6685	3.3028	0.4844	1.0118	1.8047	0.5287	0.8740	0.5089	0.9331
1.8316	3.3705	0.5028	1.1138	2.0311	0.5843	1.0114	0.5570	1.0642
2.0107	3.4064	0.5157	1.1980	2.2233	0.6300	1.1286	0.5948	1.1649
2.2073	3.3927	0.5232	1.2583	2.3678	0.6653	1.2212	0.6224	1.2303
2.4230	3.2980	0.5197	1.2781	2.4342	0.6822	1.2724	0.6334	1.2485
2.6599	3.1363	0.5085	1.2662	2.4312	0.6850	1.2921	0.6325	1.2277
2.9200	2.9250	0.4889	1.2224	2.3603	0.6727	1.2775	0.6194	1.1718
3.2055	2.7146	0.4660	1.1699	2.2591	0.6528	1.2493	0.6008	1.1008
3.5188	2.5135	0.4414	1.1115	2.1436	0.6290	1.2124	0.5795	1.0241
3.8628	2.3112	0.4148	1.0526	2.0257	0.6027	1.1738	0.5560	0.9473
4.2405	2.1010	0.3914	0.9981	1.9219	0.5820	1.1455	0.5370	0.8810
4.6551	1.8767	0.3673	0.9414	1.8201	0.5608	1.1160	0.5172	0.8184
5.1102	1.6937	0.3527	0.9080	1.7575	0.5525	1.1109	0.5087	0.7789
5.6098	1.5429	0.3376	0.8750	1.6966	0.5415	1.0984	0.4981	0.7426
6.1582	1.4799	0.3348	0.8782	1.6877	0.5456	1.1175	0.5013	0.7338
6.7603	1.4591	0.3350	0.8845	1.6850	0.5512	1.1341	0.5057	0.7303
7.4212	1.5056	0.3502	0.9240	1.7299	0.5748	1.1831	0.5257	0.7530
8.1467	1.5657	0.3718	0.9655	1.7802	0.6040	1.2323	0.5498	0.7821
8.9432	1.6125	0.3992	1.0120	1.8267	0.6378	1.2820	0.5769	0.8168
9.8175	1.6369	0.4365	1.0788	1.8791	0.6827	1.3495	0.6125	0.8666
10.7773	1.5992	0.4762	1.1468	1.8988	0.7288	1.4155	0.6476	0.9189
11.8309	1.5820	0.5335	1.2631	1.9615	0.7986	1.5364	0.7032	1.0065
12.9876	1.5520	0.5832	1.3579	1.9958	0.8582	1.6387	0.7500	1.0818
14.2573	1.5584	0.6205	1.4275	2.0338	0.9035	1.7239	0.7865	1.1381
15.6512	1.5337	0.6178	1.4040	1.9922	0.8965	1.7106	0.7797	1.1239
17.1813	1.4483	0.5841	1.3049	1.8696	0.8480	1.6149	0.7386	1.0534
18.8610	1.3005	0.5416	1.1869	1.6977	0.7848	1.4891	0.6855	0.9692
20.7050	1.1112	0.5290	1.1239	1.5322	0.7563	1.4137	0.6624	0.9365
22.7292	0.9657	0.5665	1.1718	1.4566	0.7894	1.4533	0.6930	0.9929
24.9513	0.8811	0.6681	1.3455	1.4863	0.9002	1.6217	0.7918	1.1562
27.3906	0.8643	0.8078	1.5946	1.6058	1.0578	1.8701	0.9326	1.3777
30.0685	0.8612	0.9507	1.8373	1.7414	1.2191	2.1087	1.0780	1.5930
33.0081	0.8124	1.0704	2.0108	1.8305	1.3562	2.2783	1.2023	1.7593

Grainsize (µm)	Differential volume							
	BST004	BST005	BST007	BST008	BST009	BST010	BST011	BST012
36.2352	0.6828	1.1402	2.0731	1.8175	1.4343	2.3322	1.2747	1.8399
39.7777	0.4850	1.1991	2.0973	1.7392	1.5036	2.3512	1.3377	1.9120
43.6665	0.2621	1.2520	2.1173	1.6329	1.5682	2.3652	1.3934	1.9893
47.9356	0.0971	1.3418	2.2109	1.5673	1.6830	2.4487	1.4863	2.1367
52.6220	0.0180	1.4771	2.3885	1.5716	1.8631	2.6052	1.6257	2.3550
57.7666	0.0014	1.6390	2.6038	1.6290	2.0903	2.7875	1.7926	2.5933
63.4141	0.0000	1.8324	2.8232	1.7223	2.3796	2.9892	2.0019	2.8580
69.6138	0.0000	2.0106	2.9543	1.7868	2.6735	3.1533	2.2133	3.0985
76.4196	0.0000	2.1898	2.9963	1.8044	2.9907	3.3399	2.4575	3.3855
83.8907	0.0000	2.3616	2.9504	1.7585	3.3090	3.5810	2.7314	3.7810
92.0923	0.0000	2.5370	2.8561	1.6651	3.6274	3.8977	3.0419	4.3406
101.0960	0.0000	2.7351	2.7638	1.5551	3.9517	4.2348	3.3879	5.0652
110.9790	0.0000	2.9400	2.6788	1.4426	4.2430	4.3867	3.7118	5.7579
121.8290	0.0000	3.1657	2.6180	1.3478	4.5019	4.1539	3.9847	6.1163
133.7400	0.0000	3.3894	2.5619	1.2628	4.6818	3.4288	4.1497	5.8120
146.8150	0.0000	3.6055	2.4990	1.1748	4.7583	2.3480	4.1954	4.7626
161.1680	0.0000	3.7945	2.4068	1.0610	4.6916	1.2076	4.1233	3.2228
176.9250	0.0000	3.9444	2.2524	0.8995	4.4515	0.4148	3.9433	1.6346
194.2220	0.0000	4.0605	2.0119	0.6942	4.0465	0.0720	3.6785	0.5555
213.2100	0.0000	4.1572	1.6745	0.4686	3.5076	0.0048	3.3485	0.0954
234.0540	0.0000	4.2562	1.2773	0.2484	2.9043	0.0000	2.9937	0.0063
256.9360	0.0000	4.3405	0.8958	0.0932	2.2956	0.0000	2.6631	0.0000
282.0560	0.0000	4.3581	0.6088	0.0177	1.7219	0.0000	2.4049	0.0000
309.6310	0.0000	4.2076	0.4535	0.0014	1.2063	0.0000	2.2392	0.0000
339.9020	0.0000	3.7874	0.4117	0.0000	0.7595	0.0000	2.1468	0.0000
373.1320	0.0000	3.0761	0.4367	0.0000	0.3841	0.0000	2.0610	0.0000
409.6110	0.0000	2.1578	0.4626	0.0000	0.1377	0.0000	1.8932	0.0000
449.6570	0.0000	1.1700	0.4232	0.0000	0.0253	0.0000	1.5825	0.0000
493.6170	0.0000	0.4392	0.2833	0.0000	0.0019	0.0000	1.1365	0.0000
541.8760	0.0000	0.0828	0.1247	0.0000	0.0000	0.0000	0.6234	0.0000
594.8520	0.0000	0.0064	0.0261	0.0000	0.0000	0.0000	0.2327	0.0000
653.0080	0.0000	0.0000	0.0022	0.0000	0.0000	0.0000	0.0433	0.0000
716.8490	0.0000	0.0000	0.0000	0.0000	0.0000	0.0000	0.0032	0.0000
786.9320	0.0000	0.0000	0.0000	0.0000	0.0000	0.0000	0.0000	0.0000
863.8660	0.0000	0.0000	0.0000	0.0000	0.0000	0.0000	0.0000	0.0000
948.3220	0.0000	0.0000	0.0000	0.0000	0.0000	0.0000	0.0000	0.0000
1041.0300	0.0000	0.0000	0.0000	0.0000	0.0000	0.0000	0.0000	0.0000
1142.8100	0.0000	0.0000	0.0000	0.0000	0.0000	0.0000	0.0000	0.0000
1254.5400	0.0000	0.0000	0.0000	0.0000	0.0000	0.0000	0.0000	0.0000
1377.1900	0.0000	0.0000	0.0000	0.0000	0.0000	0.0000	0.0000	0.0000
1511.8300	0.0000	0.0000	0.0000	0.0000	0.0000	0.0000	0.0000	0.0000
1659.6300	0.0000	0.0000	0.0000	0.0000	0.0000	0.0000	0.0000	0.0000
1821.8800	0.0000	0.0000	0.0000	0.0000	0.0000	0.0000	0.0000	0.0000
2000.0000	0.0000	0.0000	0.0000	0.0000	0.0000	0.0000	0.0000	0.0000

Grainsize (µm)	Differential volume							
	BST012B	BST013	BST014	BST014B	BST021	BST022	BST023	BST024
0.3751	0.0000	0.0000	0.0000	0.0000	0.0213	0.0000	0.0132	0.0240
0.4118	0.0000	0.0000	0.0000	0.0000	0.0376	0.0000	0.0223	0.0420
0.4521	0.0000	0.0001	0.0000	0.0000	0.0565	0.0000	0.0333	0.0621
0.4963	0.0000	0.0018	0.0000	0.0000	0.0844	0.0000	0.0477	0.0883
0.5448	0.0000	0.0099	0.0002	0.0000	0.1136	0.0000	0.0628	0.1116
0.5980	0.0000	0.0273	0.0031	0.0000	0.1453	0.0000	0.0764	0.1315
0.6565	0.0004	0.0545	0.0171	0.0000	0.1811	0.0000	0.0927	0.1522
0.7207	0.0055	0.0890	0.0482	0.0000	0.2222	0.0000	0.1100	0.1729
0.7911	0.0303	0.1353	0.0984	0.0000	0.2687	0.0000	0.1330	0.1966
0.8685	0.0854	0.1949	0.1637	0.0000	0.3194	0.0000	0.1575	0.2191
0.9534	0.1734	0.2689	0.2490	0.0000	0.3743	0.0000	0.1890	0.2469
1.0466	0.2832	0.3549	0.3534	0.0000	0.4307	0.0009	0.2260	0.2791
1.1489	0.4197	0.4529	0.4766	0.0000	0.4882	0.0109	0.2741	0.3228
1.2612	0.5781	0.5587	0.6130	0.0017	0.5431	0.0589	0.3313	0.3753
1.3845	0.7515	0.6682	0.7555	0.0245	0.5925	0.1569	0.3969	0.4378
1.5199	0.9254	0.7732	0.8920	0.0877	0.6320	0.2985	0.4711	0.5100
1.6685	1.0864	0.8667	1.0129	0.1735	0.6589	0.4452	0.5483	0.5884
1.8316	1.2250	0.9453	1.1123	0.2679	0.6743	0.6023	0.6348	0.6786
2.0107	1.3293	1.0014	1.1817	0.3562	0.6750	0.7528	0.7173	0.7665
2.2073	1.3928	1.0332	1.2163	0.4237	0.6640	0.8979	0.7997	0.8557
2.4230	1.4014	1.0307	1.2049	0.4640	0.6373	1.0168	0.8633	0.9249
2.6599	1.3642	1.0031	1.1570	0.4773	0.6058	1.1117	0.9212	0.9902
2.9200	1.2876	0.9526	1.0789	0.4692	0.5707	1.1795	0.9670	1.0416
3.2055	1.1975	0.8957	0.9928	0.4495	0.5405	1.2235	1.0059	1.0878
3.5188	1.1037	0.8367	0.9052	0.4253	0.5138	1.2605	1.0392	1.1272
3.8628	1.0124	0.7783	0.8197	0.4042	0.4881	1.2817	1.0592	1.1547
4.2405	0.9310	0.7289	0.7424	0.3896	0.4701	1.3230	1.0942	1.1988
4.6551	0.8536	0.6822	0.6695	0.3842	0.4538	1.3565	1.1219	1.2355
5.1102	0.8023	0.6579	0.6215	0.3883	0.4554	1.4236	1.1834	1.3097
5.6098	0.7579	0.6359	0.5818	0.3979	0.4570	1.4715	1.2254	1.3614
6.1582	0.7476	0.6412	0.5736	0.4133	0.4782	1.5451	1.2976	1.4492
6.7603	0.7439	0.6514	0.5734	0.4340	0.5009	1.6126	1.3639	1.5288
7.4212	0.7676	0.6885	0.6007	0.4642	0.5449	1.7242	1.4816	1.6656
8.1467	0.7943	0.7314	0.6346	0.4935	0.5934	1.8623	1.6222	1.8227
8.9432	0.8256	0.7804	0.6759	0.5150	0.6462	2.0227	1.7833	2.0004
9.8175	0.8753	0.8455	0.7338	0.5360	0.7106	2.2231	1.9813	2.2183
10.7773	0.9313	0.9152	0.7957	0.5562	0.7770	2.4198	2.1802	2.4352
11.8309	1.0302	1.0229	0.8929	0.6035	0.8755	2.6837	2.4601	2.7390
12.9876	1.1152	1.1158	0.9778	0.6871	0.9654	2.9209	2.7193	3.0105
14.2573	1.1752	1.1838	1.0424	0.7934	1.0434	3.1785	2.9898	3.2909
15.6512	1.1540	1.1708	1.0368	0.8978	1.0598	3.3255	3.1232	3.4280
17.1813	1.0696	1.0952	0.9730	0.8951	1.0245	3.3875	3.1410	3.4577
18.8610	0.9756	1.0079	0.8935	0.7252	0.9683	3.3604	3.0747	3.4051
20.7050	0.9409	0.9782	0.8592	0.4538	0.9490	3.3290	3.0395	3.3661
22.7292	1.0055	1.0460	0.9065	0.2734	1.0021	3.3998	3.1674	3.4535
24.9513	1.1831	1.2225	1.0524	0.3751	1.1453	3.5871	3.4717	3.6545
27.3906	1.4166	1.4505	1.2499	0.8784	1.3404	3.8941	3.9140	3.9551
30.0685	1.6365	1.6568	1.4398	1.5241	1.5304	4.1738	4.3065	4.2017
33.0081	1.7971	1.7993	1.5801	1.7011	1.6774	4.3498	4.5248	4.3416
36.2352	1.8679	1.8502	1.6362	1.1361	1.7402	4.3343	4.4802	4.3292
39.7777	1.9336	1.9025	1.6766	0.5168	1.7798	4.2016	4.3031	4.2345
43.6665	2.0087	1.9780	1.7185	0.5559	1.8104	4.0109	4.1023	4.0934
47.9356	2.1613	2.1451	1.8320	1.3401	1.9000	3.8238	3.9977	3.8925

Grainsize (µm)	Differential volume							
	BST012B	BST013	BST014	BST014B	BST021	BST022	BST023	BST024
52.6220	2.3901	2.3932	2.0336	2.0633	2.0718	3.5991	3.9417	3.5367
57.7666	2.6476	2.6514	2.2917	2.0337	2.3005	3.2230	3.7579	2.9408
63.4141	2.9458	2.9072	2.6102	1.9634	2.5966	2.6350	3.3011	2.1252
69.6138	3.2310	3.1005	2.9156	2.3884	2.8896	1.8511	2.4983	1.1818
76.4196	3.5692	3.3176	3.2338	3.5925	3.1965	1.0021	1.4519	0.4549
83.8907	4.0059	3.6648	3.5643	5.7406	3.5070	0.3723	0.5806	0.0873
92.0923	4.5624	4.2348	3.9406	8.0771	3.8419	0.0697	0.1152	0.0070
101.0960	5.2093	5.0705	4.4127	9.6047	4.2441	0.0053	0.0097	0.0000
110.9790	5.7131	5.9443	4.9368	10.9983	4.7082	0.0000	0.0000	0.0000
121.8290	5.7802	6.4676	5.4491	12.6630	5.2231	0.0000	0.0000	0.0000
133.7400	5.1775	6.2168	5.7408	11.5383	5.6671	0.0000	0.0000	0.0000
146.8150	3.9339	5.0624	5.5852	5.8245	5.8501	0.0000	0.0000	0.0000
161.1680	2.3632	3.3105	4.8589	1.1162	5.5500	0.0000	0.0000	0.0000
176.9250	1.0197	1.5826	3.6347	0.0427	4.6793	0.0000	0.0000	0.0000
194.2220	0.2623	0.4816	2.1950	0.0000	3.3675	0.0000	0.0000	0.0000
213.2100	0.0331	0.0736	0.9705	0.0000	1.9045	0.0000	0.0000	0.0000
234.0540	0.0009	0.0037	0.2663	0.0000	0.7667	0.0000	0.0000	0.0000
256.9360	0.0000	0.0000	0.0365	0.0000	0.1772	0.0000	0.0000	0.0000
282.0560	0.0000	0.0000	0.0014	0.0000	0.0194	0.0000	0.0000	0.0000
309.6310	0.0000	0.0000	0.0000	0.0000	0.0004	0.0000	0.0000	0.0000
339.9020	0.0000	0.0000	0.0000	0.0000	0.0000	0.0000	0.0000	0.0000
373.1320	0.0000	0.0000	0.0000	0.0000	0.0000	0.0000	0.0000	0.0000
409.6110	0.0000	0.0000	0.0000	0.0000	0.0000	0.0000	0.0000	0.0000
449.6570	0.0000	0.0000	0.0000	0.0000	0.0000	0.0000	0.0000	0.0000
493.6170	0.0000	0.0000	0.0000	0.0000	0.0000	0.0000	0.0000	0.0000
541.8760	0.0000	0.0000	0.0000	0.0000	0.0000	0.0000	0.0000	0.0000
594.8520	0.0000	0.0000	0.0000	0.0000	0.0000	0.0000	0.0000	0.0000
653.0080	0.0000	0.0000	0.0000	0.0000	0.0000	0.0000	0.0000	0.0000
716.8490	0.0000	0.0000	0.0000	0.0000	0.0000	0.0000	0.0000	0.0000
786.9320	0.0000	0.0000	0.0000	0.0000	0.0000	0.0000	0.0000	0.0000
863.8660	0.0000	0.0000	0.0000	0.0000	0.0000	0.0000	0.0000	0.0000
948.3220	0.0000	0.0000	0.0000	0.0000	0.0000	0.0000	0.0000	0.0000
1041.0300	0.0000	0.0000	0.0000	0.0000	0.0000	0.0000	0.0000	0.0000
1142.8100	0.0000	0.0000	0.0000	0.0000	0.0000	0.0000	0.0000	0.0000
1254.5400	0.0000	0.0000	0.0000	0.0000	0.0000	0.0000	0.0000	0.0000
1377.1900	0.0000	0.0000	0.0000	0.0000	0.0000	0.0000	0.0000	0.0000
1511.8300	0.0000	0.0000	0.0000	0.0000	0.0000	0.0000	0.0000	0.0000
1659.6300	0.0000	0.0000	0.0000	0.0000	0.0000	0.0000	0.0000	0.0000
1821.8800	0.0000	0.0000	0.0000	0.0000	0.0000	0.0000	0.0000	0.0000
2000.0000	0.0000	0.0000	0.0000	0.0000	0.0000	0.0000	0.0000	0.0000

Grainsize (µm)	Differential volume					
	AST004	AST005	AST006	AST006B	AST007	AST008
0.375124	0.0000	0.0000	0.0084	0.0050	0.0176	0.0000
0.411798	0.0000	0.0000	0.0147	0.0087	0.0311	0.0000
0.452057	0.0001	0.0000	0.0222	0.0132	0.0458	0.0000
0.496252	0.0012	0.0000	0.0343	0.0217	0.0664	0.0001
0.544768	0.0075	0.0000	0.0503	0.0350	0.0864	0.0016
0.598027	0.0241	0.0000	0.0710	0.0540	0.1076	0.0082
0.656493	0.0538	0.0004	0.0981	0.0804	0.1319	0.0224
0.720675	0.0941	0.0051	0.1329	0.1149	0.1619	0.0449
0.791132	0.1502	0.0300	0.1794	0.1623	0.1995	0.0758
0.868477	0.2221	0.0900	0.2384	0.2235	0.2466	0.1191
0.953383	0.3151	0.1937	0.3137	0.3024	0.3075	0.1781
1.046590	0.4243	0.3327	0.4044	0.3977	0.3842	0.2532
1.148910	0.5524	0.5152	0.5148	0.5137	0.4819	0.3473
1.261230	0.6936	0.7374	0.6415	0.6467	0.5999	0.4586
1.384540	0.8431	0.9955	0.7825	0.7946	0.7365	0.5849
1.519900	0.9931	1.2741	0.9293	0.9483	0.8833	0.7185
1.668490	1.1319	1.5548	1.0741	1.0992	1.0330	0.8518
1.831610	1.2611	1.8290	1.2132	1.2438	1.1786	0.9796
2.010680	1.3653	2.0712	1.3322	1.3673	1.3055	1.0902
2.207250	1.4473	2.2753	1.4269	1.4652	1.4026	1.1769
2.423040	1.4863	2.4058	1.4763	1.5158	1.4484	1.2229
2.659930	1.4973	2.4743	1.4924	1.5313	1.4493	1.2332
2.919980	1.4790	2.4744	1.4719	1.5087	1.4061	1.2074
3.205450	1.4458	2.4340	1.4369	1.4707	1.3454	1.1645
3.518830	1.4074	2.3723	1.3930	1.4235	1.2755	1.1127
3.862840	1.3576	2.2949	1.3460	1.3727	1.2059	1.0587
4.240490	1.3282	2.2405	1.3141	1.3383	1.1464	1.0134
4.655060	1.2970	2.1835	1.2845	1.3073	1.0908	0.9696
5.110170	1.3121	2.1785	1.2902	1.3135	1.0633	0.9483
5.609760	1.3184	2.1607	1.2898	1.3142	1.0376	0.9262
6.158200	1.3676	2.1943	1.3275	1.3538	1.0479	0.9310
6.760250	1.4173	2.2247	1.3630	1.3917	1.0606	0.9370
7.421170	1.5253	2.3186	1.4409	1.4739	1.1048	0.9688
8.146690	1.6639	2.4410	1.5275	1.5668	1.1485	1.0044
8.943150	1.8313	2.5861	1.6199	1.6665	1.1866	1.0410
9.817480	2.0425	2.7680	1.7273	1.7806	1.2264	1.0848
10.777300	2.2500	2.9165	1.8130	1.8700	1.2440	1.1139
11.830900	2.5376	3.1254	1.9411	2.0006	1.2925	1.1657
12.987600	2.8065	3.2862	2.0346	2.0952	1.3233	1.1965
14.257300	3.1127	3.4788	2.1283	2.1909	1.3560	1.2193
15.651200	3.3106	3.5724	2.1413	2.2042	1.3389	1.1939
17.181300	3.4048	3.5652	2.0853	2.1462	1.2720	1.1272
18.861000	3.3845	3.4291	1.9807	2.0367	1.1778	1.0414
20.705000	3.3181	3.1877	1.8627	1.9132	1.0899	0.9689
22.729200	3.3297	2.9648	1.7901	1.8392	1.0496	0.9383
24.951300	3.4344	2.7946	1.7635	1.8126	1.0681	0.9606
27.390600	3.6424	2.7546	1.7793	1.8276	1.1267	1.0179
30.068500	3.8111	2.7758	1.7958	1.8319	1.1913	1.0866
33.008100	3.8422	2.8005	1.8064	1.8110	1.2405	1.1562
36.235200	3.6327	2.7137	1.7746	1.7319	1.2382	1.1910
39.777700	3.2172	2.4420	1.7224	1.6263	1.2137	1.2148
43.666500	2.6816	1.9807	1.6121	1.4842	1.1571	1.1965
47.935600	2.1539	1.3906	1.4343	1.3214	1.1055	1.1584
52.622000	1.7365	0.7769	1.2417	1.1788	1.1004	1.1432
57.766600	1.4582	0.3108	1.1016	1.0975	1.1703	1.1947
63.414100	1.3189	0.0703	1.1855	1.1955	1.4095	1.4468

Grainsize (μm)	Differential volume					
	AST004	AST005	AST006	AST006B	AST007	AST008
69.613800	1.2557	0.0074	1.5836	1.5315	1.8304	1.9429
76.419600	1.2181	0.0001	2.4400	2.2135	2.4910	2.7847
83.890700	1.1514	0.0000	3.7049	3.2119	3.3290	3.9149
92.092300	1.0398	0.0000	5.0333	4.3257	4.2288	5.1821
101.096000	0.8990	0.0000	5.8534	5.1634	5.0193	6.3330
110.979000	0.7523	0.0000	5.6856	5.2979	5.4894	7.0441
121.829000	0.6195	0.0000	4.5077	4.5860	5.5432	7.1240
133.740000	0.4973	0.0000	2.6463	3.2325	5.1524	6.4861
146.815000	0.3772	0.0000	1.0467	1.6926	4.4196	5.2619
161.168000	0.2548	0.0000	0.2045	0.5922	3.5102	3.7437
176.925000	0.1349	0.0000	0.0164	0.1040	2.5721	2.2573
194.222000	0.0495	0.0000	0.0000	0.0071	1.7376	1.0566
213.210000	0.0091	0.0000	0.0000	0.0000	1.0690	0.3411
234.054000	0.0007	0.0000	0.0000	0.0000	0.5426	0.0571
256.936000	0.0000	0.0000	0.0000	0.0000	0.2056	0.0037
282.056000	0.0000	0.0000	0.0000	0.0000	0.0401	0.0000
309.631000	0.0000	0.0000	0.0000	0.0000	0.0035	0.0000
339.902000	0.0000	0.0000	0.0000	0.0000	0.0000	0.0000
373.132000	0.0000	0.0000	0.0000	0.0000	0.0000	0.0000
409.611000	0.0000	0.0000	0.0000	0.0000	0.0000	0.0000
449.657000	0.0000	0.0000	0.0000	0.0000	0.0000	0.0000
493.617000	0.0000	0.0000	0.0000	0.0000	0.0000	0.0000
541.876000	0.0000	0.0000	0.0000	0.0000	0.0000	0.0000
594.852000	0.0000	0.0000	0.0000	0.0000	0.0000	0.0000
653.008000	0.0000	0.0000	0.0000	0.0000	0.0000	0.0000
716.849000	0.0000	0.0000	0.0000	0.0000	0.0000	0.0000
786.932000	0.0000	0.0000	0.0000	0.0000	0.0000	0.0000
863.866000	0.0000	0.0000	0.0000	0.0000	0.0000	0.0000
948.322000	0.0000	0.0000	0.0000	0.0000	0.0000	0.0000
1,041.030000	0.0000	0.0000	0.0000	0.0000	0.0000	0.0000
1,142.810000	0.0000	0.0000	0.0000	0.0000	0.0000	0.0000
1,254.540000	0.0000	0.0000	0.0000	0.0000	0.0000	0.0000
1,377.190000	0.0000	0.0000	0.0000	0.0000	0.0000	0.0000
1,511.830000	0.0000	0.0000	0.0000	0.0000	0.0000	0.0000
1,659.630000	0.0000	0.0000	0.0000	0.0000	0.0000	0.0000
1,821.880000	0.0000	0.0000	0.0000	0.0000	0.0000	0.0000
2,000.000000	0.0000	0.0000	0.0000	0.0000	0.0000	0.0000

Grainsize (µm)	Differential volume					
	AST009	AST012	AST014	AST014B	AST015	AST015B
0.375124	0.0000	0.0000	0.0000	0.0000	0.0000	0.0000
0.411798	0.0000	0.0000	0.0000	0.0000	0.0000	0.0000
0.452057	0.0000	0.0000	0.0000	0.0000	0.0000	0.0000
0.496252	0.0000	0.0000	0.0000	0.0000	0.0000	0.0000
0.544768	0.0000	0.0000	0.0000	0.0000	0.0000	0.0000
0.598027	0.0000	0.0000	0.0000	0.0000	0.0000	0.0000
0.656493	0.0000	0.0000	0.0000	0.0000	0.0000	0.0000
0.720675	0.0000	0.0000	0.0000	0.0000	0.0000	0.0000
0.791132	0.0002	0.0000	0.0000	0.0000	0.0000	0.0000
0.868477	0.0027	0.0003	0.0000	0.0000	0.0000	0.0000
0.953383	0.0147	0.0040	0.0000	0.0000	0.0001	0.0005
1.046590	0.0409	0.0217	0.0000	0.0000	0.0022	0.0064
1.148910	0.0812	0.0588	0.0000	0.0000	0.0161	0.0342
1.261230	0.1301	0.1135	0.0031	0.0017	0.0588	0.0929
1.384540	0.1867	0.1743	0.0404	0.0245	0.1344	0.1781
1.519900	0.2494	0.2420	0.1255	0.0877	0.2311	0.2712
1.668490	0.3134	0.3119	0.2249	0.1735	0.3319	0.3685
1.831610	0.3779	0.3831	0.3316	0.2679	0.4322	0.4659
2.010680	0.4359	0.4484	0.4262	0.3562	0.5232	0.5546
2.207250	0.4862	0.5052	0.4948	0.4237	0.6010	0.6307
2.423040	0.5231	0.5465	0.5312	0.4640	0.6549	0.6818
2.659930	0.5484	0.5745	0.5359	0.4773	0.6842	0.7102
2.919980	0.5614	0.5889	0.5182	0.4692	0.6874	0.7143
3.205450	0.5644	0.5923	0.4896	0.4495	0.6731	0.7033
3.518830	0.5628	0.5904	0.4598	0.4253	0.6512	0.6846
3.862840	0.5558	0.5830	0.4370	0.4042	0.6266	0.6624
4.240490	0.5533	0.5807	0.4219	0.3896	0.6115	0.6488
4.655060	0.5485	0.5763	0.4180	0.3842	0.5977	0.6357
5.110170	0.5516	0.5808	0.4255	0.3883	0.5972	0.6368
5.609760	0.5501	0.5799	0.4411	0.3979	0.5916	0.6322
6.158200	0.5561	0.5872	0.4658	0.4133	0.5987	0.6412
6.760250	0.5617	0.5937	0.4965	0.4340	0.6054	0.6490
7.421170	0.5781	0.6126	0.5365	0.4642	0.6296	0.6754
8.146690	0.5997	0.6369	0.5730	0.4935	0.6606	0.7080
8.943150	0.6250	0.6652	0.5956	0.5150	0.6989	0.7468
9.817480	0.6564	0.7007	0.6099	0.5360	0.7512	0.7984
10.777300	0.6862	0.7348	0.6170	0.5562	0.8076	0.8513
11.830900	0.7275	0.7827	0.6523	0.6035	0.8873	0.9298
12.987600	0.7599	0.8207	0.7373	0.6871	0.9534	0.9965
14.257300	0.7855	0.8514	0.8695	0.7934	1.0069	1.0538
15.651200	0.7827	0.8501	1.0215	0.8978	1.0174	1.0635
17.181300	0.7630	0.8289	1.0593	0.8951	1.0062	1.0393
18.861000	0.7342	0.7971	0.8977	0.7252	0.9911	1.0003
20.705000	0.7227	0.7831	0.6036	0.4538	1.0045	0.9853
22.729200	0.7302	0.7912	0.3772	0.2734	1.0470	1.0117
24.951300	0.7663	0.8318	0.4492	0.3751	1.1205	1.0902
27.390600	0.8154	0.8892	0.9478	0.8784	1.2031	1.1975
30.068500	0.8696	0.9547	1.6362	1.5241	1.2869	1.3097
33.008100	0.9437	1.0405	1.8676	1.7011	1.4017	1.4257
36.235200	1.0139	1.1187	1.2747	1.1361	1.5288	1.5102
39.777700	1.1137	1.2196	0.5993	0.5168	1.7017	1.5977
43.666500	1.1887	1.2844	0.6295	0.5559	1.8278	1.6366
47.935600	1.2292	1.3074	1.4095	1.3401	1.8503	1.6368
52.622000	1.2442	1.3104	2.0926	2.0633	1.7663	1.6276

Grainsize (μm)	Differential volume					
	AST009	AST012	AST014	AST014B	AST015	AST015B
57.766600	1.2633	1.3403	1.9604	2.0337	1.6575	1.6613
63.414100	1.4562	1.5823	1.7673	1.9634	1.7858	1.9184
69.613800	1.9087	2.1250	2.2057	2.3884	2.3311	2.4781
76.419600	2.8274	3.1686	3.4720	3.5925	3.5817	3.5140
83.890700	4.2910	4.7403	5.4092	5.7406	5.5875	5.0085
92.092300	6.2350	6.7009	7.5772	8.0771	8.0021	6.7738
101.096000	8.3569	8.6753	9.3672	9.6047	9.9995	8.3963
110.979000	10.0402	10.0369	10.2466	10.9983	10.6082	9.2738
121.829000	10.6736	10.2513	10.4082	12.6630	9.4239	8.9855
133.740000	9.8455	9.0692	9.9609	11.5383	6.7925	7.4701
146.815000	7.7028	6.7780	7.4240	5.8245	3.6277	5.1643
161.168000	4.9140	4.0808	2.6565	1.1162	1.2953	2.7051
176.925000	2.3357	1.8099	0.2010	0.0427	0.2314	0.9678
194.222000	0.7336	0.5142	0.0000	0.0000	0.0162	0.1751
213.210000	0.1171	0.0740	0.0000	0.0000	0.0000	0.0128
234.054000	0.0068	0.0034	0.0000	0.0000	0.0000	0.0000
256.936000	0.0000	0.0000	0.0000	0.0000	0.0000	0.0000
282.056000	0.0000	0.0000	0.0000	0.0000	0.0000	0.0000
309.631000	0.0000	0.0000	0.0000	0.0000	0.0000	0.0000
339.902000	0.0000	0.0000	0.0000	0.0000	0.0000	0.0000
373.132000	0.0000	0.0000	0.0000	0.0000	0.0000	0.0000
409.611000	0.0000	0.0000	0.0000	0.0000	0.0000	0.0000
449.657000	0.0000	0.0000	0.0000	0.0000	0.0000	0.0000
493.617000	0.0000	0.0000	0.0000	0.0000	0.0000	0.0000
541.876000	0.0000	0.0000	0.0000	0.0000	0.0000	0.0000
594.852000	0.0000	0.0000	0.0000	0.0000	0.0000	0.0000
653.008000	0.0000	0.0000	0.0000	0.0000	0.0000	0.0000
716.849000	0.0000	0.0000	0.0000	0.0000	0.0000	0.0000
786.932000	0.0000	0.0000	0.0000	0.0000	0.0000	0.0000
863.866000	0.0000	0.0000	0.0000	0.0000	0.0000	0.0000
948.322000	0.0000	0.0000	0.0000	0.0000	0.0000	0.0000
1,041.030000	0.0000	0.0000	0.0000	0.0000	0.0000	0.0000
1,142.810000	0.0000	0.0000	0.0000	0.0000	0.0000	0.0000
1,254.540000	0.0000	0.0000	0.0000	0.0000	0.0000	0.0000
1,377.190000	0.0000	0.0000	0.0000	0.0000	0.0000	0.0000
1,511.830000	0.0000	0.0000	0.0000	0.0000	0.0000	0.0000
1,659.630000	0.0000	0.0000	0.0000	0.0000	0.0000	0.0000
1,821.880000	0.0000	0.0000	0.0000	0.0000	0.0000	0.0000
2,000.000000	0.0000	0.0000	0.0000	0.0000	0.0000	0.0000

Grainsize (µm)	Differential volume				
	AST016	AST017	AST018	AST020	AST022
0.375124	0.0000	0.0000	0.0000	0.0129	0.4057
0.411798	0.0000	0.0000	0.0000	0.0227	0.3032
0.452057	0.0000	0.0000	0.0000	0.0338	0.1778
0.496252	0.0000	0.0000	0.0000	0.0494	0.0734
0.544768	0.0000	0.0000	0.0000	0.0660	0.0148
0.598027	0.0000	0.0000	0.0000	0.0840	0.0013
0.656493	0.0000	0.0000	0.0000	0.1054	0.0000
0.720675	0.0000	0.0000	0.0000	0.1307	0.0000
0.791132	0.0000	0.0000	0.0000	0.1629	0.0000
0.868477	0.0002	0.0000	0.0000	0.2014	0.0000
0.953383	0.0028	0.0005	0.0003	0.2500	0.0018
1.046590	0.0162	0.0064	0.0047	0.3083	0.0227
1.148910	0.0470	0.0332	0.0261	0.3805	0.1225
1.261230	0.0955	0.0871	0.0736	0.4645	0.3319
1.384540	0.1521	0.1625	0.1440	0.5599	0.6348
1.519900	0.2167	0.2436	0.2239	0.6626	0.9459
1.668490	0.2842	0.3286	0.3081	0.7672	1.2281
1.831610	0.3551	0.4165	0.3948	0.8731	1.4395
2.010680	0.4218	0.4982	0.4757	0.9684	1.5534
2.207250	0.4831	0.5722	0.5489	1.0521	1.5853
2.423040	0.5322	0.6269	0.6043	1.1071	1.5382
2.659930	0.5702	0.6652	0.6429	1.1425	1.4543
2.919980	0.5976	0.6855	0.6635	1.1523	1.3580
3.205450	0.6141	0.6927	0.6702	1.1491	1.2824
3.518830	0.6259	0.6928	0.6701	1.1366	1.2442
3.862840	0.6298	0.6861	0.6634	1.1168	1.2230
4.240490	0.6383	0.6866	0.6633	1.1077	1.2286
4.655060	0.6425	0.6844	0.6608	1.0949	1.2106
5.110170	0.6550	0.6951	0.6688	1.1071	1.2099
5.609760	0.6603	0.6974	0.6695	1.1071	1.1926
6.158200	0.6720	0.7115	0.6792	1.1351	1.2119
6.760250	0.6817	0.7242	0.6873	1.1604	1.2420
7.421170	0.7035	0.7564	0.7107	1.2234	1.2909
8.146690	0.7324	0.7973	0.7413	1.2968	1.3576
8.943150	0.7671	0.8454	0.7774	1.3793	1.4011
9.817480	0.8110	0.9079	0.8237	1.4849	1.4725
10.777300	0.8549	0.9727	0.8697	1.5882	1.5207
11.830900	0.9156	1.0639	0.9349	1.7479	1.6266
12.987600	0.9696	1.1422	0.9888	1.8891	1.7409
14.257300	1.0251	1.2097	1.0343	2.0246	1.8822
15.651200	1.0503	1.2238	1.0383	2.0586	2.0034
17.181300	1.0587	1.2045	1.0176	2.0029	2.0557
18.861000	1.0479	1.1689	0.9838	1.8927	2.0598
20.705000	1.0493	1.1672	0.9754	1.8132	2.0110
22.729200	1.0694	1.2170	1.0006	1.8474	1.9849
24.951300	1.1198	1.3334	1.0682	2.0194	1.9997
27.390600	1.1921	1.4929	1.1583	2.2986	2.0546
30.068500	1.2663	1.6654	1.2505	2.5807	2.1228
33.008100	1.3555	1.8490	1.3571	2.7857	2.1399
36.235200	1.4237	1.9903	1.4486	2.8286	2.0724
39.777700	1.5020	2.1161	1.5633	2.7641	1.9210
43.666500	1.5422	2.1576	1.6473	2.6317	1.7079
47.935600	1.5524	2.1500	1.7076	2.5361	1.5053
52.622000	1.5644	2.1748	1.7647	2.5419	1.3597
57.766600	1.6322	2.3547	1.8757	2.6605	1.3228

Grainsize (µm)	Differential volume				
69.613800	2.5378	3.9951	2.8866	3.2358	1.6871
76.419600	3.6307	5.6114	4.0491	3.5804	2.0976
83.890700	5.1863	7.4413	5.6516	3.8493	2.6086
92.092300	7.0183	8.8725	7.4562	3.9579	3.1483
101.096000	8.6905	9.2050	8.9555	3.8365	3.5958
110.979000	9.5715	8.0839	9.4980	3.4274	3.8003
121.829000	9.2200	5.8246	8.7419	2.7687	3.6363
133.740000	7.5805	3.1287	6.7858	1.9620	3.0692
146.815000	5.1409	1.1277	4.2433	1.1685	2.2120
161.168000	2.6238	0.2040	1.9579	0.5337	1.2809
176.925000	0.9032	0.0145	0.5814	0.1656	0.5426
194.222000	0.1576	0.0000	0.0876	0.0266	0.1431
213.210000	0.0108	0.0000	0.0044	0.0016	0.0189
234.054000	0.0000	0.0000	0.0000	0.0000	0.0007
256.936000	0.0000	0.0000	0.0000	0.0000	0.0000
282.056000	0.0000	0.0000	0.0000	0.0000	0.0000
309.631000	0.0000	0.0000	0.0000	0.0000	0.0000
339.902000	0.0000	0.0000	0.0000	0.0000	0.0000
373.132000	0.0000	0.0000	0.0000	0.0000	0.0000
409.611000	0.0000	0.0000	0.0000	0.0000	0.0000
449.657000	0.0000	0.0000	0.0000	0.0000	0.0000
493.617000	0.0000	0.0000	0.0000	0.0000	0.0000
541.876000	0.0000	0.0000	0.0000	0.0000	0.0000
594.852000	0.0000	0.0000	0.0000	0.0000	0.0000
653.008000	0.0000	0.0000	0.0000	0.0000	0.0000
716.849000	0.0000	0.0000	0.0000	0.0000	0.0000
786.932000	0.0000	0.0000	0.0000	0.0000	0.0000
863.866000	0.0000	0.0000	0.0000	0.0000	0.0000
948.322000	0.0000	0.0000	0.0000	0.0000	0.0000
1,041.030000	0.0000	0.0000	0.0000	0.0000	0.0000
1,142.810000	0.0000	0.0000	0.0000	0.0000	0.0000
1,254.540000	0.0000	0.0000	0.0000	0.0000	0.0000
1,377.190000	0.0000	0.0000	0.0000	0.0000	0.0000
1,511.830000	0.0000	0.0000	0.0000	0.0000	0.0000
1,659.630000	0.0000	0.0000	0.0000	0.0000	0.0000
1,821.880000	0.0000	0.0000	0.0000	0.0000	0.0000
2,000.000000	0.0000	0.0000	0.0000	0.0000	0.0000

Sample	Mean GS (um)	%Sand	%Mud	SD
BST004	6.03	0.00	100.00	8.27
BST005	159.00	70.60	29.40	127.10
BST007	74.67	41.50	58.50	88.50
BST008	34.00	19.00	81.00	47.56
BST009	108.80	63.30	36.70	87.46
BST010	53.40	37.20	62.80	47.80
BST011	143.40	67.00	33.00	129.90
BST012	70.15	50.50	49.50	55.38
BST013	71.56	51.40	48.60	55.23
BST014	79.09	54.40	45.60	62.77
BST021	87.87	58.20	41.80	66.01
BST022	26.60	5.90	94.10	19.97
BST023\	28.38	8.00	92.00	21.20
BST024	25.00	3.90	96.10	18.80
AST-022	44.71	19.2	81.80	49.03
AST-020	46.51	31.4	68.60	42.38
AST-018	33.79	63.1	36.90	31.8
AST-017	68.29	56.4	43.60	43.27
AST-016	82.66	64	36.00	50.83
AST-015	81.57	63.3	36.70	51.49
AST-014	90.24	73.5	26.50	48.53
AST-012	90.97	69.6	30.40	52.62
AST-009	94.79	71.4	28.60	53.51
AST-008	75.21	55	45.00	59.58
AST-007	70.53	48.6	51.40	64.52
AST-006	47.08	33.9	66.10	46.42
AST-005	15.02	0.07	99.93	13.3
AST-004	18.8	9.5	90.50	16.6

Appendix 2: Biostratigraphic data

Branch Stream count data

Sample Number	Formation	Column Height	*Indeterminate*	*Isabelidinium pellucidum*	*Trichodinium castanea*	*Odontochitina porifera*	*Odontichitina operculata*	*Odontichitina spinosa*	*Chatangiella packhamii*	*Manumiella seymourensis*	*Pyxidinopsis c.f. epakros*	*Impletosphaeridium sp.*	*Chatangiella sp.*	*Palaeocystodinium golzowense*	*Spiniferites ramosus*	*Manumiella sp.*	*Vozzhennikovia sp.*	*Palaeocystodinium rhomboides*	*Impagidinium /Pterodium group*	*Impagidinium sp 4 (Willumsen, 2003)*	*Impag/Pteridium with horn*	*Manumiella c.f. druggii*	*Isabelidinium korojonense*	*Pyxidinopsis c.f. waipawaensis*	*Spiniferites sp.*	*Cassidium sp.*	*Xenascus ceradioides*	*Alterbidinium sp.*	*Manumiella seelandica*	*Satyrodinium haumuriense*	Total
BST-003	Mead Hill Formation	-0.15	38			1	1			28	11			4				3	108	4								2	3	rw	*203*
BST-002	Mead Hill Formation	-0.05	45				1	1	8	2			6	4					14					1		1	1				*84*
BST-004	Branch Sandstone	0.01	Barren																												*0*
BST-007	Branch Sandstone	0.25	40	2					3	18	3			14					28	2	10			3	5	3					*131*
BST-008	Branch Sandstone	0.28	4				2				2			2	1				8					2							*21*
BST-010	Branch Sandstone	0.5	58							8		5			2				18							3					*94*
BST-011	Branch Sandstone	0.6	29							10									12	1		2	2								*56*
BST-012	Branch Sandstone	1.7	Barren																												*0*
BST-014	Branch Sandstone	3.7	5																												*5*
BST-021	Branch Sandstone	4	77							20	3			7	1	3	2	7	23		9										*152*
BST-022	Herring Formation	4.1	15	1								1	2	1																	*20*
BST-024	Herring Formation	4.5	56	32	5	6	38	4.5	33	1	5																				*180*

Angora Stream count data

Sample Number	Formation	Column Height	Indeterminate	*Cordosphaeridium fibrospinosum*	*Cordosphaeridium sp.*	*Trichodinium castanea*	*Impagidinium group*	*Odontochitina operculata*	*Odontochitina porifera*	*Odontochitina spinosa*	*Batiacasphaera sp.*	*Spiniferites ramosus*	*Isabelidinium pellucidum*	*Chatangiella victoriensis*	*Cassidium sp.*	*Palaeocystodinium golzonwense*	*Manumiella seymourensis*	*Impletospaeridium sp.*	*Glaphyrocysta marlboroughensis*	*Conosphaeridium abbreviatum*	*Callaiosphaeridium sp.*	*Cymososphaedium benmorense*	*Kleithriasphaeridium seccadum*	*Diconodinium sp.*	*Sentusidinium sp.*	*Nelsoniella sp.*	*Vozzhennikovia sp.*	*Spiniferites sp.*	*Circulodinium distinctum*	*Satryodinium haumuriense*	*Oligosphaeridium sp*	*Chatangiella sp.*	*Cribroperidinium sp.*	*Spinidinium sp.*	Total
AST-022	Whangai Formation	-0.5	64						1	14			20		2	12								2										2	117
AST-020	Whangai Formation	-0.1	12						1	3			3		1	1											4							3	28
AST-019	Glenburn Formation	0	52						1	23	6		4		11	33		6		1							2				1	4	3	1	148
AST-018	Glenburn Formation	0.1	12								3		3			3														1			1		23
AST-017	Glenburn Formation	0.2	4			1						1	1			2																			9
AST-016	Glenburn Formation	0.25	2							3			2			2																			9
AST-014	Glenburn Formation	1.25	5												1																				6
AST-011	Glenburn Formation	2.75	Barren																																0
AST-008	Glenburn Formation	4	53						15	2	2	13	2			1	5		6	1						11	1	4	2						118
AST-007	Glenburn Formation	4.25	30	2	2				2	2	7		2	1	1	3		8	1	5	2	5	2	1	2								1		79
AST-005	Glenburn Formation	4.5	25			1	2	12	30	19	5	1	71	1	3	36	1	4																	211
AST-004	Glenburn Formation	4.75	12.5	1	1	1	8	6	24	11	2	1																							68

Tangaruhe Stream count data:

Sample Number	Formation	Height (m)	Indeterminate	*Isabelidinium pellucidum*	*Trithyrodinium suspectum*	*Trichodinium castanea*	*Odontochitina porifera*	*Odontochitina spinosa*	*Nelsoniella semireticulata*	*Satyrodinium haumuriense*	*Chatangiella sp.*	*Isabelidinium sp.*	*Kallosphaeridium sp.*	*Impletosphaeridium sp.*	*Palaeocystodinium golzowense*	*Palaeocystodinium granulatum*	*Palaeocystodinium sp.*	*Diconodinium vitricorne*	*Cordosphaeridium sp.*	*Senoniasphaera sp.*	*Isabelidinium sp.*	*Isabelidinium korojonense*	*Phelodinium magnificum*	*Batiacasphaera sp*	*Cribroperidinium sp.*	*Manumiella seymourensis*	*Nelsoniella sp.*	*Xenikoon sp.*	*Cassidium sp.*	*Impagidinium Group*	*Spiniferites ramosus*	*Canningopsis sp.*	*Manumiella sp.*	Total
TST005	Whangai Fm	-1	29	31				2		1					8	2				1			3	8	3			3	2					*93*
TST007	Whangai Fm	-0.25	61	58											7						1	2	1	5	3	1	1							*140*
TST008	Whangai Fm	-0.1	24												17								1	1		2				11				*56*
TST009	Tangaruhe Fm	0.1	85	1		1	36	4	11	42	1		12	4		2		7	1					1									5	*213*
TST011	Tangaruhe Fm	0.25	64				21		12	47	3		12	3			1	4	3									?1				1		*171*
TST012	Tangaruhe Fm	0.5	58		1	1	25		18	30	2	2	8					3	2	1											1			*152*

<u>List of dinoflagellate taxa</u>

A list of dinoflagellate taxa identified in this thesis is presented below. The taxonomy follows Fensome and Williams (2017). Selected dinocysts are illustrated in plates I-IX.

Genus: *Alterbidinium* Lentin and Williams, 1985

Alterbidinium sp.

IN Roncaglia et al. (1999)

Genus: Batiacasphaera Drugg, 1970. Emendations: Morgan, 1975; Dörhöfer and Davies, 1980

Batiacasphaera sp.
Plate VII, 6; Plate VI, 4

Genus: Callaiosphaeridium Davey and Williams, 1966b. Emendations: Duxbury, 1980

Calliosphaeridium sp.
Plate V, 6

IN: Schiøler and Wilson (1998)

Genus: Canninginopsis Cookson and Eisenack, 1962. Emendation: Marshall, 1990.

Canninginopsis sp.
Plate IX, 3
IN: Backhouse (2006)

Genus: Cassidium Drugg, 1967

Cassidium sp.
Plate III 5,

IN: P. S. Willumsen (2000)

Genus: Chatangiella Vozzhennikova, 1967. Emendations: Lentin and Williams, 1976; Marshall, 1988.

Chatangiella sp.
IN: Roncaglia et al. (1999)

Chatangiella packhamii Marshall, 1990

Plates I3, I4

In Roncaglia et al. (1999)

Chatangiella victoriensis (Cookson and Manum, 1964) Lentin and Williams, 1976

Plate I2

IN Helby et al. (1987)

Circulodinium distinctum (Deflandre and Cookson, 1955) Jansonius, 1986

Plate VI, 6

IN: Schiøler and Wilson (1998)

Conosphaeridium abbreviatum Wilson, 1984

Plate V, 3

IN: Schiøler and Wilson (1998)

Genus: *Cordosphaeridium* (Eisenack, 1963). Emendations: Morgenroth, 1968; Davey, 1969; Sarjeant, 1981; He Chengquan, 1991.

Cordosphaeridium sp.

Plate V,1

IN: Fensome, Williams, and MacRae (2009)

Cordosphaeridium fibrospinosum Davey and Williams, 1966. Emendation: Davey, 1969.

IN: Fensome et al. (2009)

Genus: *Cribroperidinium* Neale and Sarjeant, 1962. Emendations: Davey, 1969; Sarjeant, 1982; Helenes, 1984.

Cribroperidinium sp.

Plate VI, 3

IN: Cookson and Eisenack (1958)

Cribroperidinium c.f. edwardsii (Cookson and Eisenack, 1958) Davey, 1969a

Plate VII, 4

IN: Cookson and Eisenack (1958)

Cymososphaeridium benmorense Schiøler and Wilson, 1998

Plate V, 5

IN Schiøler and Wilson (1998)

Genus: *Diconodinium* Eisenack and Cookson, 1960. Emendation: Morgan, 1977.

Diconodinium sp.

Plate I, 1

IN Roncaglia et al. (1999)

Diconodinium vitricorne Roncaglia et al., 1999.

IN Roncaglia et al. (1999)

Fibrocysta bipolaris **(**Cookson and Eisenack, 1965b) Stover and Evitt, 1978

Plate VII, 3

IN: Roncaglia et al. (1999)

Glaphyrocysta marlboroughensis Schiøler and Wilson, 1998

Plate V, 2

IN: Schiøler and Wilson (1998)

Genus: *Impagidinium* Stover and Evitt, 1978

Impagidinium sp.

Plate II, 6

IN Bijl, Sluijs, and Brinkhuis (2013)

Impagidinium agremon Willumsen, 2011

Plate IX, 5

IN P. S. Willumsen (2011)

Genus: *Impletosphaeridium* Morgenroth, 1966. Emendation: Islam, 1993

Plate IX, 2

Impletosphaeridium sp.

Genus: *Isabelidinium* Lentin and Williams, 1977a. Emendations: Marshall, 1988, Fensome et al., 2009.

Isabelidinium sp.

Roncaglia (2000)

Isabelidinium belfastense (Cookson and Eisenack) Lentin and Williams, 1977a,

Plate I, 5

IN: Wood and Askin (1992)

Isabelidinium korojonense (Cookson and Eisenack) Lentin and Williams, 1977

IN: Roncaglia et al. (1999)

Isabelidinium pellucidum (Deflandre and Cookson, 1955) Lentin and Williams, 1977

Plate I, 6

IN: Roncaglia (2000)

Genus: *Kallosphaeridium* de Coninck, 1969. Emendation: Jan du Chêne et al., 1985

Kallosphaeridium sp.

IN: Wood, Riding, Fensome, and Williams (2016)

Genus: *Manumiella* Bujak and Davies, 1983. Emendations: Fensome et al. 2009; Thorn et al., 2009

Manumiella sp.

IN: Thorn, Riding, and Francis (2009)

Manumiella c.f. druggii (Stover, 1974) Bujak and Davies, 1983

IN Thorn et al. (2009)

Manumiella seelandica (Lange, 1969) Bujak and Davies, 1983, p.162. Emendation: Firth, 1987.

Plate II, 3

IN Thorn et al. (2009)

Manumiella seymourensis Askin 1999

Plates II, 1&2

IN: Thorn et al. (2009)

Genus: *Nelsoniella* Cookson and Eisenack, 1960a

Nelsoniella sp.

IN: Cookson and Eisenack (1960)

Nelsoniella semireticulata Cookson and Eisenack, 1960

Plate VI, 5

IN: Schiøler and Wilson (1998)

Odontochitina operculata (Wetzel, 1933a) Deflandre and Cookson, 1955

Plate IV, 1

IN: Deflandre and Cookson (1955)

Odontochitina porifera Cookson, 1956

Plate IV, 3

IN: Fensome et al. (2009)

Odontochitina spinosa Wilson, 1984

Plate IV, 2

IN: Wilson (1984b)

Genus: *Oligosphaeridium* Davey and Williams, 1966. Emendation: Davey, 1982.

Oligosphaeridium sp.

IN Schiøler and Wilson (1998)

Genus: *Palaeocystodinium* Alberti, 1961. Emendation: Fensome et al. 2009.

Palaeocystodinium sp.

IN: Fensome et al. (2009)

Palaeocystodinium golzowense Alberti, 1961

Plate VIII, 1&2

IN: Fensome et al. (2009)

Palaeocystodinium granulatum (Wilson, 1967) Lentin and Williams, 1976.

IN: Wilson (1967a)

Palaeocystodinium rhomboides (Wetzel, 1933) Lentin and Williams, 1973.

IN Roncaglia et al. (1999)

Genus: *Phelodinium* Stover and Evitt, 1978

Phelodinium sp.

Plate VIII, 2

IN P. S. Willumsen (2011)

Phelodinium magnificum (Stanley, 1965) Stover and Evitt, 1978

Plate VIII, 1

IN: P. S. Willumsen (2011)

Genus: *Pyxidinopsis* Habib, 1976

Pyxidinopsis sp.

Plate III, 2

IN: P. S. Willumsen (2000)

Pyxidinopsis c.f. epakros Willumsen, 2011

Plate III, 3

IN Willumsen (2011)

Satryodinium haumuriense (Wilson, 1984) Lentin and Manum, 1986

Plate II, 5

IN Marshall (1990)

Satryodinium bengalense Lentin and Manum, 1986

Plate II, 4

IN Roncaglia et al. (1999)

Genus: *Senoniasphaera* Clarke and Verdier, 1967

Senoniasphaera sp.

Plate VII, 1

Pers comm. Poul Schiøler, 2018.

Genus: *Sentusidinium* Sarjeant and Stover, 1978

Sentusidinium sp.

Plate III,1; IX, 6

IN: Wood et al. (2016)

Genus: Spinidinium Cookson and Eisenack, 1962. Emendations: Lentin and Williams, 1976, Quattrocchio and Sarjeant, 2003; Sluijs et al., 2009

Spinidinium sp.

IN Sluijs, Brinkhuis, Williams, and Fensome (2009)

Genus: *Spiniferites* Mantell, 1850. Emendation: Sarjeant, 1970

Spiniferites sp.

IN Fensome et al. (2009)

Spiniferites ramosus ssp. (Ehrenberg, 1837) Mantell, 1854

Plate VI, 1 & 2

IN Fensome et al. (2009)

Trichodinium castanea (Deflandre, 1935) Clarke and Verdier, 1967

Plate IX, 4

IN Atta-Peters and Salami (2006)

Trithyrodinium suspectum (Manum and Cookson, 1964) Davey, 1969b

Plate VII, 2

Pers comm. Poul Schiøler, 2018.

Genus: *Vozzhennikovia* Lentin and Williams, 1976

Vozzhennikovia sp.

Plate VII, 5

IN Wilson (1984b)

Xenascus ceradioides (Deflandre, 1937) Lentin and Williams, 1973

Genus: *Xenikoon* Cookson and Eisenack, 1960

Xenikoon sp.

IN Cookson and Eisenack (1960)

PLATE I

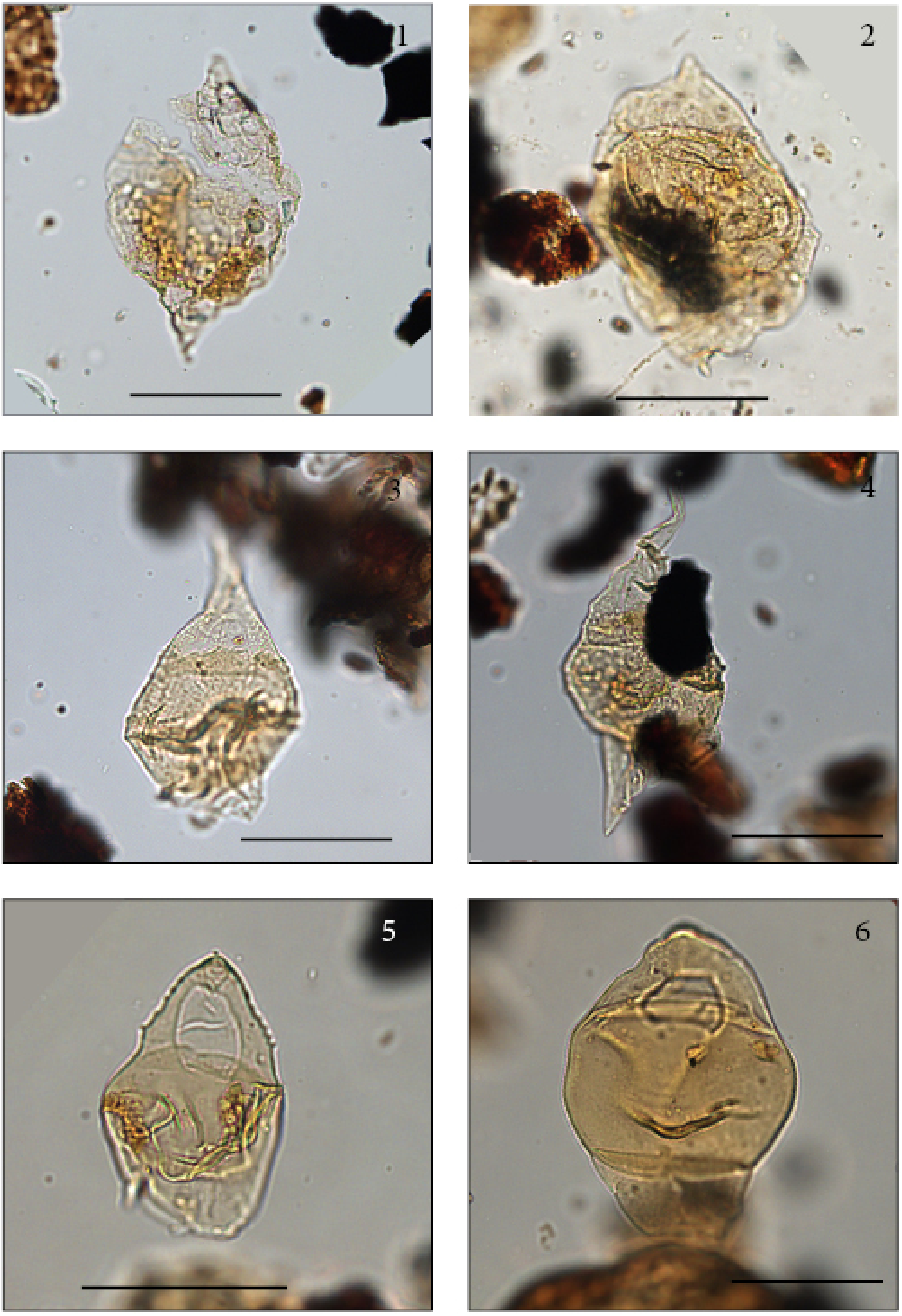

PLATE I

1. *Diconodinium sp.* (reworked)
   AST007/1
   EF coordinates: J36/1

2. *Chatangiella victoriensis*
   AST005/1
   EF coordinates: V30/2

3. *Chatangiella packhamii*
   BST024/1
   EF coordinates: L22/3

4. *Chatangiella packhamii*
   *B*ST024/1
   EF coordinates: Y32/4

5. *Isabelidinium belfastense*
   BST024/1
   EF coordinates: Q23/3

6. *Isabelidinium pellucidum*
   BST024/1
   EF coordinates: J29/2

Scale = 50um

PLATE II

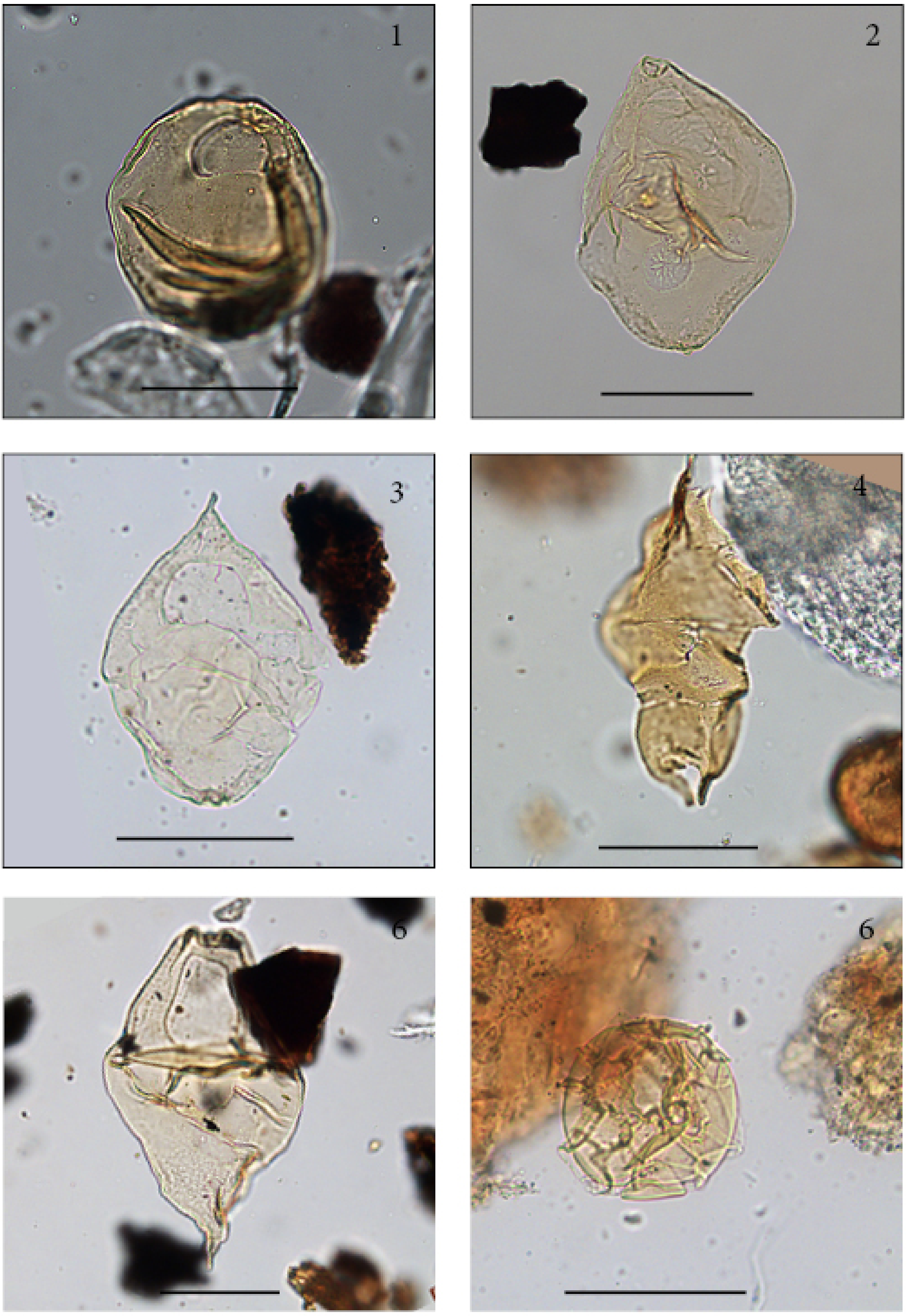

PLATE II

1. *Manumiellaseymourensis*
   BST011/3
   EF coordinates: T36/1

2. *Manumiellaseymourensis*
   BSM_NR_02/3
   EF coordinates F28/2

3. *Manumiella seelandica*
   BST003/1
   EF coordinates: P31/1

4. *Satyrodinium bengalense*
   AST018/1
   EF coordinates: X31/2

5. *Satyrodiniumhaumuriense*
   TST009/1
   EF coordinates: U31/4

6. *Impagidinium sp.*
   BST003/1
   EF coordinates: S34/2

Scale = 50um

PLATE III

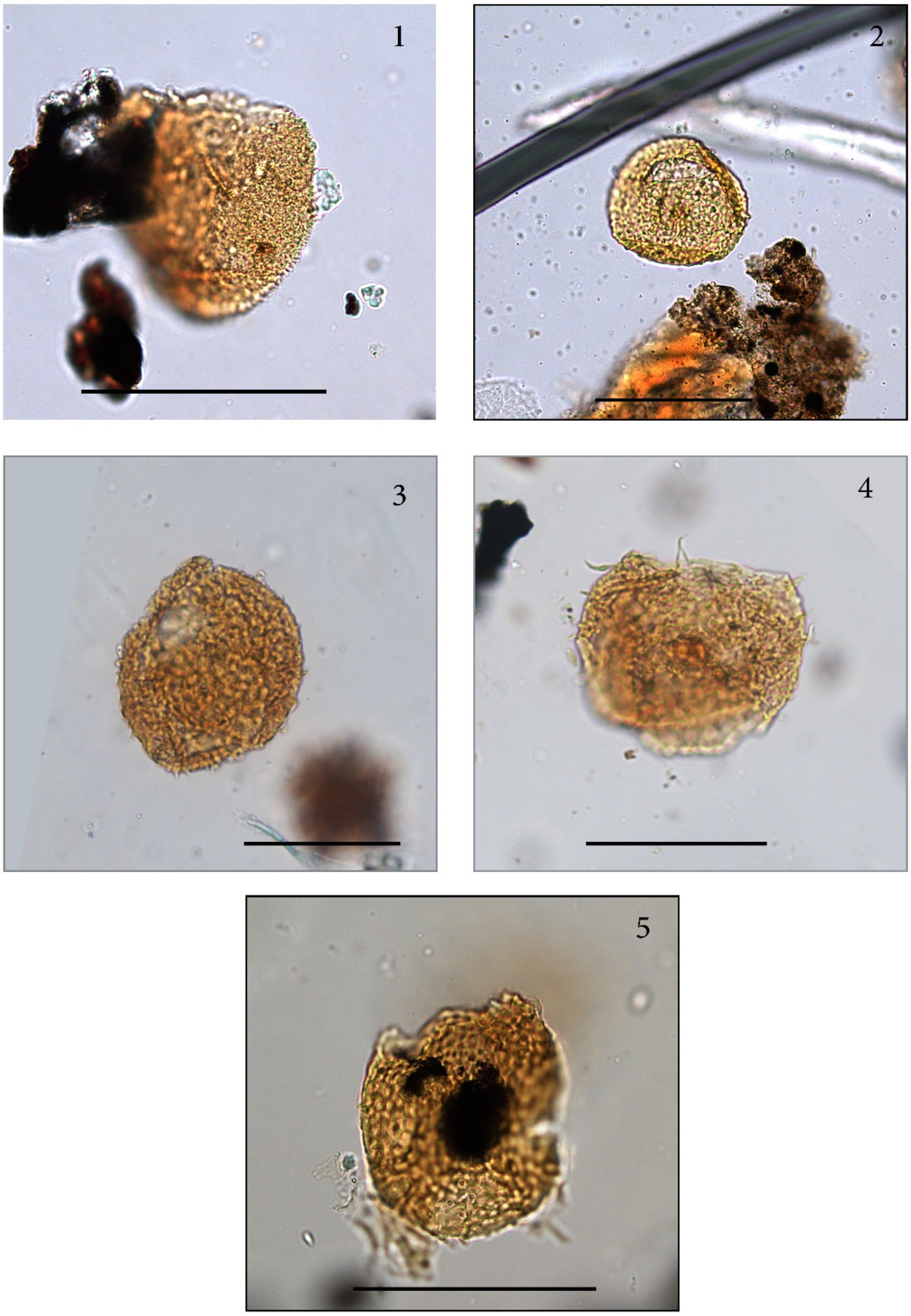

PLATE III

1. *Sentusidinium sp.*
   AST007/1
   EF coordinates: F36/2

2. *Pyxidinopsis sp*.
   BST003/1
   EF coordinates: K30/2

3. *Pyxidinopsisc.f.epakros*
   BST007/3
   EF coordinates: Z31/1

4. *Cassidium sp.*
   AST005/1
   EF coordinates: W47/3

5. *Cassidium sp.*
   BST024/1
   EF coordinates: M28/3

Scale = 50um

PLATE IV

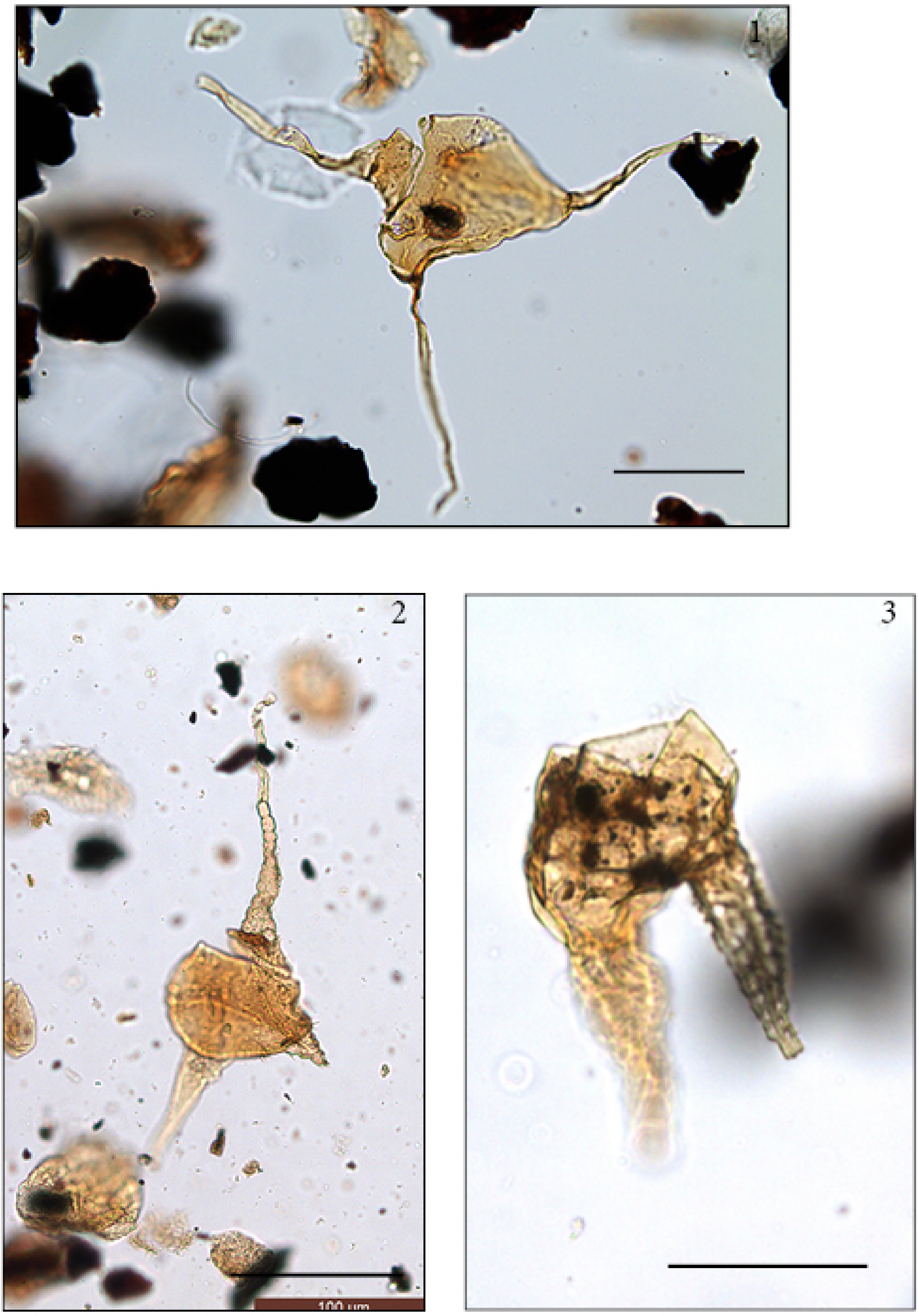

PLATE IV

1. *Odontochitina operculata*
   BST024/1
   EF coordinates: T26/3

2. *Odontochitina spinosa*
   AST005/1
   EF coordinates: V45/2

3. *Odontochitina porifera*
   TST012/1
   EF coordinates: U25/4

Scale = 50um

PLATE V

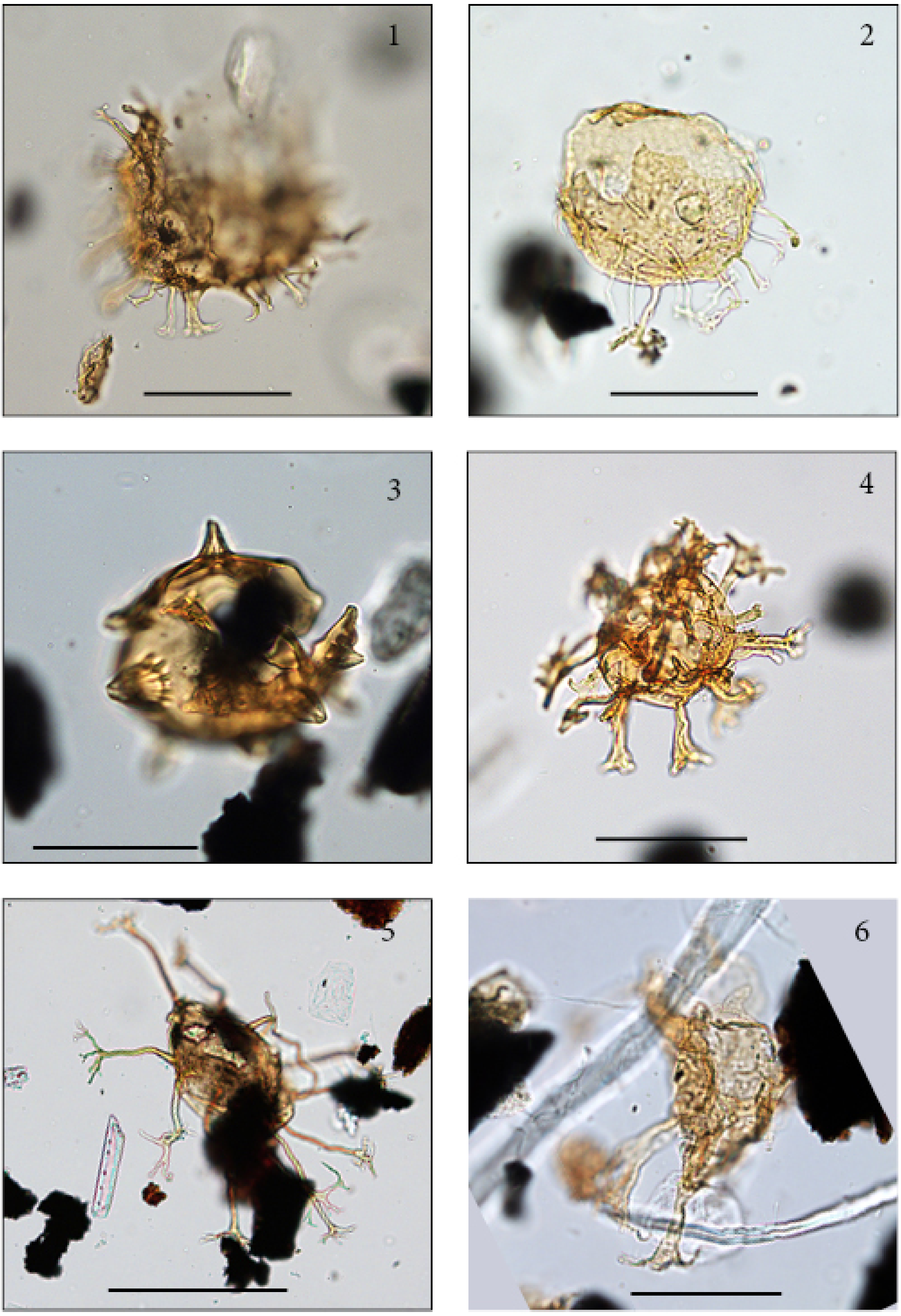

PLATE V

1. *Cordosphaeridium sp.*
   AST004/1
   EF coordinates: J38/2/3

2. *Glaphyrocysta marlboroughensis*
   AST008/1
   EF coordinates: Y29/1

3. C*onosphaeridium abbreviatum* (reworked)
   AST007/1
   EF coordinates: S35/3

4. *Kleithriasphaeridium seccadum* (reworked)
   AST007/2
   EF coordinates: K28/1

5. *Cymososphaeridium benmorense* (reworked) (scale = 100um)
   AST007//1
   EF coordinates: P30/2

6. *Callaiosphaeridium sp.* (reworked)
   AST007/1
   EF coordinates: K36/4

Scale = 50um

PLATE VI

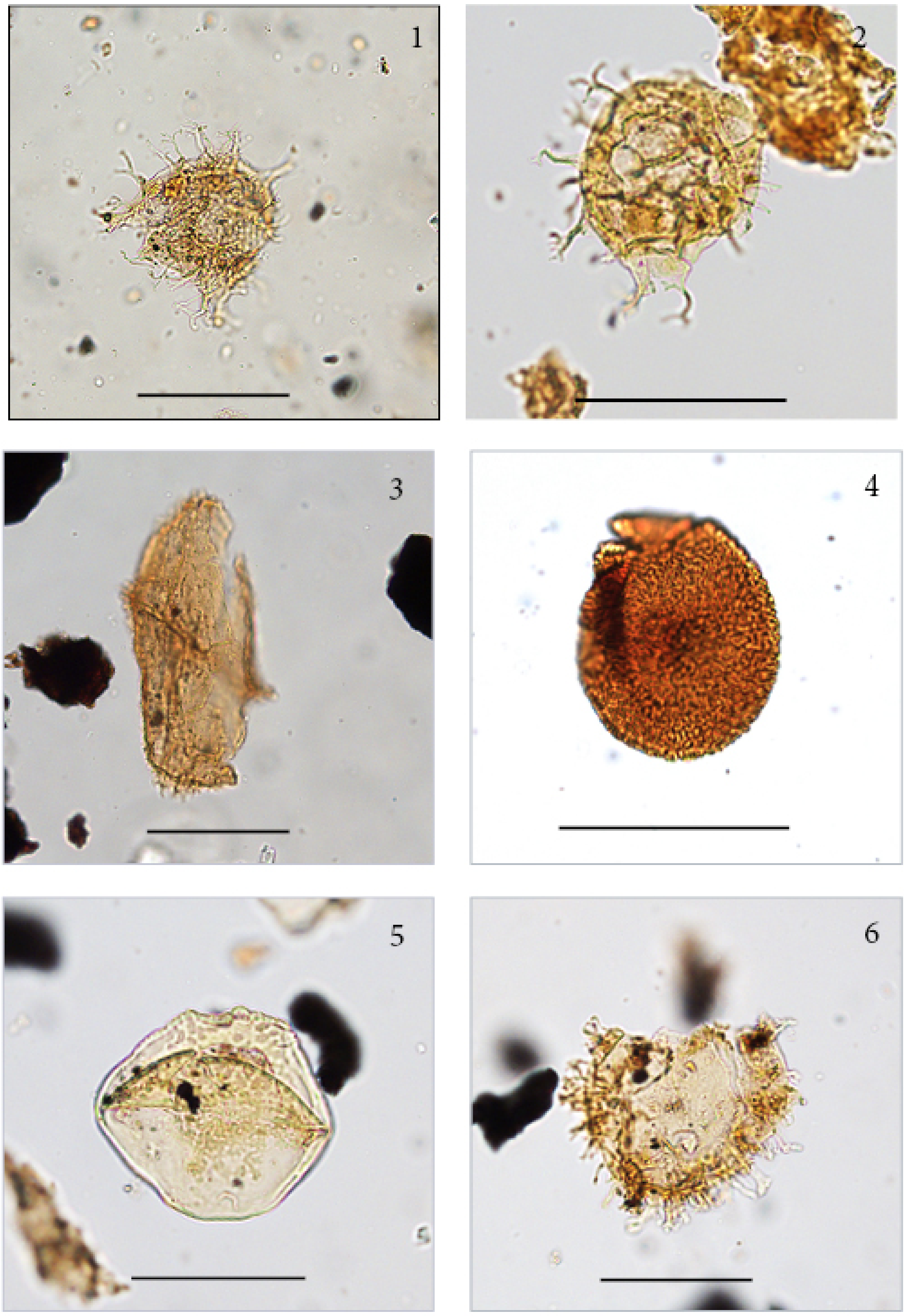

PLATE VI

1. *Spiniferites ramosus ssp.*
   BSMNR07_3
   EF coordinates: H28/2

2. *Spiniferites ramosus ssp*.
   AST007/2
   EF coordinates: F34/3

3. *Cribroperidinium sp.*
   AST007/1
   EF coordinates: F37/1

4. *Batiacasphaera sp.*
   AST004/1
   EF coordinates: Y42/1

5. *Nelsoniella semireticulata*
   TST009/1
   EF coordinates: O38/2

6. *Circulodinium distinctum*
   TST009/1
   EF coordinates: L27/2

Scale = 50um

PLATE VII

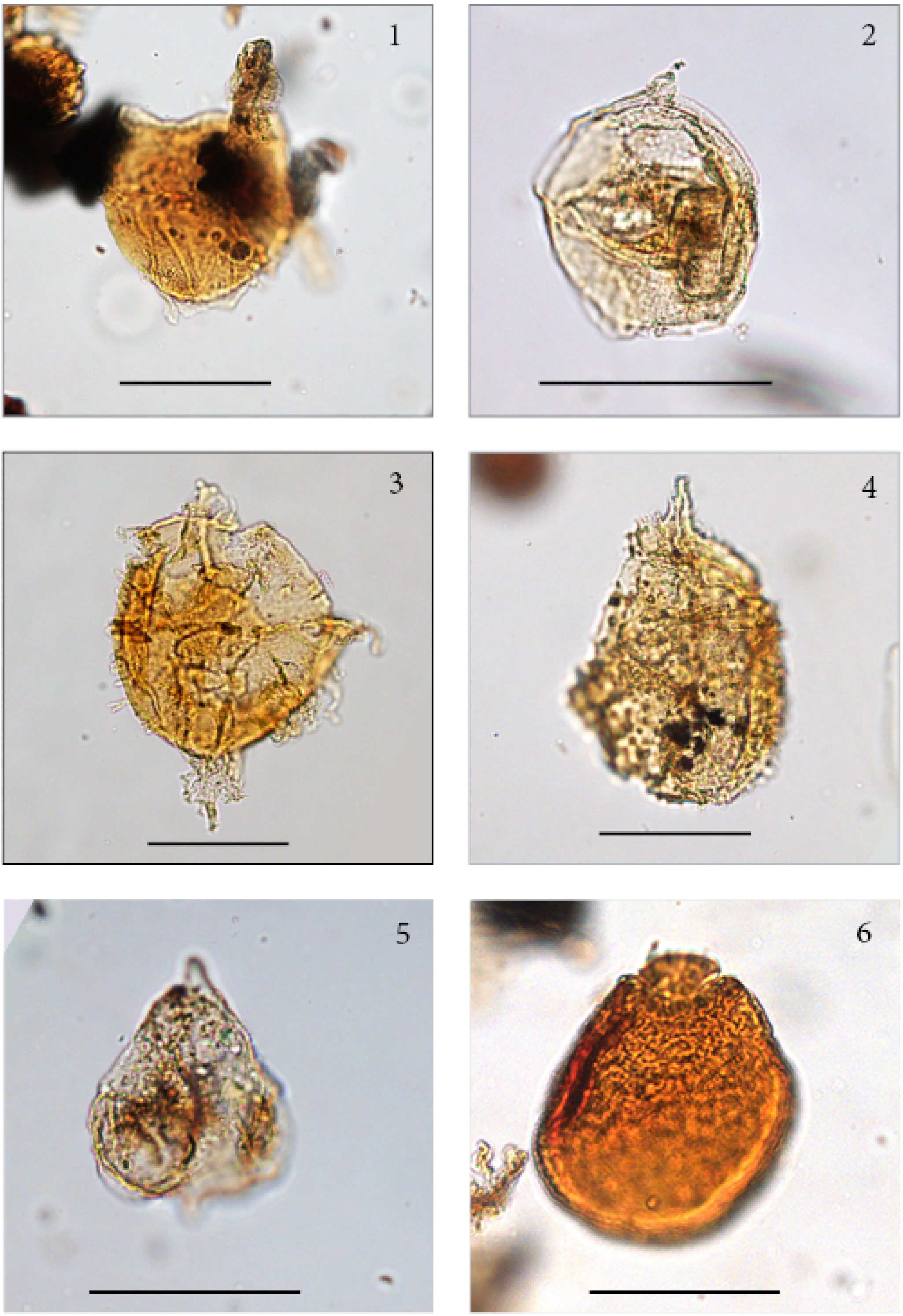

PLATE VII

1. *Senoniasphaera sp*.
   AST019/1
   EF Coordinates: O31/1

2. *Trithyrodinium suspectum*
   TST012/1
   EF coordinates: R36/4

3. *Fibrocysta bipolaris*
   BSMNR03_2
   EF coordinates: U53/4

4. *Cribroperidinium c.f. edwardsii*
   TST005/1
   EF coordinates: O25/2

5. *Vozzhenikovia sp.*
   AST020/1
   EF coordinates: Q40/1/2

6. *Batiacasphaera sp.*
   TST005/1
   EF coordinates: N19/4

Scale = 50um

PLATE VIII

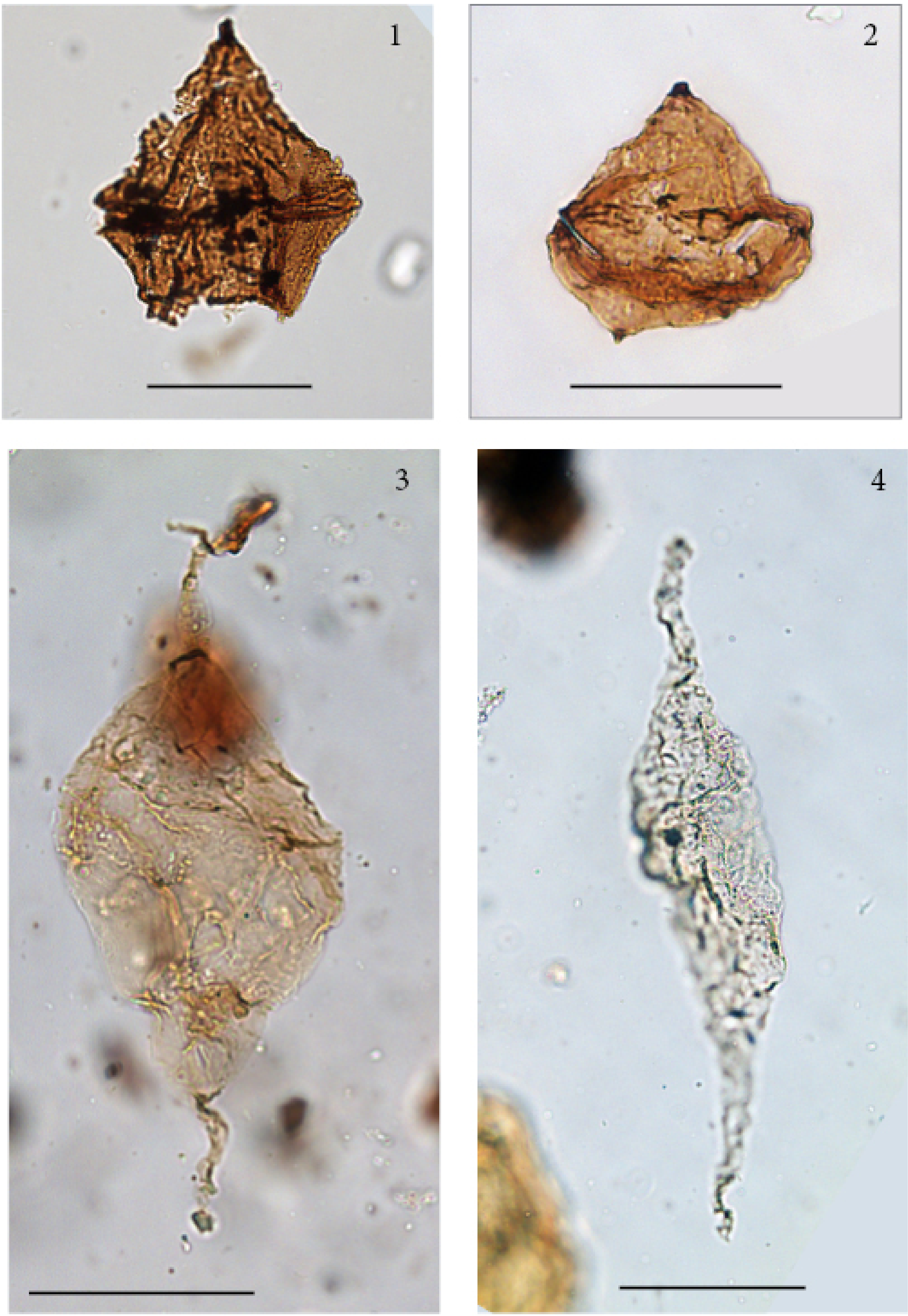

PLATE VIII

1. *Phelodinium magnificum*
   TST008/1
   EF coordinates: P23/4

2. *Phelodinium sp.*
   TST005/1
   EF coordinates: J20/2

3. *Palaeocystodinium golzowense*
   AST005/1
   EF coordinates: Y28/1

4. *Palaeocystondinium golzowense*
   BST003/1
   EF coordinates: B19/4

Scale = 50um

PLATE IX

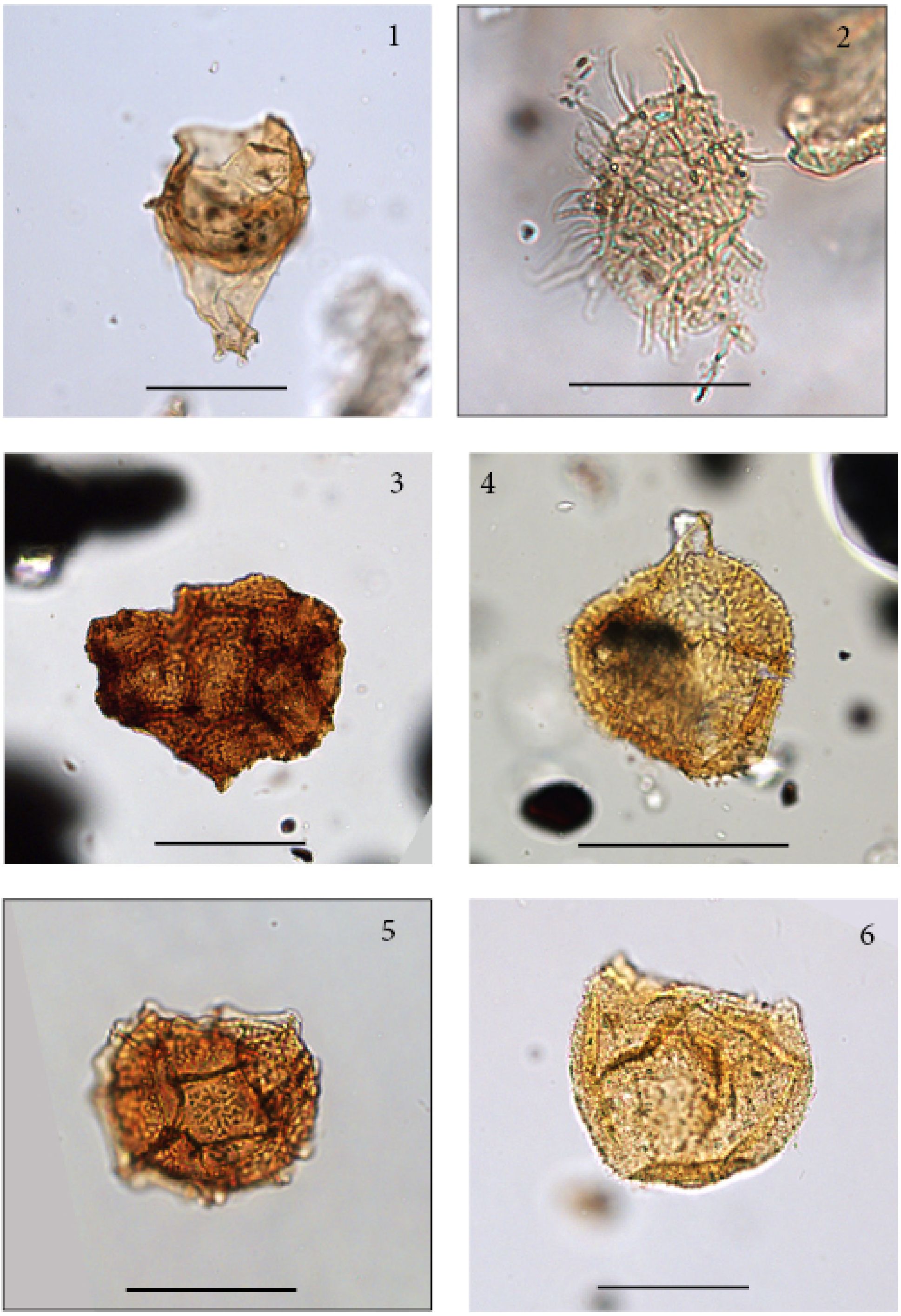

PLATE IX

1. *Xenascus ceratoides*
   BST002/1
   EF coordinates: Z26/2

2. *Impletosphaeridium sp*.
   AST005/1
   EF coordinates: J29/4

3. *Canningnopsis sp.*
   TST011/1
   EF coordinates: P22/4

4. *Trichodinium castanea*
   AST004/1
   EF coordinates: O33/2/4

5. *Impagidinium agremon*
   BSMNR04_3
   EF coordinates: K23/9

6. *Sentusidinium sp.*
   TST008/1
   EF coordinates: N25/3

Scale = 50um, except 2 where scale = 20um

Appendix 3: Palynofacies data

Branch Stream:

Raw count data

	Column height	Amorphous organic matter	Monolete spores	Trilete spores	Saccate gymnosperm pollen	Other gymnospherm pollen	Mangrove pollen	Other Angiospherm pollen	Freshwater algae	Peridinoid dinoflagellate cysts	Gonyaulacoid dinoflagellate cysts	Indeterminate and other dino cysts	Acritarchs and other marine 'algae'	Foraminiferal test linings	Other zoomorphs	Indeterminate and unknown palynomorphs	Fungal remains	Cellular membranes	Non-cellular membranes	Brown structured phytoclasts	Degraded phytoclasts	Opaque elongate phytoclasts	Opaque equidimensional phytoclasts	Opaque 'other' phytoclasts	Resin/Humic gel	Total
BST003	**-0.15**	142	0	1	0	1	0	0	0	4	5	9	6	0	0	1	3	31	1	10	49	1	25	4	7	300
BST002	**-0.05**	95	2	5	3	0	0	0	0	4	3	2	3	0	0	5	1	21	2	46	38	5	50	7	8	300
BST005	**0.1**	107	1	0	0	0	0	0	0	1	2	6	0	0	1	0	1	5	1	2	11	8	37	17	0	200
BST007	**0.25**	148	0	0	0	0	0	0	0	15	6	3	0	0	1	6	0	3	6	16	7	2	76	5	6	300
BST008	**0.28**	67	0	1	0	0	0	0	0	1	0	2	0	0	1	2	0	1	6	7	3	0	24	1	2	118
BST010	**0.5**	66	0	0	0	0	0	0	0	3	2	2	1	0	0	3	1	6	3	46	26	0	120	13	8	300
BST011	**0.6**	97	0	0	0	0	0	0	0	9	7	2	2	0	1	0	7	21	1	31	1	3	79	35	4	300
BST012	**1.7**	12	0	0	0	0	0	0	0	1	0	0	0	0	1	0	0	6	2	4	7	2	24	13	0	72
BST014	**3.7**	33	0	3	0	1	0	0	0	0	0	1	0	0	0	0	3	12	6	10	0	2	12	4	1	88
BST021	**4**	17	1	2	2	0	0	0	0	12	17	9	13	0	1	15	0	6	12	41	1	1	147	1	2	300
BST022	**4.1**	3	0	0	0	0	0	0	0	0	0	0	0	0	0	0	0	1	15	28	0	5	248	0	0	300
BST024	**4.5**	2	0	1	0	0	0	0	0	6	1	5	0	0	0	2	0	8	0	48	2	4	51	0	0	130

Normalised data

	Column height	Amorphous organic matter	Monolete spores	Trilete spores	Saccate gymnosperm pollen	Other gymnospherm pollen	Mangrove pollen	Other Angiospherm pollen	Freshwater algae	Peridinoid dinoflagellate cysts	Gonyaulacoid dinoflagellate cysts	Indeterminate and other dino cysts	Acritarchs and other marine 'algae'	Foraminiferal test linings	Other zoomorphs	Indeterminate and unknown palynomorphs	Fungal remains	Cellular membranes	Non-cellular membranes	Brown structured phytoclasts	Degraded phytoclasts	Opaque elongate phytoclasts	Opaque equidimensional phytoclasts	Opaque 'other' phytoclasts	Resin/Humic gel	Total
BST003	**-0.15**	32	1	2	1	0	0	0	0	1	1	1	1	0	0	2	0	7	1	15	13	2	17	2	3	100
BST002	**-0.05**	47	0	0	0	0	0	0	0	1	2	3	2	0	0	0	1	10	0	3	16	0	8	1	2	100
BST005	**0.1**	54	1	0	0	0	0	0	0	1	1	3	0	0	1	0	1	3	1	1	6	4	19	9	0	100
BST007	**0.25**	49	0	0	0	0	0	0	0	5	2	1	0	0	0	2	0	1	2	5	2	1	25	2	2	100
BST008	**0.28**	57	0	1	0	0	0	0	0	1	0	2	0	0	1	2	0	1	5	6	3	0	20	1	2	100
BST010	**0.5**	22	0	0	0	0	0	0	0	1	1	1	0	0	0	1	0	2	1	15	9	0	40	4	3	100
BST011	**0.6**	32	0	0	0	0	0	0	0	3	2	1	1	0	0	0	2	7	0	10	0	1	26	12	1	100
BST012	**1.7**	17	0	0	0	0	0	0	0	1	0	0	0	0	1	0	0	8	3	6	10	3	33	18	0	100
BST014	**3.7**	38	0	3	0	1	0	0	0	0	0	1	0	0	0	0	3	14	7	11	0	2	14	5	1	100
BST021	**4**	6	0	1	1	0	0	0	0	4	6	3	4	0	0	5	0	2	4	14	0	0	49	0	1	100
BST022	**4.1**	1	0	0	0	0	0	0	0	0	0	0	0	0	0	0	0	0	5	9	0	2	83	0	0	100
BST024	**4.5**	2	0	1	0	0	0	0	0	5	1	4	0	0	0	2	0	6	0	37	2	3	39	0	0	100

Raw count summary

	Column height	AOM	terrestrial palynomorphs	marine palynomorphs	indeterminate palynomorphs	brown phytoclasts	black phytoclasts	other phytoclasts
BST003	-0.15	142	2	24	1	59	30	42
BST002	-0.05	95	10	12	5	84	62	32
BST005	0.1	107	1	10	0	13	62	7
BST007	0.25	148	0	25	6	23	83	15
BST008	0.28	67	1	4	2	10	25	9
BST010	0.5	66	0	8	3	72	133	18
BST011	0.6	97	0	21	0	32	117	33
BST012	1.7	12	0	2	0	11	39	8
BST014	3.7	33	4	1	0	10	18	22
BST021	4	17	5	52	15	42	149	20
BST022	4.1	3	0	0	0	28	253	16
BST024	4.5	2	1	12	2	50	55	8

Normalised summary data

	Column height	AOM	terrestrial palynomorphs	marine palynomorphs	indeterminate palynomorphs	brown phytoclasts	black phytoclasts	other phytoclasts	black_brown_ratio	Impagidinium group
BST003	-0.15	32	3	4	2	28	21	11	-0.13	55
BST002	-0.05	47	1	8	0	20	10	14	-0.29	17
BST005	0.1	54	1	5	0	7	31	4	0.678	0
BST007	0.25	49	0	8	2	8	28	5	0.557	19
BST008	0.28	57	1	3	2	8	21	8	0.398	41
BST010	0.5	22	0	3	1	24	44	6	0.267	21
BST011	0.6	32	0	7	0	11	39	11	0.563	23
BST012	1.7	17	0	3	0	15	54	11	0.55	0
BST014	3.7	38	5	1	0	11	20	25	0.255	0
BST021	4	6	2	17	5	14	50	7	0.55	17
BST022	4.1	1	0	0	0	9	84	5	0.956	0
BST024	4.5	2	1	9	2	38	42	6	0.041	0

Angora Stream:

Raw count data

	Column height	Amorphous organic matter	Monolete spores	Trilete spores	Saccate gymnosperm pollen	Other gymnospherm pollen	Mangrove pollen	Other Angiospherm pollen	Freshwater algae	Peridinoid dinoflagellate cysts	Gonyaulacoid dinoflagellate cysts	Indeterminate and other dino cysts	Acritarchs and other marine 'algae'	Foraminiferal test linings	Other zoomorphs	Indeterminate and unknown palynomorphs	Fungal remains	Cellular membranes	Non-cellular membranes	Brown structured phytoclasts	Degraded phytoclasts	Opaque elongate phytoclasts	Opaque equidimensional phytoclasts	Opaque 'other' phytoclasts	Resin/Humic gel	Total
AST022	**-0.5**	18	1	3	1	1	0	0	0	15	1	3	0	0	0	16	0	0	2	71	2	3	159	2	2	300
AST020	**-0.1**	6	0	1	0	0	0	0	0	11	0	4	0	0	0	6	1	7	1	109	2	2	144	0	6	300
AST019	**0**	6	0	1	1	0	0	0	0	10	4	10	4	0	0	16	0	18	2	86	41	16	80	3	2	300
AST018	**0.1**	58	1	2	5	21	0	0	0	0	1	3	0	0	0	5	4	20	2	21	5	3	132	17	0	300
AST017	**0.2**	55	1	4	29	1	0	0	0	3	0	2	3	0	0	0	0	21	0	55	27	4	84	8	3	300
AST016	**0.25**	21	0	0	5	1	0	0	0	0	0	1	6	0	0	1	0	42	2	41	39	6	127	6	2	300
AST014	**1.25**	49	1	1	3	2	0	0	0	2	0	3	4	0	0	2	2	104	0	33	12	4	67	11	0	300
AST011	**2.75**	7	0	1	3	0	0	0	0	0	0	0	25	0	0	6	17	10	3	48	1	7	168	1	3	300
AST008	**4**	1	0	0	0	0	0	0	0	8	1	4	0	0	0	7	0	17	0	16	3	34	206	2	1	300
AST007	**4.25**	10	0	0	1	0	0	0	0	2	0	0	2	0	0	3	0	5	0	40	10	28	190	4	5	300
AST005	**4.5**	23	1	5	0	0	0	0	0	27	1	5	7	0	0	13	2	35	4	81	1	6	83	2	4	300
AST004	**4.75**	6	0	0	2	0	0	0	0	1	4	4	3	0	0	6	1	22	2	6	8	5	222	0	8	300

Normalised data

	Column height	Amorphous organic matter	Monolete spores	Trilete spores	Saccate gymnosperm pollen	Other gymnosperm pollen	Mangrove pollen	Other Angiosperm pollen	Freshwater algae	Peridinoid dinoflagellate cysts	Gonyaulacoid dinoflagellate cysts	Indeterminate and other dino cysts	Acritarchs and other marine 'algae'	Foraminiferal test linings	Other zoomorphs	Indeterminate and unknown palynomorphs	Fungal remains	Cellular membranes	Non-cellular membranes	Brown structured phytoclasts	Degraded phytoclasts	Opaque elongate phytoclasts	Opaque equidimensional phytoclasts	Opaque 'other' phytoclasts	Resin/Humic gel	Total
AST022	**-0.5**	6	0	1	0	0	0	0	0	5	0	1	0	0	0	5	0	0	1	24	1	1	53	1	1	100
AST020	**-0.1**	2	0	0	0	0	0	0	0	4	0	1	0	0	0	2	0	2	0	36	1	1	48	0	2	100
AST019	**0**	2	0	0	0	0	0	0	0	3	1	3	1	0	0	5	0	6	1	29	14	5	27	1	1	100
AST018	**0.1**	19	0	1	2	7	0	0	0	0	0	1	0	0	0	2	1	7	1	7	2	1	44	6	0	100
AST017	**0.2**	18	0	1	10	0	0	0	0	1	0	1	1	0	0	0	0	7	0	18	9	1	28	3	1	100
AST016	**0.25**	7	0	0	2	0	0	0	0	0	0	0	2	0	0	0	0	14	1	14	13	2	42	2	1	100
AST014	**1.25**	16	0	0	1	1	0	0	0	1	0	1	1	0	0	1	1	35	0	11	4	1	22	4	0	100
AST011	**2.75**	2	0	0	1	0	0	0	0	0	0	0	8	0	0	2	6	3	1	16	0	2	56	0	1	100
AST008	**4**	0	0	0	0	0	0	0	0	3	0	1	0	0	0	2	0	6	0	5	1	11	69	1	0	100
AST007	**4.25**	3	0	0	0	0	0	0	0	1	0	0	1	0	0	1	0	2	0	13	3	9	63	1	2	100
AST005	**4.5**	8	0	2	0	0	0	0	0	9	0	2	2	0	0	4	1	12	1	27	0	2	28	1	1	100
AST004	**4.75**	2	0	0	1	0	0	0	0	0	1	1	1	0	0	2	0	7	1	2	3	2	74	0	3	100

Raw count summary

	Column height	AOM	terrestrial palynomorphs	marine palynomorphs	indeterminate palynomorphs	brown phytoclasts	black phytoclasts	other phytoclasts
AST022	-0.5	18	6	19	16	73	164	4
AST020	-0.1	6	1	15	6	111	146	15
AST019	0	6	2	28	16	127	99	22
AST018	0.1	58	29	4	5	26	152	26
AST017	0.2	55	35	8	0	82	96	24
AST016	0.25	21	6	7	1	80	139	46
AST014	1.25	49	7	9	2	45	82	106
AST011	2.75	7	4	25	6	49	176	33
AST008	4	1	0	13	7	19	242	18
AST007	4.25	10	1	4	3	50	222	10
AST005	4.5	23	6	40	13	82	91	45
AST004	4.75	6	2	12	6	14	227	33

Normalised summary data

	Column height	AOM	terrestrial_palynomorphs	marine_palynomorphs	indeterminate_palynomorphs	brown_phytoclasts	black_phytoclasts	other_phytoclasts	black_brown_ratio	Impagidinium group
AST022	-0.5	6	2	6	5	24	55	1	0.352	0
AST020	-0.1	2	0	5	2	37	49	5	0.119	0
AST019	0	2	1	9	5	42	33	7	-0.11	0
AST018	0.1	19	10	1	2	9	51	9	0.767	0
AST017	0.2	18	12	3	0	27	32	8	0.068	0
AST016	0.25	7	2	2	0	27	46	15	0.24	0
AST014	1.25	16	2	3	1	15	27	35	0.261	0
AST011	2.75	2	1	8	2	16	59	11	0.555	0
AST008	4	0	0	4	2	6	81	6	1.105	0
AST007	4.25	3	0	1	1	17	74	3	0.647	0
AST005	4.5	8	2	13	4	27	30	15	0.045	1
AST004	4.75	2	1	4	2	5	76	11	1.21	12

Tangaruhe Stream:

Raw count data

	Column height	Amorphous organic matter	Monolete spores	Trilete spores	Saccate gymnosperm pollen	Other gymnosperm pollen	Mangrove pollen	Other Angiosperm pollen	Freshwater algae	Peridinoid dinoflagellate cysts	Gonyaulacoid dinoflagellate cysts	Indeterminate and other dino cysts	Acritarchs and other marine 'algae'	Foraminiferal test linings	Other zoomorphs	Indeterminate and unknown palynomorphs	Fungal remains	Cellular membranes	Non-cellular membranes	Brown structured phytoclasts	Degraded phytoclasts	Opaque elongate phytoclasts	Opaque equidimensional phytoclasts	Opaque 'other' phytoclasts	Resin/Humic gel	Total
TST005	**-1**	191	0	1	0	0	0	0	0	16	2	2	1	0	1	1	2	2	2	18	0	10	44	7	0	300
TST007	**-0.25**	154	2	0	0	2	0	0	0	23	6	4	4	0	2	4	2	2	0	23	0	9	47	12	4	300
TST008	**-0.1**	177	1	0	1	0	0	0	0	8	3	4	2	0	0	2	0	3	0	22	0	8	56	10	3	300
TST009	**0.1**	76	0	0	0	0	0	0	0	8	1	3	1	0	0	1	0	1	0	36	0	6	153	14	0	300
TST011	**0.25**	62	0	1	0	0	0	0	0	17	0	2	1	0	1	3	0	2	1	39	0	13	145	12	1	300
TST012	**0.5**	54	1	1	0	0	0	0	0	8	1	4	0	2	1	0	1	0	0	43	1	13	154	16	0	300

Normalised data

	Column height	Amorphous organic matter	Monolete spores	Trilete spores	Saccate gymnosperm pollen	Other gymnosperm pollen	Mangrove pollen	Other Angiosperm pollen	Freshwater algae	Peridinoid dinoflagellate cysts	Gonyaulacoid dinoflagellate cysts	Indeterminate and other dino cysts	Acritarchs and other marine 'algae'	Foraminiferal test linings	Other zoomorphs	Indeterminate and unknown palynomorphs	Fungal remains	Cellular membranes	Non-cellular membranes	Brown structured phytoclasts	Degraded phytoclasts	Opaque elongate phytoclasts	Opaque equidimensional phytoclasts	Opaque 'other' phytoclasts	Resin/Humic gel	Total
TST005	**-1**	64	0	0	0	0	0	0	0	5	1	1	0	0	0	0	1	1	1	6	0	3	15	2	0	100
TST007	**-0.25**	51	1	0	0	1	0	0	0	8	2	1	1	0	1	1	1	1	0	8	0	3	16	4	1	100
TST008	**-0.1**	59	0	0	0	0	0	0	0	3	1	1	1	0	0	1	0	1	0	7	0	3	19	3	1	100
TST009	**0.1**	25	0	0	0	0	0	0	0	3	0	1	0	0	0	0	0	0	0	12	0	2	51	5	0	100
TST011	**0.25**	21	0	0	0	0	0	0	0	6	0	1	0	0	0	1	0	1	0	13	0	4	48	4	0	100
TST012	**0.5**	18	0	0	0	0	0	0	0	3	0	1	0	1	0	0	0	0	0	14	0	4	51	5	0	100

Raw count summary

Column height	AOM	terrestrial palynomorphs	marine palynomorphs	indeterminate palynomorphs	brown phytoclasts	black phytoclasts	other phytoclasts
-1	191	1	22	1	18	61	6
-0.25	154	4	39	4	23	68	8
-0.1	177	2	17	2	22	74	6
0.1	76	0	13	1	36	173	1
0.25	62	1	21	3	39	170	4
0.5	54	2	16	0	44	183	1

Normalised summary data

Column height	AOM	terrestrial palynomorphs	marine palynomorphs	indeterminate palynomorphs	brown phytoclasts	black phytoclasts	other phytoclasts	black brown ratio	Impagindinium group
-1	64	0	7	0	6	20	2	0.53	0
-0.25	51	1	13	1	8	23	3	0.471	0
-0.1	59	1	6	1	7	25	2	0.527	20
0.1	25	0	4	0	12	58	0	0.682	0
0.25	21	0	7	1	13	57	1	0.639	0
0.5	18	1	5	0	15	61	0	0.619	1